7 SOUND AND SOLID SURFACES

The interaction of sound with solid surfaces could well be taken as the beginning of architectural acoustics. Sound undergoes three types of fundamental interactions upon encountering an object: reflection, absorption, and transmission. Each of these occurs to some degree when an impact takes place, although usually we are concerned with only one at a time.

7.1 PERFECTLY REFLECTING INFINITE SURFACES

Incoherent Reflections

Up to this point we have considered sound waves to be free to propagate in any direction, unaffected by walls or other surfaces. Now we will examine the effect of reflections, beginning with a perfectly reflecting infinite surface. The simplest model of this interaction occurs with sound sources that can be considered incoherent; that is, where phase is not a consideration. If an omnidirectional source is placed near a perfectly reflecting surface of infinite extent, the surface acts like a mirror for the sound energy emanating from the source. The intensity of the sound in the far field, where the distance is large compared to the separation distance between the source and its mirror image, is twice the intensity of one source. Figure 7.1 shows this geometry. In terms of the relationship between the sound power and sound pressure levels for a point source given in Eq. 2.61,

$$L_p = L_w + 10 \log \frac{Q}{4 \pi r^2} + K \tag{7.1}$$

where L_p = sound pressure level (dB re 20 μN/ m^2)
L_w = sound power level (dB re 10^{-12} W)
Q = directivity
r = measurement distance (m or ft)
K = constant (0.13 for meters or 10.45 for ft)

When the source is near a perfectly reflecting plane, the sound power radiates into half a sphere. This effectively doubles the Q since the area of half a sphere is 2 πr^2. If the source is near two perfectly reflecting planes that are at right angles to one another, such as a floor and a wall, there is just one quarter of a sphere to radiate into, and the effective Q is 4.

FIGURE 7.1 Construction of an Image Source

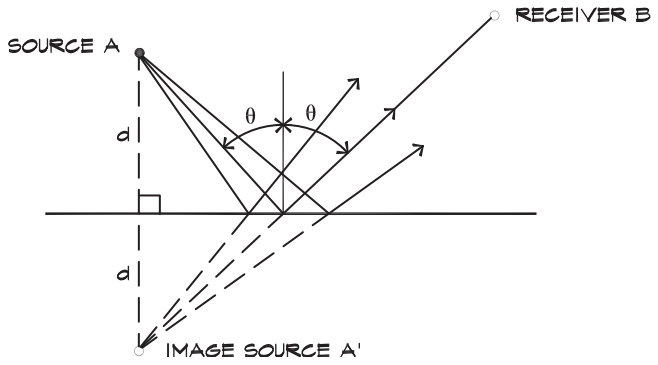

FIGURE 7.2 Multiple Image Sources

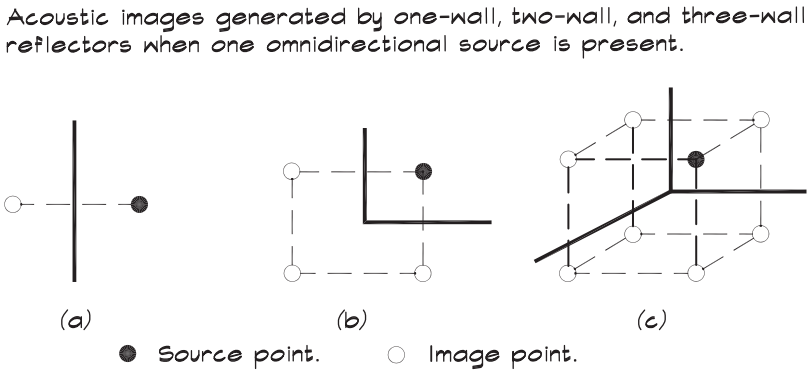

For a source located in a corner bounded by three perpendicular surfaces, the effective Q is 8. Figure 7.2 illustrates these conditions. For a nondirectional source such as a subwoofer, clearly the corner of a room is the most efficient location.

Note that the concept of Q is slightly different here than it is for the inherent directivity associated with a source. The directivity associated with the position of a source must be employed with some discretion. If a directional source such as a horn loudspeaker is placed in the corner of a room pointed outward, then the overall directivity does not increase by a factor of 8, since most of the energy already is focused away from the reflecting surfaces. The mirror image of the horn, pointed away from the corner, also contributes, but only a small amount at high frequencies. Thus changes in Q due to reflecting surfaces must also account for the inherent directivity of the source.

Coherent Reflections—Normal Incidence

When the sound is characterized as a plane wave, moving in the positive x direction, we can write an expression for the behavior of the pressure in space and time

$$\mathbf{p}\,(\mathrm{x}) = \mathbf{A}\,\mathrm{e}^{\,\mathrm{j}\,(\omega\,\mathrm{t}\,-\,\mathrm{k}\,\mathrm{x})} \tag{7.2}$$

If we place an infinite surface at $\mathrm{x} = 0$, with its normal along the x axis, the equation for the combined incident and reflected waves in front of the surface is

$$\mathbf{p}\,(\mathrm{x}) = \mathbf{A}\,\mathrm{e}^{\,\mathrm{j}\,(\omega\,\mathrm{t}\,-\,\mathrm{k}\,\mathrm{x})} + \mathbf{B}\,\mathrm{e}^{\mathrm{j}\,(\omega\,\mathrm{t}\,+\,\mathrm{k}\,\mathrm{x})} \tag{7.3}$$

The particle velocity, **u**, defined in Eq. 6.31 as

$$\mathbf{u}(x) = \frac{j}{k\,\rho_0 c_0}\left(\frac{\partial \mathbf{p}}{\partial x}\right) \tag{7.4}$$

becomes

$$\mathbf{u}(x) = \frac{j}{k\,\rho_0 c_0}\left[-j\,k\,\mathbf{A} + j\,k\,\mathbf{B}\right] e^{j\omega t} \tag{7.5}$$

or

$$\mathbf{u}(x) = \frac{1}{\rho_0 c_0}\left[\mathbf{A} - \mathbf{B}\right] e^{j\omega t} \tag{7.6}$$

When the surface is perfectly reflecting, the amplitude $\mathbf{A} = \mathbf{B}$ and the particle velocity is zero at the boundary. Mathematically the reflected particle velocity cancels out the incident particle velocity at $x = 0$.

The ratio of the incident and reflected-pressure amplitudes can be written as a complex amplitude ratio

$$\boldsymbol{r} = \frac{\mathbf{B}}{\mathbf{A}} \tag{7.7}$$

When $\boldsymbol{r} = 1$, Eq. 7.2 can be written as

$$\mathbf{p}(x) = \mathbf{A}\, e^{j\omega t}\left[e^{j\,k\,x} + e^{-j\,k\,x}\right] = 2\,\mathbf{A}\,\cos(k\,x)\, e^{j\omega t} \tag{7.8}$$

which has a real part

$$p(x) = 2\,A\,\cos(k\,x)\,\cos(\omega t + \varphi) \tag{7.9}$$

The corresponding real part of the particle velocity is

$$u(x) = \frac{2\,A}{\rho_0 c_0}\sin(k\,x)\cos\left(\omega t + \varphi - \frac{\pi}{2}\right) \tag{7.10}$$

so the velocity lags the pressure by a 90° phase angle.

Equation 7.8 shows that the pressure amplitude, 2 A at the boundary, is twice that of the incident wave alone. Thus the sound pressure level measured there is 6 dB greater than that of the incident wave measured in free space. Figure 7.3 (Waterhouse, 1955) gives a plot of the behavior of a unit-amplitude plane wave incident on a perfectly reflecting surface at various angles of incidence. Note that since both the incident and reflected waves are included, the sound pressure level of the combined waves at the wall is only 3 dB higher than farther away.

The equations illustrated in Fig. 7.3a describe a standing (frozen) wave, whose pressure peaks and valleys are located at regular intervals away from the wall at a spacing that is related to frequency. The velocity in Fig. 7.3b exhibits a similar behavior. As we have seen, the particle velocity goes to zero at a perfectly reflecting wall. There is a maximum in the particle velocity at a distance $(2n + 1)\,\lambda/4$ away from the wall, where $n = 0, 1, 2$, and so on.

FIGURE 7.3 Interference Patterns When Sound Is Incident on a Plane Reflector from Various Angles (Waterhouse, 1955)

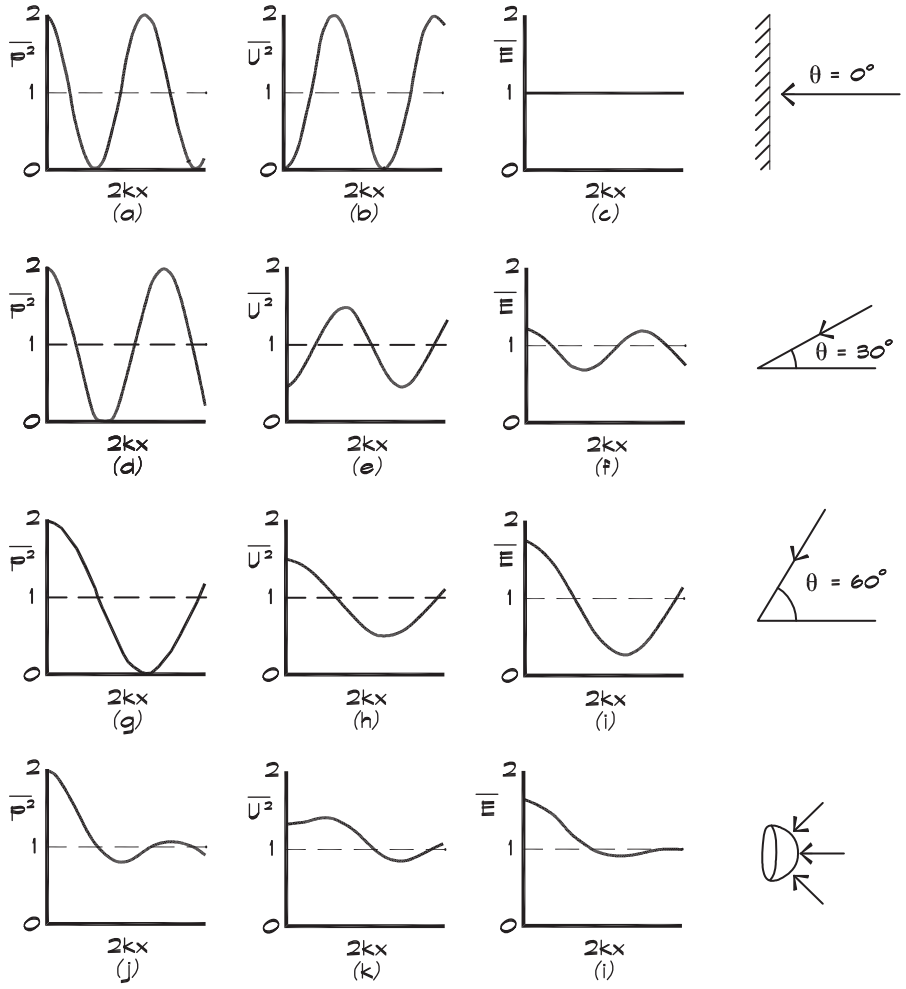

Interference patterns produced when sound is incident on a plane reflector at angles of 0°, 30°, 60°, and from all directions over a hemisphere. $\overline{p^2}$ is the normalized mean squared pressure, k the wave number, and x the distance from the reflector. $\overline{U^2}$ is the normalized mean square velocity and $\overline{E}$ is the normalized mean energy density.

Coherent Reflections—Oblique Incidence

When a plane wave moving in the $-$x direction is incident at an oblique angle as in Fig. 7.4, the incident pressure along the x axis is given by

$$\mathbf{p} = \mathbf{A}\, e^{j\,k\,(x\,\cos\,\theta - y\,\sin\,\theta) + j\,\omega t} \tag{7.11}$$

For a perfectly reflecting surface the combined incident and reflected waves are

$$\mathbf{p} = \mathbf{A}\left[e^{j\,k\,x\cos\,\theta - j\,k\,y\,\sin\,\theta} + e^{-j\,k\,x\,\cos\,\theta - j\,k\,y\,\sin\,\theta}\right] e^{j\,\omega t} \tag{7.12}$$

FIGURE 7.4 Oblique Incidence Reflection

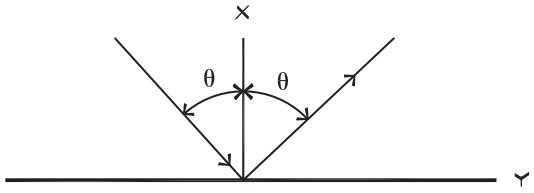

which is

$$\mathbf{p} = 2\,\mathbf{A}\,e^{-j\,k\,y\,\sin\,\theta + j\,\omega\,t}\cos\,(k\,x\,\cos\,\theta) \tag{7.13}$$

and the interference is still sinusoidal but has a longer wavelength. Looking along the x axis, the combined incident and reflected waves produce a pattern, which can be written in terms of the mean-square unit-amplitude pressure wave for perfectly reflecting surface given by

$$\langle \mathbf{p}^2 \rangle = [1 + \cos\,(2\,k\,x\,\cos\,\theta)] \tag{7.14}$$

As the angle of incidence θ increases, the wavelength of the pattern also increases. Figures 7.3a, d, and g show the pressure patterns for angles of incidence of 0°, 30°, and 60°.

Coherent Reflections—Random Incidence

When there is a reverberant field, the sound is incident on a boundary from any direction with equal probability, and the expression in Eq. 7.14 is averaged (integrated) over a hemisphere. This yields

$$\langle \mathbf{p}_r^2 \rangle = [1 + \sin\,(2\,k\,x)/\,2\,k\,x] \tag{7.15}$$

which is plotted in Fig. 7.3j.

The velocity plots in this figure are particularly interesting. Porous sound absorbing materials are most effective when they are placed in an area of high particle velocity. For normal incidence this is at a quarter wavelength from the surface. For off-axis and random incidence the maximum velocity is still at a quarter wavelength; however, there is some positive particle velocity even at the boundary surface that has a component perpendicular to the normal. Thus materials can absorb sound energy even when they are placed close to a reflecting boundary; however, they are more effective, particularly at low frequencies, when located away from the boundary.

Coherent Reflections—Random Incidence, Finite Bandwidth

When the sound is not a simple pure tone, there is a smearing of the peaks and valleys in the pressure and velocity standing waves. Both functions must be integrated over the bandwidth of the frequency range of interest.

$$\langle \mathbf{p}_r^2 \rangle = \left[1 + \frac{1}{k_2 - k_1} \int_{k_1}^{k_2} \frac{\sin\,(2\,k\,x)}{2\,k\,x}\,dk \right] \tag{7.16}$$

FIGURE 7.5 Intensity vs Distance from a Reflecting Wall (Waterhouse, 1955)

Normalized intensity or mean square pressure $\overline{p^2}$ versus distance x of the sound reflected from a solid wall in a reverberant sound field for various bandwidths. In the abscissa $k = (k_1 + k_2) / 2$ where k_1 and k_2 are the wave numbers at the extremes of the band.

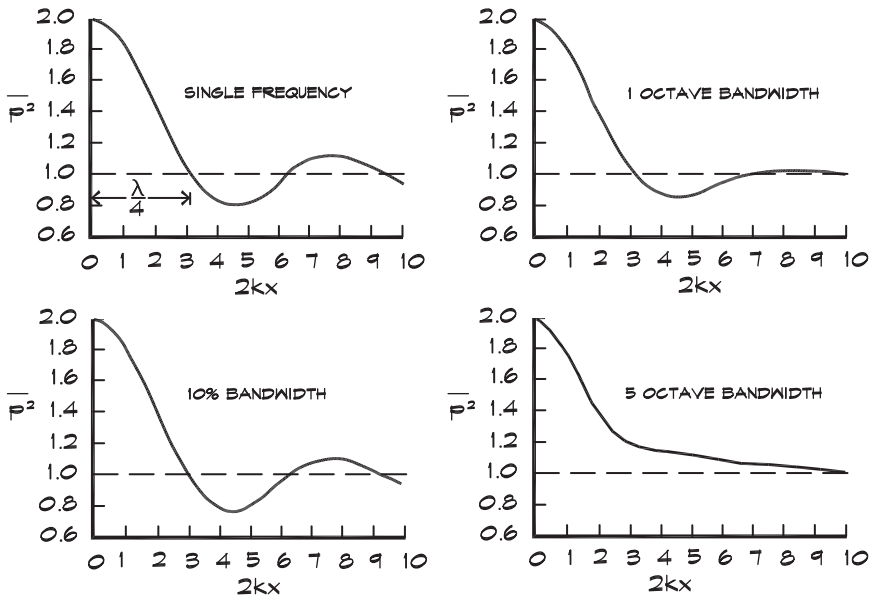

The second term is a well-known tabulated integral. Figure 7.5 shows the result of the integration. Near the wall the mean-square pressure still exhibits a doubling (6 dB increase) and the particle velocity is zero.

7.2 REFLECTIONS FROM FINITE OBJECTS

Scattering from Finite Planes

Reflection from finite planar surfaces is of particular interest in concert hall design, where panels are frequently suspended as "clouds" above the orchestra. Usually these clouds are either flat or slightly convex toward the audience. A convex surface is more forgiving of imperfect alignment since the sound tends to spread out somewhat after reflecting.

If a sound wave is incident on a finite panel, there are several factors that influence the scattered wave. For high frequencies impacting near the center of the panel, the reflection is the same as that which an infinite panel would produce. Near the edge of the panel, diffraction (bending) can occur. Here the reflected amplitude is reduced and the angle of incidence may not be equal to the angle of reflection. At low frequencies, where the wavelength is much larger than the panel, the sound energy simply flows around it like an ocean wave does around a boulder.

Figure 7.6 shows the geometry of a finite reflector having length 2b. When sound impacts the panel at a distance e from the edge, the diffraction attenuation depends on the closeness of the impact point to the edge, compared with the wavelength of sound. The reflected sound field at the receiver is calculated by adding up contributions from all parts of the reflecting surface. The solution of this integral is treated in detail using the

FIGURE 7.6 Geometry of the Reflection from a Finite Panel

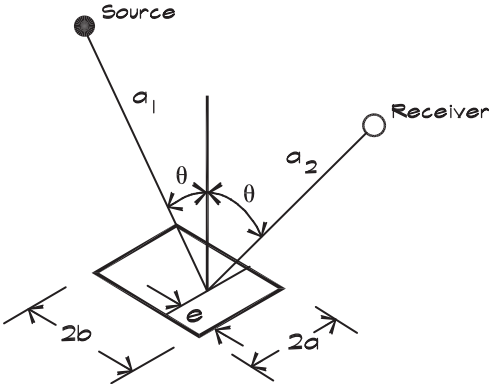

Kirchoff-Fresnel approximation by Leizer (1966) or Ando (1985). The reflected intensity can be expressed as a diffraction coefficient K multiplied times the intensity that would be reflected from a corresponding infinite surface. For a rectangular reflector the attenuation due to diffraction is

$$\Delta L_{dif} = 10 \log K = 10 \log (K_1 K_2) \tag{7.17}$$

where K = diffraction coefficient for a finite panel
K_1 = diffraction coefficient for the x panel dimension
K_2 = diffraction coefficient for the y panel dimension

The orthogonal-panel dimensions can be treated independently. Rindel (1986) gives the coefficient for one dimension

$$K_1 = \frac{1}{2}\left\{\left[C(v_1) + C(v_2)\right]^2 + \left[S(v_1) + S(v_2)\right]^2\right\} \tag{7.18}$$

where

$$v_1 = \sqrt{\frac{\lambda}{2}\left[\frac{1}{a_1} + \frac{1}{a_2}\right]}\, e \cos\theta \tag{7.19}$$

and

$$v_2 = \sqrt{\frac{\lambda}{2}\left[\frac{1}{a_1} + \frac{1}{a_2}\right]}\, (2b - e) \cos\theta \tag{7.20}$$

The terms C and S in Eq. 7.18 are the Fresnel integrals

$$C(v) = \int_0^v \cos\left(\frac{\pi}{2} z^2\right) dz, \quad S(v) = \int_0^v \sin\left(\frac{\pi}{2} z^2\right) dz \tag{7.21}$$

FIGURE 7.7 Attenuation of a Reflection Due to Diffraction (Rindel, 1986)

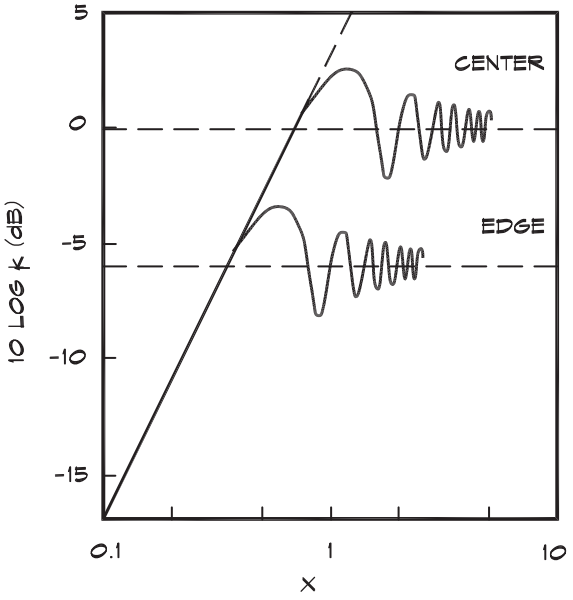

The integration limit v takes on the values of v_1 or v_2 according to the term of interest in Eq. 7.18. For everyday use these calculations are cumbersome. Accordingly we examine approximate solutions appropriate to regions of the reflector.

Rindel (1986) considers the special case of the center of the panel where e = b and $v_1 = v_2 = x$. Then Eq. 7.18 becomes

$$K_{1,\ \text{center}} = 2\left\{[C\ (x)]^2 + [S\ (x)]^2\right\} \tag{7.22}$$

where

$$x = 2b\cos\theta/\sqrt{\lambda\, a^*} \tag{7.23}$$

and the characteristic distance a^* is

$$a^* = 2\, a_1 a_2 / (a_1 + a_2) \tag{7.24}$$

Figure 7.7 gives the value of the diffraction attenuation. At high frequencies where $x > 1$, although there are fluctuations due to the Fresnel zones, a panel approaches zero diffraction attenuation as x increases. At low frequencies ($x < 0.7$) the approximation

$$K_{1,\ \text{center}} \cong 2\, x^2 \quad \text{for} \quad x < 0.7 \tag{7.25}$$

yields a good result.

At the edge of the panel where e = 0, $v_1 = 0$, and $v_2 = 2x$ we can solve for the value of the diffraction coefficient (Rindel, 1986)

$$K_{1,\ \text{edge}} = \frac{1}{2}\left\{[C\ (2x)]^2 + [S\ (2x)]^2\right\} \tag{7.26}$$

which is also shown in Fig. 7.7. The approximations in this case are

$$K_{1,\ \text{edge}} \cong 2\,x^2 \quad \text{for} \quad x \leq 0.35 \tag{7.27}$$

and

$$K_{1,\ \text{edge}} \cong 1/4 \quad \text{for} \quad x > 1 \tag{7.28}$$

Based on these special cases Rindel (1986) divides the panel into three zones according to the nearness to the edge of the impact point

a) $x \leq 0.35$: $K_1 \cong 2\,x^2$, independent of the value of e.

b) $0.35 < x \leq 0.7$: $K_1 \cong \frac{1}{4} + (e/b)\left(2\,x^2 - \frac{1}{4}\right)$, is a linear interpolation between the edge and center values.

c) $x > 0.7$: Here the concept of an edge zone is introduced whose width, e_o, is given by

$$e_o = \frac{b}{x\sqrt{2}} = \frac{1}{\cos\theta}\sqrt{\frac{1}{8}\lambda\, a^*} \tag{7.29}$$

If $e \geq e_o$, then we are in the region of specular reflection. When $e < e_o$, then diffraction attenuation must be considered. Rindel (1986) gives

$$K_1 \cong \begin{cases} 1 & \text{for } e \geq e_o \\ \frac{1}{4} + \frac{3\,e}{4\,e_o} & \text{for } e < e_o \end{cases} \tag{7.30}$$

Figure 7.8 compares these approximate values to those obtained from a more detailed analysis.

Rindel (1986) also cites results of measurements carried out in an anechoic chamber using gated impulses, which are reproduced in Fig. 7.9. He concludes that for values of

FIGURE 7.8 Calculated Values of K_1 (Rindel, 1986)

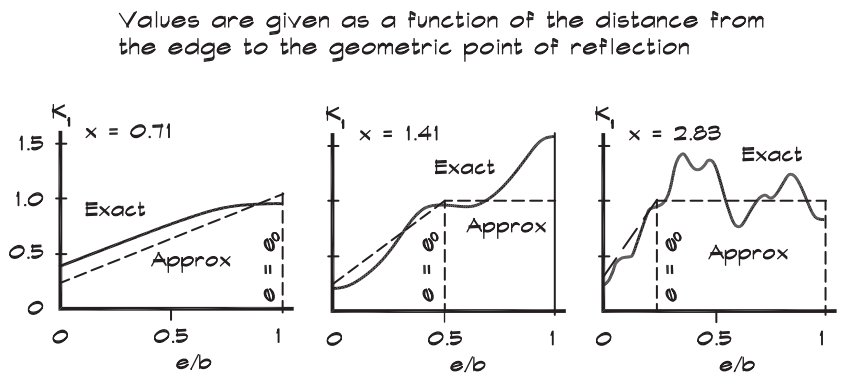

FIGURE 7.9 Measured and Calculated Attenuation of a Sound Reflection from a Square Surface (Rindel, 1986)

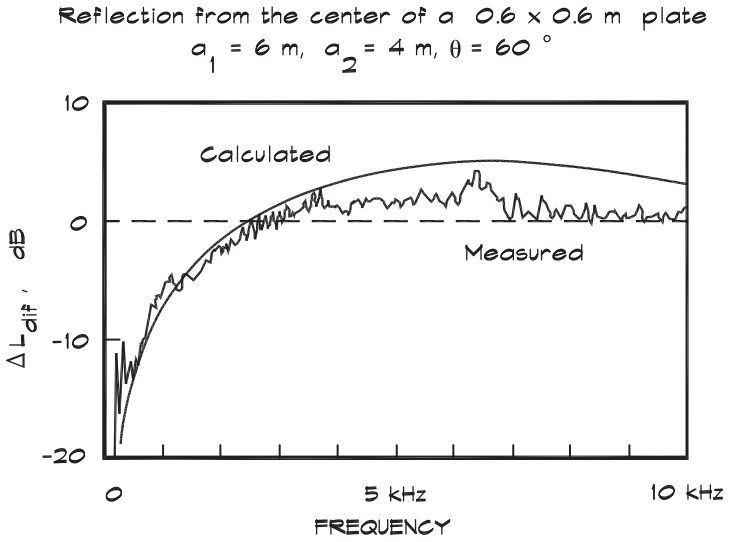

x greater than 0.7, edge diffraction is of minor importance. This corresponds to a limiting frequency

$$f_g > \frac{c\, a^*}{2\, S\, \cos\theta} \tag{7.31}$$

where S is the panel area. For a 2 m square panel the limiting frequency is about 360 Hz for a 45° angle of incidence and a characteristic distance of 6 m, typical of suspended reflectors.

Panel Arrays

When reflecting panels are arrayed as in Fig. 7.10, the diffusion coefficients must account for multipanel scattering. The coefficient in the direction shown is (Finne, 1987 and Rindel, 1990)

$$K_1 = \frac{1}{2}\left\{\sum_{i=1}^{I}\left[C\,(v_{1,i}) - C\,(v_{2,i})\right]^2 + \sum_{i=1}^{I}\left[S\,(v_{1,i}) - S\,(v_{2,i})\right]^2\right\} \tag{7.32}$$

FIGURE 7.10 Section through a Reflector Array with Five Rows of Reflectors (Rindel, 1990)

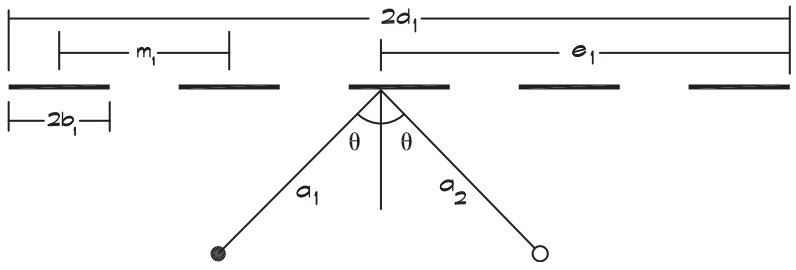

FIGURE 7.11 Simplified Illustration of the Attenuation of Reflections from an Array with Relative Density μ (Rindel, 1990)

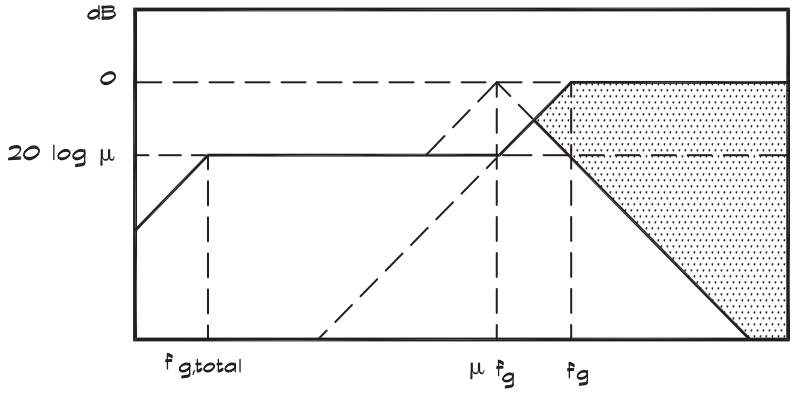

where

$$v_{1,i} = \frac{2}{\sqrt{\lambda\, a^*}}(e_1 - (i-1)\, m_1)\cos\,\theta \tag{7.33}$$

and

$$v_{2,i} = \frac{2}{\sqrt{\lambda\, a^*}}(e_1 - 2b_1 - (i-1)\, m_1)\cos\,\theta \tag{7.34}$$

where i is the running row number and I is the total number of rows in the x-direction.

At high frequencies the v values increase and the reflection is dominated by an individual panel. The single-panel limiting frequency from Eq. 7.31 sets the upper limit for this dependence. At low frequencies the v values decrease, but the reflected vectors combine in phase. The diffusion attenuation becomes dependent on the relative panel area density, μ, (the total array area divided by the total panel area), not the size of the individual reflectors. Figure 7.11 shows a design guide.

The K values are approximately

$$K \cong \mu^2 \quad \text{in the frequency range } f_{g,total} \le f \le \mu f_g \tag{7.35}$$

where the limiting frequency for the total array is given by Eq. 7.31, with the total area of the array used instead of the individual panel area. The shaded area indicates the possible variation depending on whether the sound ray strikes a panel or empty space. Beranek (1992) published relative reflection data based on laboratory tests by Watters et al., (1963), which are shown in Fig. 7.12. In general a large number of small panels is preferable to a few large ones.

Bragg Imaging

Since individual reflectors have to be relatively large to reflect bass frequencies, they are used in groups to improve their low-frequency response (see Leonard, Delsasso, and Knudsen, 1964; or Beranek, 1992). This can be tricky because if they are not arranged in a single plane there can be destructive interference at certain combinations of frequency and angle

FIGURE 7.12 Scattering from Panel Arrays (Beranek, 1992)

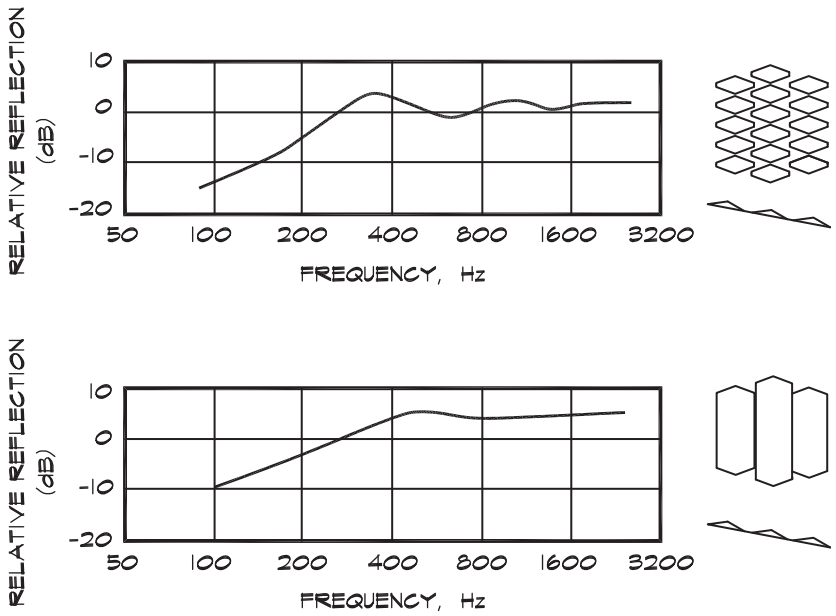

of incidence. When two planes of reflectors are employed, for a given separation distance there is a relationship between the angle of incidence and the frequency of cancellation of the reflected sound. This effect was used by Bragg to study the crystal structure of materials with x-rays. When sound is scattered from two reflecting planes, certain frequencies are missing in the reflected sound. This was one cause of the problems in Philharmonic Hall in New York (Beranek, 1996).

An illustration of this phenomenon, known as Bragg imaging, is shown in Fig. 7.13. When two rows of reflecting panels are placed one above the other, there is destructive interference between reflected sound waves when the combined path-length difference has the relationship

$$2\,\mathrm{d}\,\cos\,\theta = \frac{(2\,\mathrm{n}-1)\,\lambda}{2} \tag{7.36}$$

FIGURE 7.13 Geometry of Bragg Scattering from Rows of Parallel Reflectors

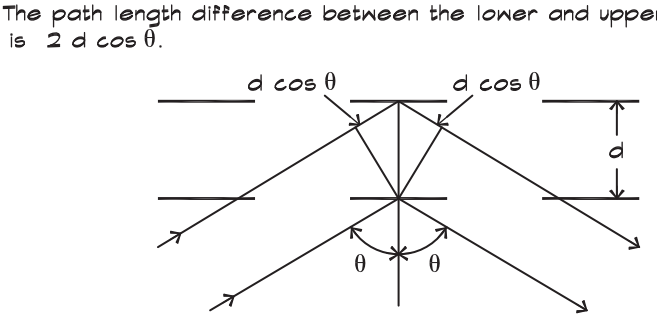

where λ = wavelength of the incident sound (m or ft)
d = perpendicular spacing between rows of reflectors (m or ft)
n = positive integer 1, 2, 3, . . . etc.
θ = angle of incidence and reflection with respect to the normal (rad or deg)

The use of slightly convex reflectors can help diffuse the sound energy and smooth out the interferences; however, stacked planes of reflecting panels can produce a loss of bass energy in localized areas of the audience.

Scattering from Curved Surfaces

When sound is scattered from a curved surface, the curvature induces diffusion of the reflected energy when the surface is convex, or focusing when it is concave. The attenuation associated with the curvature can be calculated using the geometry shown in Fig. 7.14. If we consider a rigid cylinder having a radius R, the loss in intensity is proportional to the ratio of the incident-to-reflected beam areas (Rindel, 1986). At the receiver, M, the sound energy is proportional to the width of the reflected beam tube $(a + a_2)\, d\beta$. If there were no curvature the beam width would be $(a_1 + a_2)\, d\beta_1$ at the image point M_1.

Accordingly the attenuation due to the curvature is

$$\Delta L_{curv} = -10 \log \frac{(a + a_2)\, d\beta}{(a_1 + a_2)\, d\beta_1} = -10 \log \frac{(a + a_2)(d\beta/d\beta_1)}{(a_1 + a_2)} \tag{7.37}$$

Using Fig. 7.14 we see that $a\, d\beta = a_1\, d\beta_1 = R\, d\phi \cos\theta$, and that $d\beta = d\beta_1 + 2\, d\phi$, from which it follows that

$$\frac{d\beta}{d\beta_1} = 1 + \frac{2\, a_1}{R \cos\theta} \tag{7.38}$$

and plugging this into Eq. 7.37 yields

$$\Delta L_{curv} = -10 \log \left| 1 + \frac{a^*}{R \cos\theta} \right| \tag{7.39}$$

where a^* is given in Eq. 7.24. For concave surfaces the same equation can be used with a negative value for R. Figure 7.15 shows the results for both convex and concave surfaces.

FIGURE 7.14 Geometry of the Reflection from a Curved Surface (Rindel, 1986)

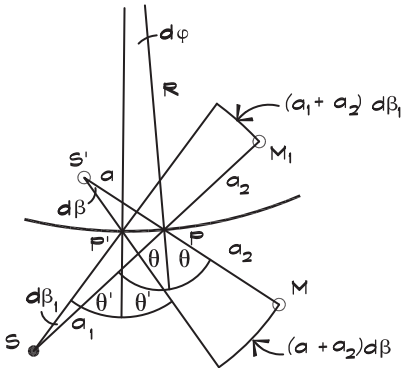

FIGURE 7.15 Attenuation or Gain Due to Curvature (Rindel, 1985)

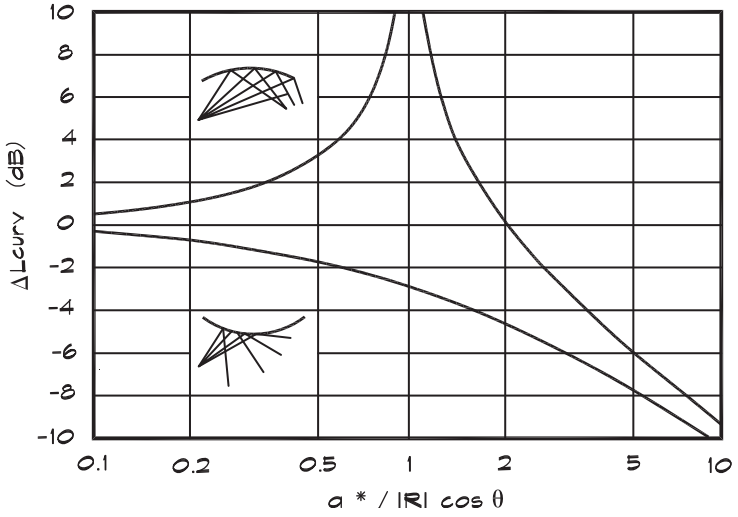

FIGURE 7.16 Calculated and Measured Values of ΔL_{curv} (Rindel, 1985)

Sketch				
Radius R	2.0 m	0.5 m	-2.0 m	-0.5 m
a * / R cos θ	0.5	2.0	0.5	-2.0
ΔL_{curv} (calc.)	-1.8 dB	-4.8 dB	3.0 dB	0.0 dB
ΔL_{curv} (meas.)	-2 ± 0.5 dB	-5 ± 1 dB	3 ± 1 dB	-1 ± 2 dB

This analysis assumes that both the source and the receiver are in a plane whose normal is the axis of the cylinder. If this is not the case, both a* and θ must be deduced from a normal projection onto that plane (Rindel, 1985). Where there is a double-curved surface with two radii of curvature, the attenuation term must be applied twice, using the appropriate projections onto the two normal planes of the surface.

Figure 7.16 gives the results of measurements using TDS on a small (1.4 m × 1.0 m) curved panel at a distance of 1 m for a zero angle of incidence over a frequency range of 3 to 19 kHz. The data also show the variation in the measured values, which Rindel (1985) attributes to diffraction effects.

Combined Effects

When sound is reflected from finite curved panels, the combined effects of distance, absorption, size, and curvature must be included. For an omnidirectional source, the level of the reflected sound relative to the direct sound is

$$L_{refl} - L_{dir} = \Delta L_{dist} + \Delta L_{abs} + \Delta L_{dif} + \Delta L_{curv} \tag{7.40}$$

where the absorption term will be addressed later in this chapter, and the distance term is

$$\Delta L_{dist} = 20 \log \frac{a_0}{a_1 + a_2} \tag{7.41}$$

The other terms have been treated earlier.

Whispering Galleries

If a source of sound is located in a circular space, very close to the outside wall, some of the sound rays strike the surface at a shallow angle and are reflected again and again, and so propagate within a narrow band completely around the room. A listener located on the opposite side of the space can clearly hear conversations that occur close to the outside wall. This phenomenon, which is called a whispering gallery since even whispered conversations are audible, occurs in circular or domed spaces such as the statuary gallery in the Capital building in Washington, DC.

7.3 ABSORPTION

Reflection and Transmission Coefficients

When sound waves interact with real materials the energy contained in the incident wave is reflected, transmitted through the material, and absorbed within the material. The surfaces treated in this model are generally planar, although some curvature is tolerated as long as the radius of curvature is large when compared to a wavelength. The energy balance is illustrated in Fig. 7.17.

$$E_i = E_r + E_t + E_a \tag{7.42}$$

Since this analysis involves only the interaction at the boundary of the material, the difference between absorption, where energy is converted to heat, and transmission, where energy passes through the material, is not relevant. Both mechanisms are absorptive from the standpoint of the incident side because the energy is not reflected. Because we are only interested in the incident side of the boundary, we can combine the transmitted and

FIGURE 7.17 Interaction of Sound Waves with a Surface

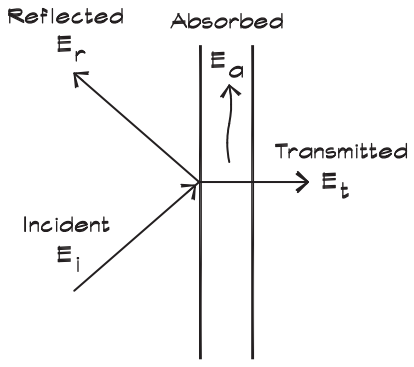

absorbed energies. If we divide Eq. 7.42 by E_i,

$$1 = \frac{E_r}{E_i} + \frac{E_{t+a}}{E_i} \tag{7.43}$$

We can express each energy ratio as a coefficient of reflection or transmission. The fraction of the incident energy that is absorbed (or transmitted) at the surface boundary is the coefficient

$$\alpha_\theta = \frac{E_{t+a}}{E_i} \tag{7.44}$$

and the reflection coefficient is

$$\alpha_r = \frac{E_r}{E_i} \tag{7.45}$$

Substituting these coefficients into Eq. 7.43,

$$1 = \alpha_\theta + \alpha_r \tag{7.46}$$

The reflection coefficient can be expressed in terms of the complex reflection amplitude ratio $\boldsymbol{r}$ for pressure that was defined in Eq. 7.7

$$\alpha_r = \boldsymbol{r}^2 \tag{7.47}$$

and the absorption coefficient is

$$\alpha_\theta = 1 - \boldsymbol{r}^2 \tag{7.48}$$

The reflected energy is

$$E_r = (1 - \alpha_\theta)E_i \tag{7.49}$$

Impedance Tube Measurements

When a plane wave is normally incident on the boundary between two materials, 1 and 2, we can calculate the strength of the reflected wave from a knowledge of their impedances. (This solution was published by Rayleigh in 1896.) Following the approach taken in Eq. 7.3, the sound pressure from the incident and reflected waves is written as

$$\mathbf{p}(x) = \mathbf{A}\, e^{j(\omega t - k x)} + \mathbf{B}\, e^{j(\omega t + k x)} \tag{7.50}$$

If we square and average this equation, we obtain the mean-squared acoustic pressure of a normally incident and reflected wave (Pierce, 1981)

$$\langle \mathbf{p}^2 \rangle = \frac{1}{2}\mathbf{A}^2\left[1 + |\boldsymbol{r}^2| + 2|\boldsymbol{r}|\cos(2kx + \delta_r)\right] \tag{7.51}$$

where δ_r is the phase of $\boldsymbol{r}$. Equation 7.51 describes a standing wave and gives a method for measuring the normal-incidence absorption coefficient of a material placed in the end of a tube, called an *impedance tube*, pictured in Fig. 7.18.

FIGURE 7.18 Impedance Tube Measurements of the Absorption Coefficient

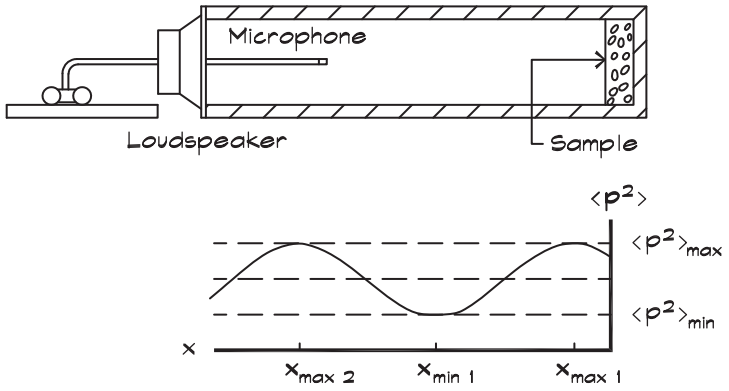

An incident and reflected wave combine to produce a standing wave in a tube. The pressure maximum and minimum are measured and their ratio determines the impedance.

The maximum value of the mean-squared pressure is $\frac{1}{2}\,\mathbf{A}^2\,[1 + |\,\boldsymbol{r}\,|]^2$, which occurs whenever $2\,\mathrm{k}\,\mathrm{x} + \delta_\mathrm{r}$ is an even multiple of π. The minimum is $\frac{1}{2}\,\mathbf{A}^2\,[1 - |\,\boldsymbol{r}\,|]^2$, which occurs at odd multiples of π. The ratio of the maximum-to-minimum pressures is an easily measured quantity called the *standing wave ratio*, s, which is usually obtained from its square

$$\mathrm{s}^2 = \frac{\langle \mathbf{p}^2 \rangle_{\max}}{\langle \mathbf{p}^2 \rangle_{\min}} = \left| \frac{\mathbf{A} + \mathbf{B}}{\mathbf{A} - \mathbf{B}} \right|^2 = \frac{[1 + |\,\boldsymbol{r}\,|]^2}{[1 - |\,\boldsymbol{r}\,|]^2} \tag{7.52}$$

The phase angle is

$$\delta_\mathrm{r} = -2\,\mathrm{k}\,\mathrm{x}_{\mathrm{max}\ 1} + 2\,\mathrm{m}\,\pi = -2\,\mathrm{k}\,\mathrm{x}_{\mathrm{min}\ 1} + (2\,\mathrm{n} + 1)\,\pi \tag{7.53}$$

where $\mathrm{x}_{\mathrm{min}\ 1}$ is the smallest distance to a minimum and $\mathrm{x}_{\mathrm{max}\ 1}$ is the smallest distance to a maximum, measured from the surface of the material. The numbers m and n are arbitrary integers, which do not affect the relative phase. Equation 7.52 can be solved for the magnitude and phase of the reflection amplitude ratio

$$\boldsymbol{r} = |\,\boldsymbol{r}\,|\,\mathrm{e}^{\mathrm{j}\,\delta_\mathrm{r}} \tag{7.54}$$

from which the normal incidence material impedance can be obtained.

$$\mathbf{z}_\mathrm{n} = \rho_0 \mathrm{c}_0 \frac{(1 + \boldsymbol{r})}{(1 - \boldsymbol{r})} \tag{7.55}$$

Oblique Incidence Reflections—Finite Impedance

When sound is obliquely incident on a surface having a finite impedance, the pressure of the incident and reflected waves is given by

$$\mathbf{p} = \mathbf{A}\left[\mathrm{e}^{\mathrm{j}\,\mathrm{k}\,(\mathrm{x}\,\cos\theta - \mathrm{y}\sin\theta)} + \boldsymbol{r}\,\mathrm{e}^{-\mathrm{j}\,\mathrm{k}\,(\mathrm{x}\cos\theta + \mathrm{y}\sin\theta)}\right] \tag{7.56}$$

and the velocity in the x direction at the boundary (x = 0) using Eq. 6.31 is

$$\mathbf{u}(\mathrm{x}) = \frac{\mathbf{A}}{\rho_0 \mathrm{c}_0}\left[\cos\theta\, \mathrm{e}^{-\mathrm{j\,k\,y\,\sin\theta}} - \boldsymbol{r}\cos\theta\, \mathrm{e}^{-\mathrm{j\,k\,y\,\sin\theta}}\right] \tag{7.57}$$

The normal specific acoustic impedance, expressed as the ratio of the pressure to the velocity at the surface is

$$\mathbf{z}_\mathrm{n} = \left(\frac{\mathbf{p}}{\mathbf{u}_\mathrm{x}}\right)_{\mathrm{x}=0} = \frac{\rho_0 \mathrm{c}_0}{\cos\theta}\frac{(1+\boldsymbol{r})}{(1-\boldsymbol{r})} \tag{7.58}$$

The reflection coefficient can then be written in terms of the boundary's specific acoustic impedance

$$\boldsymbol{r} = \frac{\mathbf{z} - \rho_0 \mathrm{c}_0}{\mathbf{z} + \rho_0 \mathrm{c}_0} \tag{7.59}$$

where $\mathbf{z} = \mathbf{z}_\mathrm{n}\cos\theta$ and $\mathbf{z}_\mathrm{n} = w_\mathrm{n} + \mathrm{j}\, x_\mathrm{n}$
$\mathbf{z}$ = complex specific acoustic impedance
= (pressure or force) / (particle or volume velocity)
w = specific acoustic resistance or real part of the impedance
x = specific acoustic reactance or the imaginary part of the impedance
- when positive it is mass like and when negative it is stiffness like
$\rho_0 \mathrm{c}_0$ = characteristic acoustic resistance of the incident medium
(about 412 Ns/m ^{3} - mks rayls in air)
$\mathrm{j} = \sqrt{-1}$

Now these relationships contain a good deal of information about the reflection process. When $|\mathbf{z}| \gg \rho_0 \mathrm{c}_0$ the reflection coefficient approaches a value of + 1, there is perfect reflection, and the reflected wave is in phase with the incident wave. If $|\mathbf{z}| \ll \rho_0 \mathrm{c}_0$, the boundary is resilient like the open end of a tube, and the value of $\boldsymbol{r}$ approaches −1. Here the reflected wave is 180° out of phase with the incident wave and there is cancellation. When $|\mathbf{z}| = \rho_0 \mathrm{c}_0$, no sound is reflected.

For any finite value of $\mathbf{z}_\mathrm{n}$, as θ approaches $\pi/2$, the incident wave grazes over the boundary and the value of $\boldsymbol{r}$ approaches − 1. Under this condition the incident and reflected waves are out of phase and interfere with one another. This is an explanation of the ground effect, which was discussed previously. Note that in both cases—that is, when $\boldsymbol{r}$ is either ± 1—there is no sound absorption by the surface. The $|\boldsymbol{r}| = -1$ case is rarely encountered in architectural acoustics and only over limited frequency ranges (Kuttruff, 1973).

Reflection and transmission coefficients can also be written in terms of the normal acoustic impedance of a material. The energy reflection coefficient using Eq. 7.59 is

$$\alpha_\mathrm{r} = \left|\frac{\left(\mathbf{z}_\mathrm{n}/\rho_0 \mathrm{c}_0\right)\cos\theta - 1}{\left(\mathbf{z}_\mathrm{n}/\rho_0 \mathrm{c}_0\right)\cos\theta + 1}\right|^2 \tag{7.60}$$

and in terms of the real and imaginary components of the impedance,

$$\alpha_r = \frac{\left(w_n \cos\theta - \rho_0 c_0\right)^2 + x_n^2 \cos^2\theta}{\left(w_n \cos\theta + \rho_0 c_0\right)^2 + x_n^2 \cos^2\theta} \tag{7.61}$$

The absorption coefficient is set equal to the absorption/transmission coefficient given in Eq. 7.44, since it is defined at a surface where it does not matter whether the energy is transmitted through the material or absorbed within the material, as long as it is not reflected back. The specular absorption coefficient is

$$\alpha_\theta = 1 - \left| \frac{\left(\mathbf{z}_n/\rho_0 c_0\right)\cos\theta - 1}{\left(\mathbf{z}_n/\rho_0 c_0\right)\cos\theta + 1} \right|^2 \tag{7.62}$$

which in terms of its components is

$$\alpha_\theta = \frac{4\,\rho_0 c_0 w_n \cos\theta}{\left(w_n \cos\theta + \rho_0 c_0\right)^2 + x_n^2 \cos^2\theta} \tag{7.63}$$

For most architectural situations the incident conducting medium is air; however, it could be any material with a characteristic resistance. Since solid surfaces such as walls or absorptive panels have a resistance $w_n \gg \rho_0 c_0$, the magnitude of the absorption coefficient yields a maximum value when $w_n \cos\theta_i = \rho_0 c_0$. For normal incidence, when $\mathbf{z}_n = \rho_0 c_0$, the transmission coefficient is unity as we would expect.

Figure 7.19 shows the behavior of a typical absorption coefficient with angle of incidence. As the angle of incidence increases, the apparent depth of the material increases, thereby increasing the absorption. At very high angles of incidence there is no longer a velocity component into the material so the coefficient drops off rapidly.

FIGURE 7.19 Absorption Coefficient as a Function of Angle of Incidence for a Porous Absorber (Benedetto and Spagnolo, 1985)

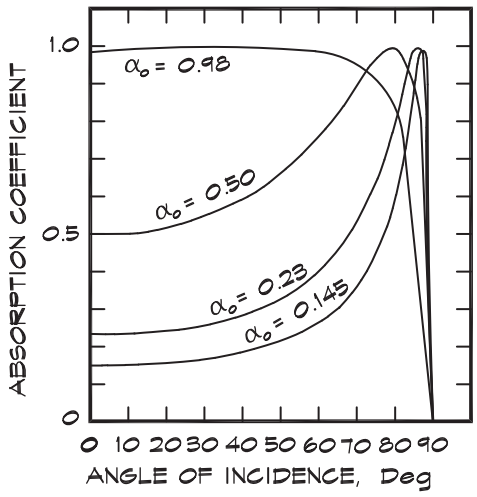

FIGURE 7.20 Geometry of the Diffuse Field Absorption Coefficient Calculation (Cremer et al., 1982)

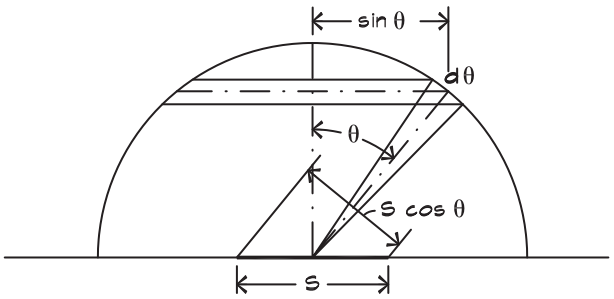

Calculated Diffuse Field Absorption Coefficients

In Eq. 7.63 we saw that we could write the absorption coefficient as a function of the angle of incidence, in terms of the complex impedance. Although direct-field absorption coefficients are useful for gaining an understanding of the physics of the absorption process, for most architectural applications a measurement is made of the diffuse-field absorption coefficient. Recall that a diffuse field implies that incident sound waves come from any direction with equal probability. The diffuse-field absorption coefficient is the average of the coefficient α_θ, taken over all possible angles of incidence. The geometry is shown in Fig. 7.20. The energy from a uniformly radiating hemisphere that is incident on the surface **S** is proportional to the area that lies between the angle $\theta - \Delta\theta/2$ and $\theta + \Delta\theta/2$. The fraction of the total energy coming from this angle is

$$\frac{\mathrm{dE}}{\mathrm{E}} = \frac{2\pi \mathrm{r} \sin\theta \, \mathrm{r} \, \mathrm{d}\theta}{4\pi \mathrm{r}^2} = \frac{1}{2} \sin\theta \, \mathrm{d}\theta \tag{7.64}$$

and the total power sound absorbed by a projected area S cos θ is

$$\mathrm{W} = \mathrm{E}\,\mathrm{c}\,\mathrm{S} \int_0^{\pi/2} \alpha_\theta \sin\theta \quad \cos\theta \, \mathrm{d}\theta \tag{7.65}$$

The total incident power from all angles is the value of Eq. 7.65, with a perfectly absorptive material ($\alpha_\theta = 1$). The average absorption coefficient is the ratio of the absorbed to the total power

$$\alpha = \frac{\int_0^{\pi/2} \alpha_\theta \sin\theta \quad \cos\theta \, \mathrm{d}\theta}{\int_0^{\pi/2} \sin\theta \quad \cos\theta \, \mathrm{d}\theta} \tag{7.66}$$

which can be simplified to (Paris, 1928)

$$\alpha = 2 \int_0^{\pi/2} \alpha_\theta \sin\theta \quad \cos\theta \, \mathrm{d}\theta \tag{7.67}$$

Here the sine term is the probability that energy will originate at a given angle and the cosine term is the projection of the receiving area.

Measurement of Diffuse Field Absorption Coefficients

Although diffuse-field absorption coefficients can be calculated from impedance tube data, more often they are measured directly in a reverberant space. Values of α are published for a range of frequencies between 125 Hz and 4 kHz. Each coefficient represents the diffuse-field absorption averaged over a band of frequencies one octave wide. Occasionally absorption data are required for calculations beyond this range. In these cases estimates can be made from impedance tube data, by extrapolation from known data, or by calculating the values from first principles.

Some variability arises in the measurement of the absorption coefficient. The diffuse-field coefficient is, in theory, always less than or equal to a value of one. In practice, when the reverberation time method discussed in Chapt. 8, is employed, values of α greater than 1 are sometimes measured. This normally is attributed to diffraction, the lack of a perfectly diffuse field in the measuring room, and edge conditions. At low frequencies diffraction seems to be the main cause (Beranek, 1971). Since it is easier and more consistent to measure the absorption using the reverberation time method, this is the value that is found in the published literature.

Diffuse-field measurements of the absorption coefficient are carried out in a reverberation chamber, which is a room with little or no absorption. Data are taken with and without the panel under test in the room and the resulting reverberation times are used to calculate the absorptive properties of the material. The test standard, ASTM C423, specifies several mountings as shown in Fig 7.21. Mountings A, B, D, and E are used for most prefabricated products. Mounting F is for duct liners and C is used for specialized applications. When data are reported, the test mounting method must also be included since the airspace behind the material greatly affects the results. The designation E-400, for example, indicates that mounting E was used and there was a 400 mm (16”) airspace behind the test sample.

Noise Reduction Coefficient (NRC)

Absorptive materials, such as acoustical ceiling tile, wall panels, and other porous absorbers are often characterized by their noise reduction coefficient, which is the average diffuse field absorption coefficient over the speech frequencies, 250 Hz to 2 kHz, rounded to the nearest 0.05.

$$\mathrm{NRC} = \frac{1}{4}\left(\alpha_{250} + \alpha_{500} + \alpha_{1\,\mathrm{k}} + \alpha_{2\,\mathrm{k}}\right) \tag{7.68}$$

Although these single-number metrics are useful as a means of getting a general idea of the effectiveness of a particular material, for critical applications calculations should be carried out over the entire frequency range of interest.

Absorption Data

Table 7.1 shows a representative sample of measured absorption data. The list is by no means complete but care has been taken to include a reasonable sample of different types of materials. When layering materials or when using them in a manner that is not representative

FIGURE 7.21 Laboratory Absorption Test Mountings

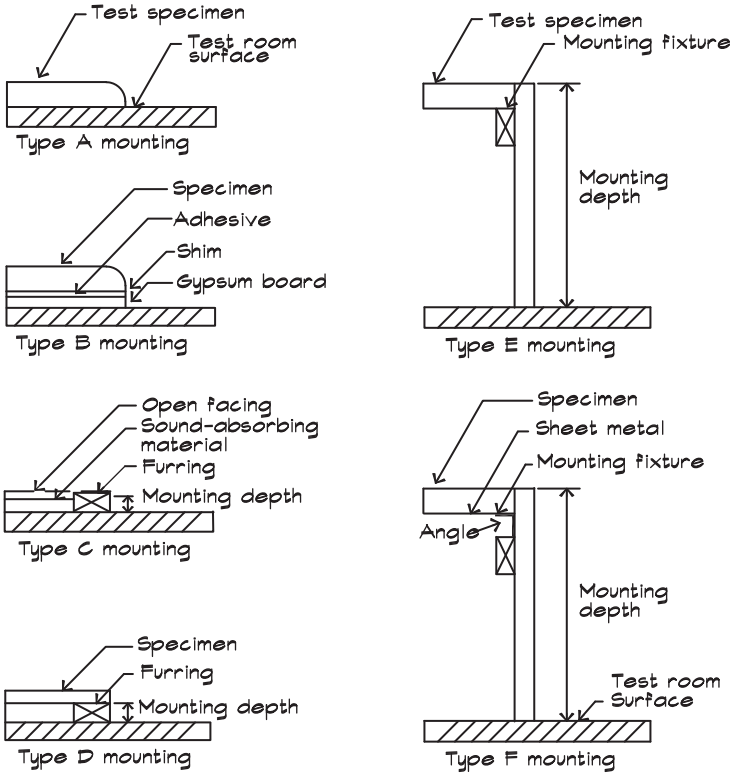

of the measured data, some adjustments may have to be made to account for different air cavity depths or mounting methods.

Occasionally it is necessary to estimate the absorption of materials beyond the range of measured data. Most often this occurs in the 63 Hz octave band, but sometimes occurs at lower frequencies. Data generally are not measured in this frequency range because of the size of reverberant chamber necessary to meet the diffuse field requirements. In these cases it is particularly important to consider the contributions to the absorption of the structural elements behind any porous panels.

Layering Absorptive Materials

It is the rule rather than the exception that acoustical materials are layered in real applications. For example a 25 mm (1 in) thick cloth-wrapped fiberglass material might be applied over a 16 mm (5/8 in) thick gypsum board wall. A detailed mathematical analysis of the impedance of the composite material is beyond the scope of a typical architectural project, and when one seeks the absorption coefficient from tables such as those in Table 7.1, one finds data on the panel, tested in an A-mounting condition, and data on the gypsum board wall, but no data on the combination.

If the panel data were used without consideration of the backing, the listed value at 125 Hz would suggest that there would be a decrease in absorption from the application of the panel relative to the drywall alone. This is due to the lower absorption coefficient that comes about from the test mounting method (on concrete), rather than from the panel itself.

TABLE 7.1 Absorption Coefficients of Common Materials

Material	Mount	Frequency, Hz					
		125	250	500	1k	2k	4k
Walls							
Glass, 1/4", heavy plate		0.18	0.06	0.04	0.05	0.02	0.02
Glass, 3/32", ordinary window		0.55	0.25	0.18	0.12	0.07	0.04
Gypsum board, 1/2", on 2×4 studs		0.29	0.10	0.05	0.04	0.07	0.09
Plaster, 7/8", gypsum or lime, on brick		0.013	0.015	0.02	0.03	0.04	0.05
Plaster, on concrete block		0.12	0.09	0.07	0.05	0.05	0.04
Plaster, 7/8", on lath		0.14	0.10	0.06	0.04	0.04	0.05
Plaster, 7/8", lath on studs		0.30	0.15	0.10	0.05	0.04	0.05
Plywood, 1/4", 3" air space, 1" batt,		0.60	0.30	0.10	0.09	0.09	0.09
Soundblox, type B, painted		0.74	0.37	0.45	0.35	0.36	0.34
Wood panel, 3/8", 3-4" air space		0.30	0.25	0.20	0.17	0.15	0.10
Concrete block, unpainted		0.36	0.44	0.51	0.29	0.39	0.25
Concrete block, painted		0.10	0.05	0.06	0.07	0.09	0.08
Concrete poured, unpainted		0.01	0.01	0.02	0.02	0.02	0.03
Brick, unglazed, unpainted		0.03	0.03	0.03	0.04	0.05	0.07
Wood paneling, 1/4",		0.42	0.21	0.10	0.08	0.06	0.06
with airspace behind							
Wood, 1", paneling with airspace behind		0.19	0.14	0.09	0.06	0.06	0.05
Shredded-wood fiberboard, 2", on concrete	A	0.15	0.26	0.62	0.94	0.64	0.92
Carpet, heavy, on 5/8-in perforated mineral fiberboard		0.37	0.41	0.63	0.85	0.96	0.92
Brick, unglazed, painted	A	0.01	0.01	0.02	0.02	0.02	0.03
Light velour, 10 oz per sq yd, hung straight, in contact with wall		0.03	0.04	0.11	0.17	0.24	0.35
Medium velour, 14 oz per sq yd, draped to half area		0.07	0.31	0.49	0.75	0.70	0.60
Heavy velour, 18 oz per sq yd, draped to half area		0.14	0.35	0.55	0.72	0.70	0.65

continued

TABLE 7.1 Absorption Coefficients of Common Materials, (*Continued*)

Material	Mount	Frequency, Hz					
		125	250	500	1k	2k	4k
Floors							
Floors, concrete or terrazzo	A	0.01	0.01	0.015	0.02	0.02	0.02
Floors, linoleum, vinyl on concrete	A	0.02	0.03	0.03	0.03	0.03	0.02
Floors, linoleum, vinyl on subfloor		0.02	0.04	0.05	0.05	0.10	0.05
Floors, wooden		0.15	0.11	0.10	0.07	0.06	0.07
Floors, wooden platform w/airspace		0.40	0.30	0.20	0.17	0.15	0.10
Carpet, heavy on concrete	A	0.02	0.06	0.14	0.57	0.60	0.65
Carpet, on 40 oz (1.35 kg/sq m) pad	A	0.08	0.24	0.57	0.69	0.71	0.73
Indoor-outdoor carpet	A	0.01	0.05	0.10	0.20	0.45	0.65
Wood parquet in asphalt on concrete	A	0.04	0.04	0.07	0.06	0.06	0.07
Ceilings							
Acoustical coating K-13, 1”	A	0.08	0.29	0.75	0.98	0.93	0.96
1.5”	A	0.16	0.50	0.95	1.06	1.00	0.97
2”	A	0.29	0.67	1.04	1.06	1.00	0.97
Acoustical coating K-13 “fc” 1”	A	0.12	0.38	0.88	1.16	1.15	1.12
Glass-fiber roof fabric, 12 oz/yd		0.65	0.71	0.82	0.86	0.76	0.62
Glass-fiber roof fabric, 37.5 oz/yd		0.38	0.23	0.17	0.15	0.09	0.06
Acoustical Tile							
Standard mineral fiber, 5/8”	E400	0.68	0.76	0.60	0.65	0.82	0.76
Standard mineral fiber, 3/4”	E400	0.72	0.84	0.70	0.79	0.76	0.81
Standard mineral fiber, 1”	E400	0.76	0.84	0.72	0.89	0.85	0.81
Energy mineral fiber, 5/8”	E400	0.70	0.75	0.58	0.63	0.78	0.73
Energy mineral fiber, 3/4”	E400	0.68	0.81	0.68	0.78	0.85	0.80
Energy mineral fiber, 1”	E400	0.74	0.85	0.68	0.86	0.90	0.79
Film faced fiberglass, 1”	E400	0.56	0.63	0.69	0.83	0.71	0.55
Film faced fiberglass, 2”	E400	0.52	0.82	0.88	0.91	0.75	0.55
Film faced fiberglass, 3”	E400	0.64	0.88	1.02	0.91	0.84	0.62

continued

TABLE 7.1 Absorption Coefficients of Common Materials, (*Continued*)

Material	Mount	Frequency, Hz					
		125	250	500	1k	2k	4k
Glass Cloth Acoustical Ceiling Panels							
Fiberglass tile, 3/4”	E400	0.74	0.89	0.67	0.89	0.95	1.07
Fiberglass tile, 1”	E400	0.77	0.74	0.75	0.95	1.01	1.02
Fiberglass tile, 1 1/2”	E400	0.78	0.93	0.88	1.01	1.02	1.00
Seats and Audience							
Audience in upholstered seats		0.39	0.57	0.80	0.94	0.92	0.87
Unoccupied well-upholstered seats		0.19	0.37	0.56	0.67	0.61	0.59
Unoccupied leather covered seats		0.19	0.57	0.56	0.67	0.61	0.59
Wooden pews, occupied		0.57	0.44	0.67	0.70	0.80	0.72
Leather-covered upholstered seats, unoccupied		0.44	0.54	0.60	0.62	0.58	0.50
Congregation, seated in wooden pews		0.57	0.61	0.75	0.86	0.91	0.86
Chair, metal or wood seat, unoccupied		0.15	0.19	0.22	0.39	0.38	0.30
Students, informally dressed, seated in tablet-arm chairs		0.30	0.41	0.49	0.84	0.87	0.84
Duct Liners							
1/2”		0.11	0.51	0.48	0.70	0.88	0.98
1”		0.16	0.54	0.67	0.85	0.97	1.01
1 1/2”		0.22	0.73	0.81	0.97	1.03	1.04
2”		0.33	0.90	0.96	1.07	1.07	1.09
Aeroflex Type 150, 1”	F	0.13	0.51	0.46	0.65	0.74	0.95
Aeroflex Type 150, 2”	F	0.25	0.73	0.94	1.03	1.02	1.09
Aeroflex Type 200, 1/2”	F	0.10	0.44	0.29	0.39	0.63	0.81
Aeroflex Type 200, 1”	F	0.15	0.59	0.53	0.78	0.85	1.00
Aeroflex Type 200, 2”	F	0.28	0.81	1.04	1.10	1.06	1.09
Aeroflex Type 300, 1/2”	F	0.09	0.43	0.31	0.43	0.66	0.98
Aeroflex Type 300, 1”	F	0.14	0.56	0.63	0.82	0.99	1.04
Aeroflex Type 150, 1”	A	0.06	0.24	0.47	0.71	0.85	0.97
Aeroflex Type 150, 2”	A	0.20	0.51	0.88	1.02	0.99	1.04
Aeroflex Type 300, 1”	A	0.08	0.28	0.65	0.89	1.01	1.04

continued

TABLE 7.1 Absorption Coefficients of Common Materials, (*Continued*)

Material	Mount	Frequency, Hz					
		125	250	500	1k	2k	4k
Building Insulation - Fiberglass							
3.5" (R-11) (insulation exposed to sound)	A	0.34	0.85	1.09	0.97	0.97	1.12
6" (R-19) (insulation exposed to sound)	A	0.64	1.14	1.09	0.99	1.00	1.21
3.5" (R11) (FRK facing exposed to sound)	A	0.56	1.11	1.16	0.61	0.40	0.21
6" (R-19) (FRK facing exposed to sound)	A	0.94	1.33	1.02	0.71	0.56	0.39
Fiberglass Board (FB)							
FB, 3lb/ft^3, 1" thick	A	0.03	0.22	0.69	0.91	0.96	0.99
FB, 3 lb/ft^3, 2" thick	A	0.22	0.82	1.21	1.10	1.02	1.05
FB, 3 lb/ft^3, 3" thick	A	0.53	1.19	1.21	1.08	1.01	1.04
FB, 3 lb/ft^3, 4" thick	A	0.84	1.24	1.24	1.08	1.00	0.97
FB, 3 lb/ft^3, 1" thick	E400	0.65	0.94	0.76	0.98	1.00	1.14
FB, 3 lb/ft^3, 2" thick	E400	0.66	0.95	1.06	1.11	1.09	1.18
FB, 3 lb/ft^3, 3" thick	E400	0.66	0.93	1.13	1.10	1.11	1.14
FB, 3 lb/ft^3, 4" thick	E400	0.65	1.01	1.20	1.14	1.10	1.16
FB, 6 lb/ft^3, 1" thick	A	0.08	0.25	0.74	0.95	0.97	1.00
FB, 6 lb/ft^3, 2" thick	A	0.19	0.74	1.17	1.11	1.01	1.01
FB, 6 lb/ft^3, 3" thick	A	0.54	1.12	1.23	1.07	1.01	1.05
FB, 6 lb/ft^3, 4" thick	A	0.75	1.19	1.17	1.05	0.97	0.98
FB, 6 lb/ft^3, 1" thick	E400	0.68	0.91	0.78	0.97	1.05	1.18
FB, 6 lb/ft^3, 2" thick	E400	0.62	0.95	0.98	1.07	1.09	1.22
FB, 6 lb/ft^3, 3" thick	E400	0.66	0.92	1.11	1.12	1.10	1.19
FB, 6 lb/ft^3, 4" thick	E400	0.59	0.91	1.15	1.11	1.11	1.19
FB, FRK faced, 1" thick	A	0.12	0.74	0.72	0.68	0.53	0.24
FB, FRK faced, 2" thick	A	0.51	0.65	0.86	0.71	0.49	0.26
FB, FRK faced, 3" thick	A	0.84	0.88	0.86	0.71	0.52	0.25
FB, FRK faced, 4" thick	A	0.88	0.90	0.84	0.71	0.49	0.23
FB, FRK faced, 1" thick	E400	0.48	0.60	0.80	0.82	0.52	0.35
FB, FRK faced, 2" thick	E400	0.50	0.61	0.99	0.83	0.51	0.35
FB, FRK faced, 3" thick	E400	0.59	0.64	1.09	0.81	0.50	0.33
FB, FRK faced, 4" thick	E400	0.61	0.69	1.08	0.81	0.48	0.34
Miscellaneous							
Musician (per person), with instrument		4.0	8.5	11.5	14.0	15.0	12.0
Air, Sabins per 1000 cubic feet @ 50% RH					0.9	2.3	7.2

In cases where materials are applied in ways that differ from the manner in which they were tested, estimates must be made based on the published absorptive properties of the individual elements. For example, a drywall wall has an absorptive coefficient of 0.29 at 125 Hz since it is acting as a panel absorber, having a resonant frequency of about 55 Hz. A one-inch (25 mm) thick fiberglass panel has an absorption coefficient of 0.03 at 125 Hz since it is measured in the A-mounting position. When a panel is mounted on drywall, the low-frequency sound passes through the fiberglass panel and interacts with the drywall surface. Assuming the porous material does not significantly increase the mass of the wall surface, the absorption at 125 Hz should be at least 0.29, and perhaps a little more due to the added flow resistance of the fiberglass. Consequently when absorptive materials are layered we must consider the combined result, rather than the absorption coefficient of only the surface material alone.

7.4 ABSORPTION MECHANISMS

Absorptive materials used in architectural applications tend to fall into three categories: porous absorbers, panel absorbers, and resonant absorbers. Of these, the porous absorbers are the most frequently encountered and include fiberglass, mineral fiber products, fiberboard, pressed wood shavings, cotton, felt, open-cell neoprene foam, carpet, sintered metal, and many other products. Panel absorbers are nonporous lightweight sheets, solid or perforated, that have an air cavity behind them, which may be filled with an absorptive material such as fiberglass. Resonant absorbers can be lightweight partitions vibrating at their mass-air-mass resonance or they can be Helmholtz resonators or other similar enclosures, which absorb sound in the frequency range around their resonant frequency. They also may be filled with absorbent porous materials.

Porous Absorbers

Several mechanisms contribute to the absorption of sound by porous materials. Air motion induced by the sound wave occurs in the interstices between fibers or particles. The movement of the air through narrow constrictions, as illustrated in Fig. 7.22, produces losses of momentum due to viscous drag (friction) as well as changes in direction. This accounts for most of the high-frequency losses. At low frequencies absorption occurs because fibers are relatively efficient conductors of heat. Fluctuations in pressure and density are isothermal, since thermal equilibrium is restored so rapidly. Temperature increases in the gas cause heat

FIGURE 7.22 Viscous Drag Mechanism of Absorption in Porous Materials

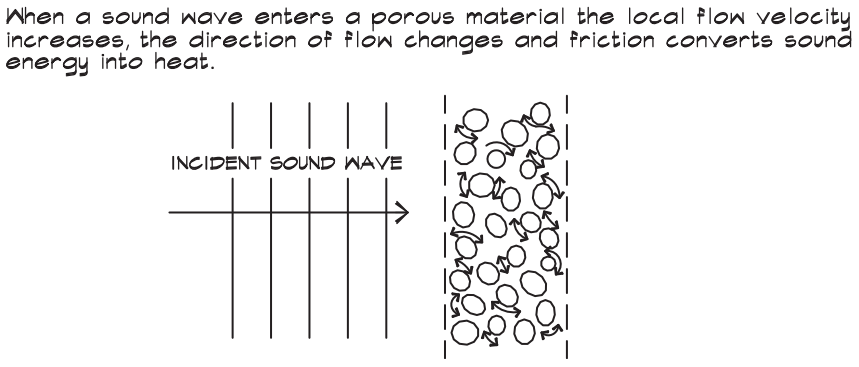

to be transported away from the interaction site to dissipate. Little attenuation seems to occur as a result of induced motion of the fibers (Mechel and Ver, 1992).

A lower (isothermal) sound velocity within a porous material also contributes to absorption. Friction forces and direction changes slow down the passage of the wave, and the isothermal nature of the process leads to a different equation of state. When sound waves travel parallel to the plane of the absorber some of the wave motion occurs within the absorber. Waves near the surface are diffracted, drawn into the material, due to the lower sound velocity.

In general, porous absorbers are too complicated for their precise impedances to be predicted from first principles. Rather, it is customary to measure the flow resistance, r_f, of the bulk material to determine the resistive component of the impedance. The bulk flow resistance is defined as the ratio between the pressure drop ΔP across the absorbing material and the steady velocity u_s of the air passing through the material.

$$r_f = -\frac{\Delta P}{u_s} \tag{7.69}$$

Since this is dependent on the thickness of the absorber it is not a fundamental property of the material. The material property is the *specific flow resistance*, r_s, which is independent of the thickness.

$$r_s = -\frac{1}{u_s}\frac{\Delta P}{\Delta x} = \frac{r_f}{\Delta x} \tag{7.70}$$

Flow resistance can be measured (Ingard, 1994) using a weighted piston as in Fig. 7.23. When the piston reaches its steady velocity, the resistance can be determined by measuring the time it takes for the piston to travel a given distance and the mass of the piston. Flow resistance is expressed in terms of the pressure drop in Newtons per square meter divided by the velocity in meters per second and is given in units of mks rayls, the same unit as the specific acoustic impedance. The specific flow resistance has units of mks rayls/m.

FIGURE 7.23 A Simple Device to Measure the Flow Resistance of a Porous Material (Ingard, 1994)

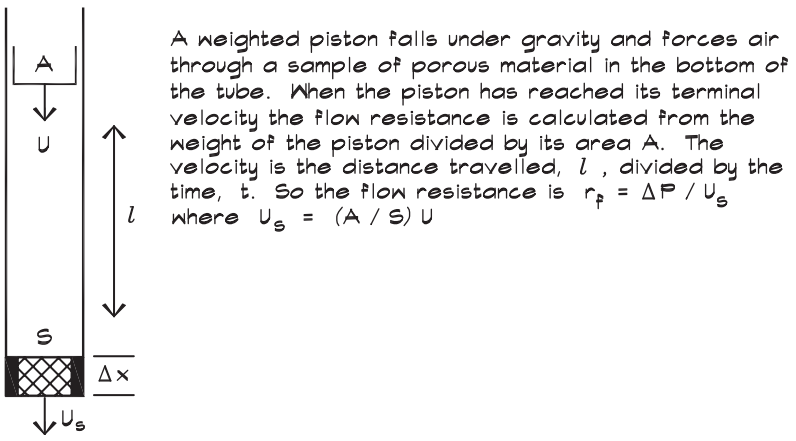

FIGURE 7.24 Geometry of a Spaced Porous Absorber (Kuttruff, 1973)

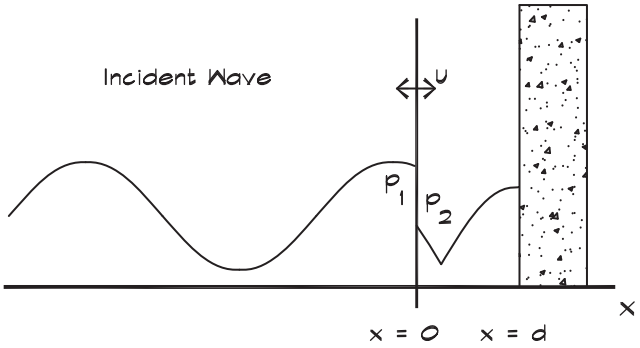

The porous absorber does not move but air flows through it, creating a standing wave in the cavity behind.

Spaced Porous Absorbers—Normal Incidence, Finite Impedance

If a thin porous absorber is positioned such that it has an airspace behind it, the composite impedance at the surface of the material and thus the absorption coefficient, is influenced by the backing. Figure 7.24 shows a porous absorber located a distance d away from a solid wall. The flow resistance, which is approximately the resistive component of the impedance, is the difference in pressure across the material divided by the velocity through the material.

$$r_f = \frac{\mathbf{p}_1 - \mathbf{p}_2}{\mathbf{u}} \tag{7.71}$$

where $\mathbf{p}_1$ is the pressure on the left side of the sheet and $\mathbf{p}_2$ is the pressure just to the right of the sheet. In this analysis it is assumed that the resistance is the same for steady and alternating flow. The velocity on either side of the sheet is the same due to conservation of mass. Equation 7.71 can be written in terms of the impedance at the surface of the absorber (at $x = 0$) on either side of the sheet.

$$r_f = \mathbf{z}_1 - \mathbf{z}_2 \tag{7.72}$$

which implies that the impedance of the composite sheet plus the air backing is the sum of the sheet flow resistance and the impedance of the cavity behind the absorber.

$$\mathbf{z}_1 = r_f + \mathbf{z}_2 \tag{7.73}$$

To calculate the impedance of the air cavity for a normally incident sound wave we write the equations for a rightward moving wave and the reflected leftward moving wave, assuming perfect reflection from the wall.

$$\begin{aligned} \mathbf{p}_2(x) &= \mathbf{A}\left[e^{-j\,k(x-d)} + e^{j\,k(x-d)}\right] \\ &= 2\,\mathbf{A}\cos\left[k\,(x-d)\right] \end{aligned} \tag{7.74}$$

The velocity in the cavity is

$$\begin{aligned}\mathbf{u}_2(x) &= \frac{\mathbf{A}}{\rho_0 c_0}\left[e^{-j\,k\,(x-d)} - e^{j\,k\,(x-d)}\right] \\ &= -\frac{2\,j\,\mathbf{A}}{\rho_0 c_0}\sin\left[k\,(x-d)\right]\end{aligned} \tag{7.75}$$

The ratio of the pressure to the velocity at the sheet surface (x = 0) is the impedance of the cavity

$$\mathbf{z}_2 = \left(\frac{\mathbf{p}_2}{\mathbf{u}_2}\right)_{x=0} = -j\,\rho_0 c_0 \cot(k\,d) \tag{7.76}$$

The normal impedance of the porous absorber and the air cavity is

$$\mathbf{z}_n = r_f - j\,\rho_0 c_0 \cot(k\,d) \tag{7.77}$$

By plugging this expression into Eq. 7.63 we get the absorption coefficient for normal incidence (Kuttruff, 1973)

$$\alpha_n = 4\left\{\left[\sqrt{\frac{r_f}{\rho_0 c_0}} + \sqrt{\frac{\rho_0 c_0}{r_f}}\right]^2 + \frac{\rho_0 c_0}{r_f}\cot^2\left(\frac{2\pi\,f\,d}{c_0}\right)\right\}^{-1} \tag{7.78}$$

Figure 7.25 (Ginn, 1978) shows the behavior of this equation with frequency for a flow resistance $r_f \cong 2\rho_0 c_0$.

FIGURE 7.25 Absorptive Material Near a Hard Surface (Ginn, 1978)

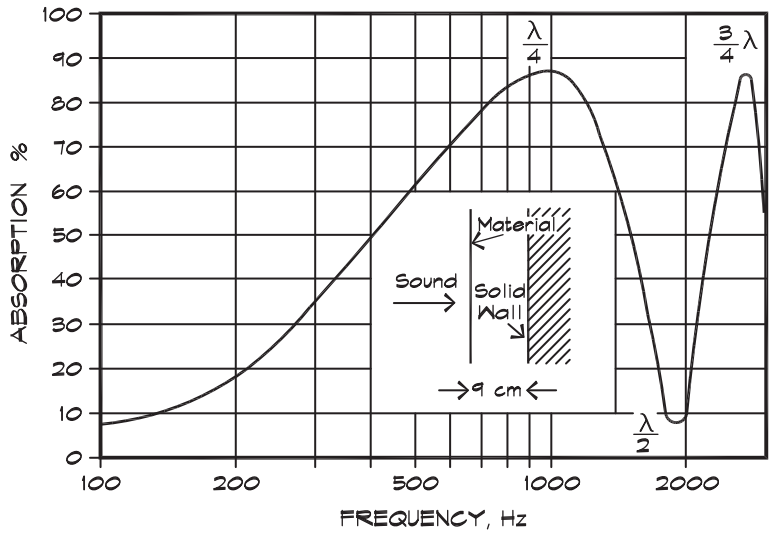

Absorption of freely suspended, thin porous material arranged parallel to a plane hard surface.

A thin porous absorber located at multiples of a quarter wavelength from a reflecting surface is in an optimum position to absorb sound since the particle velocity is at a maximum at this point. An absorber located at multiples of one-half wavelength from a wall is not particularly effective since the particle velocity is low. Thin curtains are not good broadband absorbers unless there is considerable (usually 100%) gather or unless there are several curtains hung one behind another. Note that in real rooms it is rare to encounter a condition of purely normal incidence. For diffuse fields the phase interference patterns are much less pronounced than those shown in Fig. 7.25.

Porous Absorbers with Internal Losses—Normal Incidence

When there are internal losses that attenuate the sound as it passes through a material, the attenuation can be written as an exponentially decaying sinusoid

$$\mathbf{p}\,(\mathrm{x}) = \mathbf{A}\,\mathrm{e}^{\mathrm{j}\omega\mathrm{t}}\,\mathrm{e}^{-\mathrm{j}\boldsymbol{q}\mathrm{x}} \tag{7.79}$$

where $\boldsymbol{q} = \delta + \mathrm{j}\,\beta$ is the complex *propagation constant* within the absorbing material. It is much like the wave number in that its real part, δ, is close to ω/c. However, it has an imaginary part, β, which is the attenuation constant, in nepers/meter, of the sound passing through an absorber. To convert nepers per meter to dB/meter, multiply nepers by 8.69.

For a thick porous absorber with a characteristic wave impedance $\mathbf{z}_\mathrm{w}$, we write the equations for a normally incident and reflected plane wave with losses

$$\mathbf{p} = \mathbf{A}\,\mathrm{e}^{\mathrm{j}\boldsymbol{q}\mathrm{x}} + \mathbf{B}\,\mathrm{e}^{-\mathrm{j}\boldsymbol{q}\mathrm{x}} \tag{7.80}$$

and the particle velocity is

$$\mathbf{u} = \frac{1}{\mathbf{z}_\mathrm{w}}\left[\mathbf{A}\,\mathrm{e}^{\mathrm{j}\boldsymbol{q}\mathrm{x}} - \mathbf{B}\,\mathrm{e}^{-\mathrm{j}\boldsymbol{q}\mathrm{x}}\right] \tag{7.81}$$

We use the indices 1 and 2 for the left- and right-hand sides of the material and make the end of the material $\mathrm{x} = 0$ and the beginning of the material $\mathrm{x} = -\mathrm{d}$. The incident wave is moving in the positive x direction. At $\mathrm{x} = 0$,

$$\mathbf{p}_2 = \mathbf{A} + \mathbf{B} \tag{7.82}$$

and

$$\mathbf{u}_2 = \frac{1}{\mathbf{z}_\mathrm{w}}(\mathbf{A} - \mathbf{B}) \tag{7.83}$$

Solving for the amplitudes A and B,

$$\mathbf{A} = (\mathbf{p}_2 + \mathbf{z}_\mathrm{w}\,\mathbf{u}_2)\,/\,2 \tag{7.84}$$

$$\mathbf{B} = (\mathbf{p}_2 - \mathbf{z}_\mathrm{w}\,\mathbf{u}_2)\,/\,2 \tag{7.85}$$

Plugging these into Eqs. 7.80 and 7.81 at $\mathrm{x} = -\mathrm{d}$,

$$\mathbf{p}_1 = \mathbf{p}_2 \cos(\boldsymbol{q}\,\mathrm{d}) - \mathrm{j}\,\mathbf{z}_\mathrm{w}\,\mathbf{u}_2 \sin(\boldsymbol{q}\,\mathrm{d}) \tag{7.86}$$

and

$$\mathbf{u}_1 = \left(\frac{-\mathrm{j}}{\mathbf{z}_\mathrm{w}}\right) \mathbf{p}_2 \sin(\boldsymbol{q}\,\mathrm{d}) + \mathbf{u}_2 \cos(\boldsymbol{q}\,\mathrm{d}) \tag{7.87}$$

The ratio of these two equations yields the input impedance of the absorbing surface in terms of the characteristic wave impedance of the material and its propagation constant, and the back impedance $\mathbf{z}_2$ of the surface behind the absorber.

$$\mathbf{z}_1 = \mathbf{z}_\mathrm{w} \left(\frac{\mathbf{z}_2 \coth(\boldsymbol{q}\,\mathrm{d}) + \mathbf{z}_\mathrm{w}}{\mathbf{z}_2 + \mathbf{z}_\mathrm{w} \coth(\boldsymbol{q}\,\mathrm{d})}\right) \tag{7.88}$$

When the material is backed by a rigid wall ($\mathbf{z}_2 = \infty$), then we obtain

$$\mathbf{z}_1 = \mathbf{z}_\mathrm{w} \coth(\boldsymbol{q}\,\mathrm{d}) \tag{7.89}$$

Empirical Formulas for the Impedance of Porous Materials

It is difficult to predict the complex characteristic impedance of a material from the flow resistance based on theory alone, so empirical formulas have been developed that give good results. Delany and Bazley (1969) published a useful relationship for the wave impedance of a porous material such as fiberglass

$$\mathbf{z}_\mathrm{w} = w + \mathrm{j}\,x \tag{7.90}$$

$$w = \rho_0\,\mathrm{c}_0 \left[1 + 0.0571 \left(\rho_0\,\mathrm{f}/\mathrm{r}_\mathrm{s}\right)^{-0.754}\right] \tag{7.91}$$

$$x = -\rho_0\,\mathrm{c}_0 \left[0.0870 \left(\rho_0\,\mathrm{f}/\mathrm{r}_\mathrm{s}\right)^{-0.732}\right] \tag{7.92}$$

and the propagation constant is

$$\boldsymbol{q} = \delta + \mathrm{j}\,\beta \tag{7.93}$$

$$\delta \cong \frac{\omega}{\mathrm{c}_0} \left[1 + 0.0978 \left(\rho_0\,\mathrm{f}/\mathrm{r}_\mathrm{s}\right)^{-0.700}\right] \tag{7.94}$$

$$\beta = \frac{\omega}{\mathrm{c}_0} \left[0.189 \left(\rho_0\,\mathrm{f}/\mathrm{r}_\mathrm{s}\right)^{-0.595}\right] \tag{7.95}$$

where $\mathbf{z}_\mathrm{w}$ = complex characteristic impedance of the material
w = resistance or real part of the wave impedance
x = reactance or imaginary part of the wave impedance
$\boldsymbol{q}$ = complex propagation constant
δ = real part of the propagation constant $\cong \omega/\mathrm{c}_0$
β = imaginary part of the propagation constant
= attenuation (nepers/m)

$\rho_0 c_0$ = characteristic acoustic resistance of air (about 412 Ns/m^3 – mks rayls)
r_s = specific flow resistance (mks rayls)
d = thickness of the material (m)
f = frequency (Hz)
$j = \sqrt{-1}$

Figure 7.26 shows measured absorption data versus frequency compared to calculated data using the relationships just shown for two different flow resistance and thickness values. Note that manufacturers usually give the specific flow resistance in cgs rayls/cm (1 cgs rayl = 10 mks rayls). The shape of the curve is determined by the total flow resistance, and the thickness sets the cutoff point for low-frequency absorption.

Diffuse-field absorption coefficients show a similar behavior with thickness. For oblique incidence there is a component of the velocity parallel to the surface so there is some absorption, even near the wall. The thickness and spacing of a porous absorber such as a pressed-fiberglass panel, mounted on a concrete wall or other highly reflecting surface, still determines the frequency range of its absorption characteristics. Figure 7.27 shows the measured diffuse-field absorption coefficients of various thicknesses of felt panel.

Thick Porous Materials with an Air Cavity Backing

When a thick porous absorber is backed by an air cavity and then a rigid wall, the back impedance behind the absorber is given in Eq. 7.76. This value can be inserted into Eq. 7.63 to get the overall impedance of the composite. The absorption coefficient is plotted in Fig. 7.28 for several thicknesses. In each case the total depth and total flow resistance are the same. Note that the specific flow resistance has been changed to offset the changes in thickness. When materials are spaced away from the wall, they should have a higher characteristic resistance. It is interesting that, as the material thickness decreases, the effect of the quarter-wave spacing becomes more noticeable since its behavior approaches that of a thin resistive absorber.

FIGURE 7.26 Normal Absorption Coefficient vs Frequency for Pressed Fiberglass Board (Hamet, 1997)

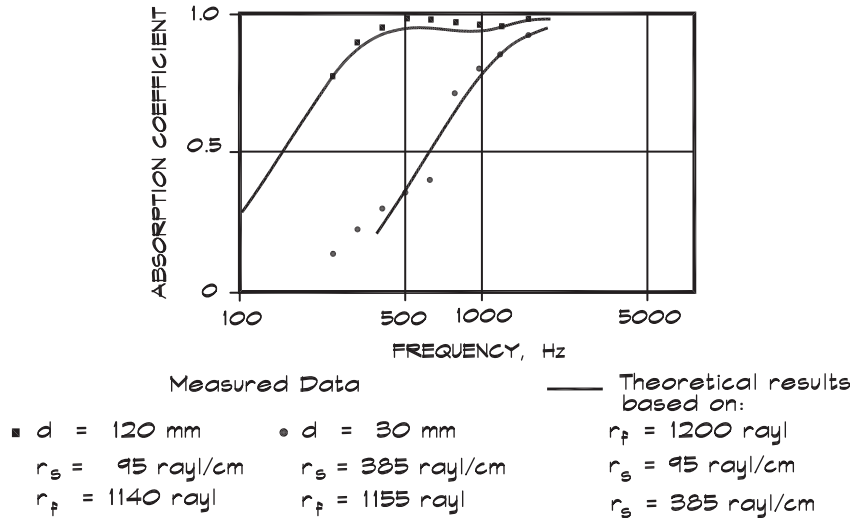

FIGURE 7.27 Dependence of Absorption on Thickness (Ginn, 1978)

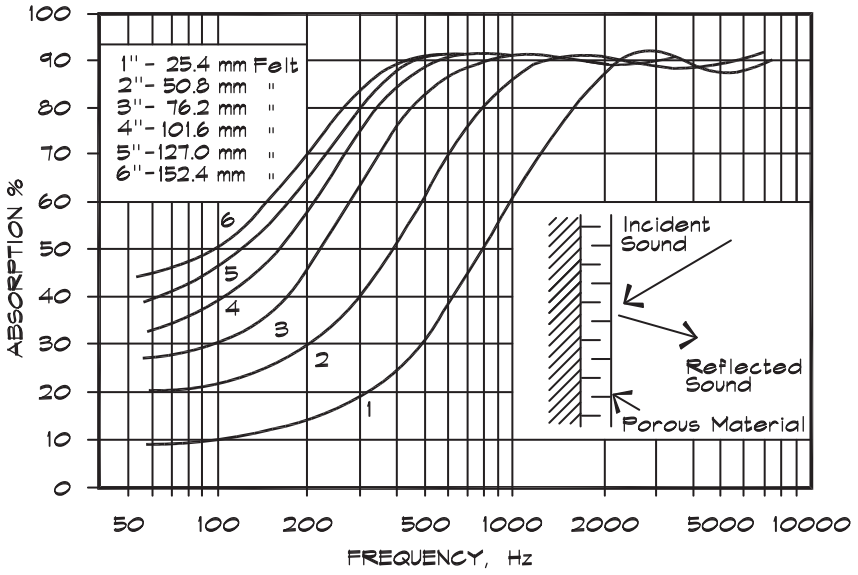

FIGURE 7.28 Absorption of Thick Materials with Air Backing (Ingard, 1994)

The absorption coefficient of a nonlocally reacting porous layer backed by an air cavity and a rigid wall. The overall thickness of the layer-cavity combination is 20 cm (8") and the different layer thicknesses are 5 cm (2"), 10 cm (4"), 15 cm (6") and 20 cm (8"). The total flow resistance in each case is $2\rho_0 c_0$.

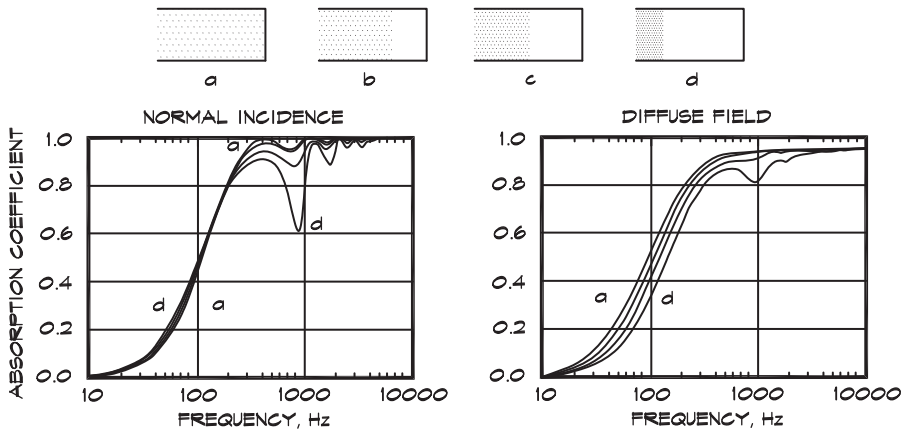

Practical Considerations in Porous Absorbers

For most architectural applications, a 1" (25 mm) thick absorbent fiberglass panel applied over a hard surface is the minimum necessary to control reverberation for speech intelligibility. Some localized effects such as high-frequency flutter echoes can be reduced using thinner materials such as 3/16" (5 mm) wall fabric or 1/4" (6 mm) carpet, but these materials are not thick enough for general applications. If low-frequency energy in the 125 Hz. octave band is of concern, then at least 2" (50 mm) panels are necessary. At even lower frequencies, 63 Hz and below, panel absorbers such as a gypboard wall, or Helmholtz bass traps are required.

FIGURE 7.29 Diffuse Field Absorption Coefficient (Ingard, 1994)

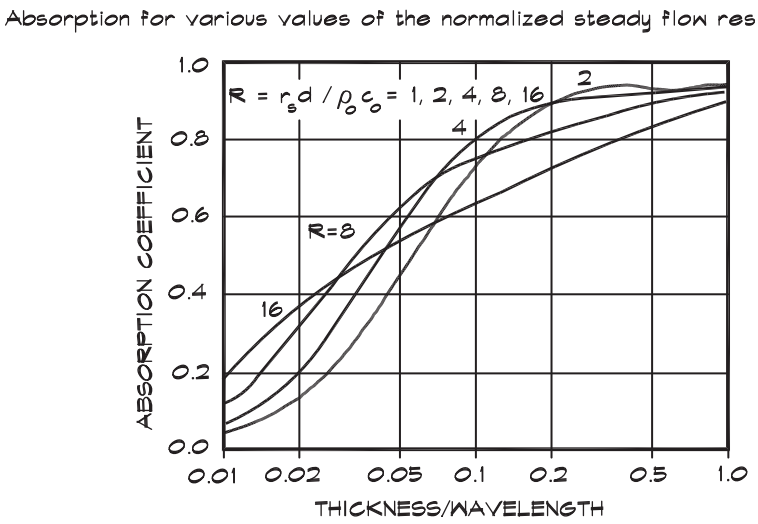

Figure 7.29 shows the absorption of materials of the same thickness but having different flow resistances. Normally a value around 2 $\rho_0 c_0$ of total flow resistance is optimal at the mid and high frequencies for a wall-mounted absorber (Ingard, 1994). At lower frequencies, or when there is an air cavity backing, higher resistances are better.

When a relatively dense material such as acoustical tile is suspended over an airspace, it can be an effective broadband absorber. Figure 7.30 shows the difference in low-frequency performance for acoustical tiles applied with adhesive directly to a reflecting surface and those supported in a suspension system. The thickness of the material is still important so that the absorption coefficient does not exhibit the high-frequency dependence shown earlier. In general, fiberglass tiles are more effective at high frequencies than mineral-fiber tiles since their characteristic resistance is lower.

Wrapping materials with a porous cloth covering has little effect on the absorption coefficient. The flow resistance of the cloth must be low. If it is easy to blow through it there is little change in the absorption. Paper or vinyl backings raise the resistance and lower the high-frequency absorption. Small perforations made in a vinyl fabric can reduce the flow resistance while delivering a product that is washable.

Screened Porous Absorbers

Absorptive materials can be overlaid by a porous screen with little effect on their properties, so long as the covering is sufficiently open. Slats of wood or metal are commonly used to protect these soft absorbers from wear and to improve their appearance. Perforated metals and wire mesh screens are also employed and can be effective as long as there is sufficient open area and the hole sizes are not so large that the spaces between the holes become reflecting surfaces, or so small that they become clogged with dirt or paint. Figure 7.31 (Doelle, 1972) shows the behavior of a porous absorber covered with a perforated facing. If there is at least 15 to 20% open area, the material works as if it were unfaced. Several examples of spaced facings are shown in Fig. 7.32.

FIGURE 7.30 Average Absorption of Acoustical Tiles (Doelle, 1972)

(A) Applied with adhesive, (B) In a suspended grid

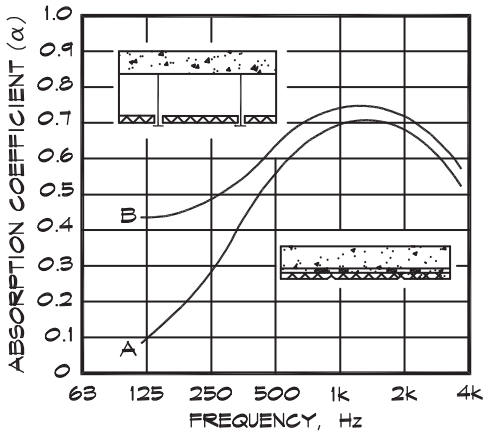

FIGURE 7.31 Sound Absorption of Perforated Panels (Doelle, 1972)

Sound absorption of perforated panel resonators with an isolation blanket in the air space. The open area (sound transparency) of the perforated facing has a considerable effect on the absorption.

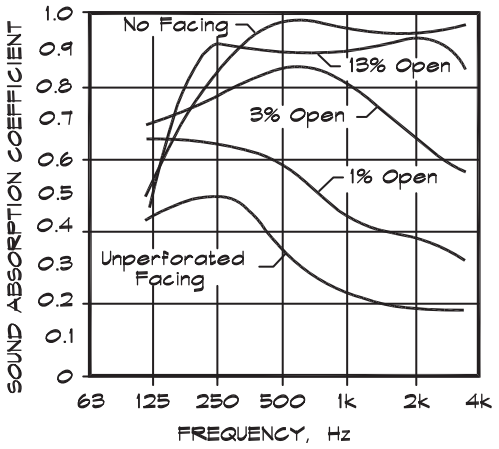

The effects of painting tiles are shown in Fig. 7.33 (Doelle, 1972). When a porous absorber is painted, its effectiveness can drop dramatically if the passage of air through its surface is impeded. This is especially true of acoustical tiles, which rely on holes or perforations to achieve their porosity. Unfaced fiberglass and duct liner boards that have a cloth face can be painted once with a light spray coat of nonbridging (water-base) paint without undue degradation. Multiple coats progressively reduce the high-frequency absorption. Clearly there are marked differences in absorptivity attributable to the thickness and number of coats of paint. Porous materials such as concrete block or certain types of stone need to be coated with paint or sealer to decrease their absorptivity (and increase their transmission loss) when they are used in churches or other spaces where a long reverberation time is desired.

FIGURE 7.32 Various Configurations of Wood Slats (Doelle, 1972)

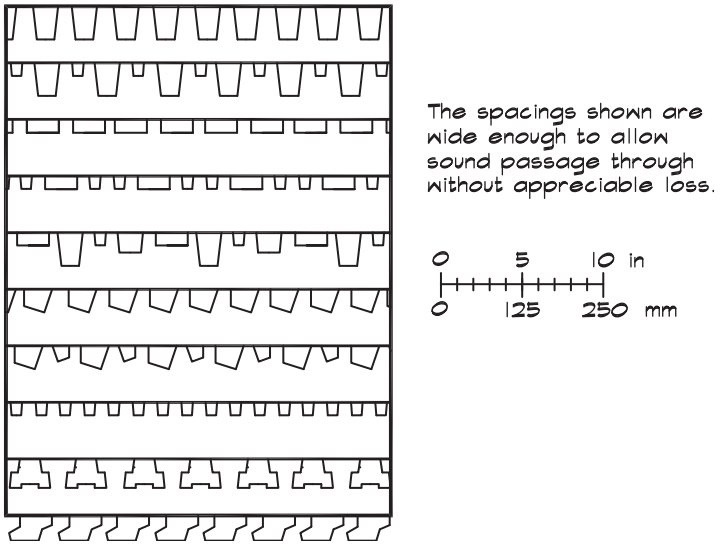

FIGURE 7.33 Effect of Paint on Absorptive Panels (Doelle, 1972)

The effect of paint on porous prefabricated acoustical units: (A) untreated surface (B) one coat of paint applied with a spray gun (C) one coat of paint applied with a brush (D) two coats of paint applied with a brush.

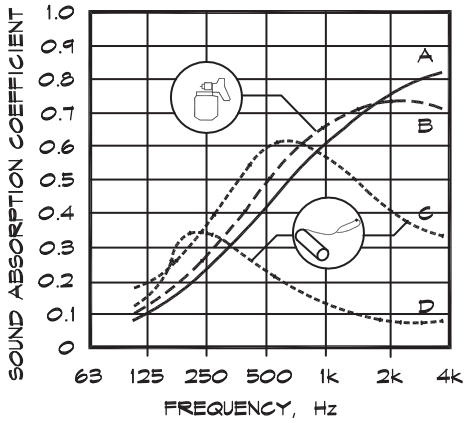

7.5 ABSORPTION BY NONPOROUS ABSORBERS

Unbacked Panel Absorbers

A freely suspended nonporous panel can absorb sound simply due to its mass reactance: that is, its induced motion. For this reason even solid walls provide some residual absorption, which may be only a few percentage points. Figure 7.34 shows the geometry of a normally incident sound wave impacting a solid plate. On the source side we have the incident pressure $\mathbf{p}_1$ and the reflected pressure $\mathbf{p}_3$; on the opposite side we have the transmitted pressure $\mathbf{p}_2$. The total pressure acting on the wall, $\mathbf{p}_1 + \mathbf{p}_3 - \mathbf{p}_2$, induces a motion in the panel according to Newton's law, $\mathbf{p}_1 + \mathbf{p}_2 - \mathbf{p}_3 = \mathrm{j}\,\omega\, m\,\mathbf{u}$. Since the sound wave on the right side is radiating

FIGURE 7.34 Geometry of an Unbacked Panel Absorber

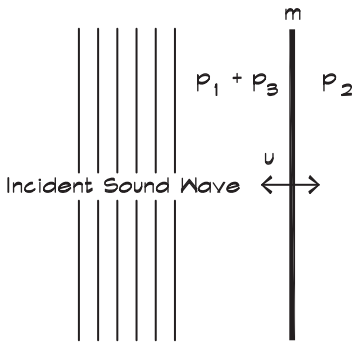

into free space we can write the pressure in terms of the particle velocity $\mathbf{p}_2 = \rho_0 \, c_0 \, \mathbf{u}$ to obtain the relationship $\mathbf{p}_1 + \mathbf{p}_3 - \rho_0 \, c_0 \, \mathbf{u} = j \, \omega \, m \, \mathbf{u}$ and from this, the impedance of the panel is (Kuttruff, 1963)

$$\mathbf{z} = j \, \omega \, m + \rho_0 \, c_0 \tag{7.96}$$

Now this expression can be inserted into Eq. 7.63 to calculate the normal incidence absorption coefficient

$$\alpha_n = \left[1 + \left(\frac{\omega \, m}{2 \, \rho_0 \, c_0} \right)^2 \right]^{-1} \tag{7.97}$$

From this expression the absorption of windows and solid walls can be calculated; however, their residual absorption is small and only significant at low frequencies.

Air Backed Panel Absorbers

When a nonporous panel, as in Fig. 7.35, is placed in front of a solid surface with no contact between the panel and the surface, the panel can move back and forth, but is resisted by the air spring force.

FIGURE 7.35 Geometry of an Air Backed Panel Absorber

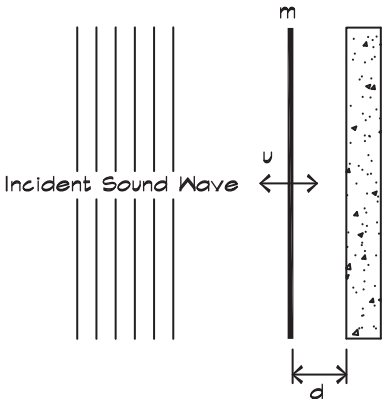

When there is a pressure differential across the panel Newton's law governs the motion

$$\Delta \mathbf{p} = \mathrm{m}\frac{\mathrm{d}\,\mathbf{u}}{\mathrm{d}\,\mathrm{t}} = \mathrm{j}\,\omega\,\mathrm{m}\,\mathbf{u} \tag{7.98}$$

where m is the mass of the panel per unit area. Using the same notation as before, with $\mathbf{p}_1 + \mathbf{p}_3$ being the pressure in front of the panel and $\mathbf{p}_2$ the pressure behind the absorber, we obtain

$$\frac{\mathbf{p}_1 + \mathbf{p}_3 - \mathbf{p}_2}{\mathbf{u}} = \mathrm{r_f} + \mathrm{j}\,\omega\,\mathrm{m} \tag{7.99}$$

and in a similar manner the composite assembly impedance is

$$\mathbf{z} = \mathrm{r_f} + \mathrm{j}\left[\omega\,\mathrm{m} - \rho_0\,\mathrm{c}_0\,\cot(\mathrm{k\,d})\right] \tag{7.100}$$

When the depth, d, of the airspace behind the sheet is small compared to a wavelength, we can use the approximation $\cot(\mathrm{k\,d}) \cong (\mathrm{k\,d})^{-1}$ so that

$$\mathbf{z} \cong \mathrm{r_f} + \mathrm{j}\left[\omega\,\mathrm{m} - \frac{\rho_0 \mathrm{c}_0^2}{\omega\,\mathrm{d}}\right] \tag{7.101}$$

As before, we can insert this expression into Eq. 7.63 to obtain the normal-incidence absorption coefficient (Kuttruff, 1973)

$$\alpha_\mathrm{n} = \frac{4\,\mathrm{r_f}\,\rho_0\,\mathrm{c}_0}{\left(\mathrm{r_f} + \rho_0\mathrm{c}_0\right)^2 + \left[(\mathrm{m}/\omega)\left(\omega^2 - \omega_0^2\right)\right]^2} \tag{7.102}$$

where we have used the resonant frequency from the bracketed term in Eq. 7.101, whose terms are equal at resonance.

$$\omega_\mathrm{r} = \left(\frac{\rho_0\,\mathrm{c}_0^2}{\mathrm{m\,d}}\right)^{\frac{1}{2}} \tag{7.103}$$

A simpler version of Eq. 7.103 is

$$\mathrm{f_r} = \frac{600}{\sqrt{\mathrm{m\,d}}} \tag{7.104}$$

where m is the panel mass in kg / m^2 and d is the thickness of the airspace in cm. When the airspace is filled with batt insulation the resonant frequency is reduced to

$$\mathrm{f_r} = \frac{500}{\sqrt{\mathrm{m\,d}}} \tag{7.105}$$

due to the change in sound velocity.

If the panel is impervious to flow, the flow resistance is infinite, and the absorption is theoretically infinite at resonance. Above and below resonance the absorption coefficient falls

FIGURE 7.36 Sound Absorption of a Suspended Panel (Doelle, 1972)

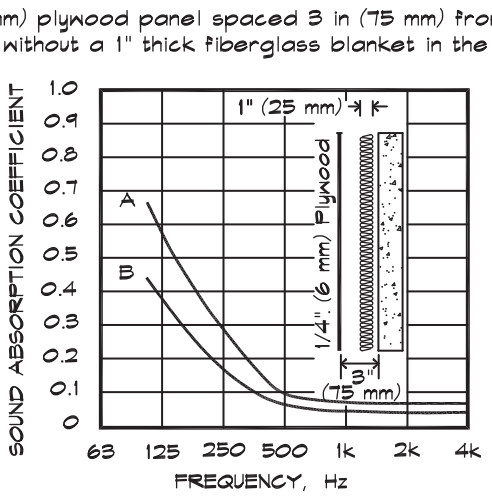

off. In this model the sharpness of the peak is determined by the amount of flow resistance provided by the panel. When damping is added to the cavity the propagation constant in the airspace becomes complex and adds a real part to the impedance, which broadens the resonance. The damping is provided by fiberglass boards or batting suspended in the airspace behind the panel. Figure 7.36 shows the typical behavior of a panel absorber with and without insulation.

Panel absorbers of this type that are tuned to a low resonant frequency are used as bass traps in studios and control rooms. Thin wood panels, mounted over an air cavity, produce considerable low-frequency absorption and, when there is little or no absorptive treatment behind the panel, this absorption is frequently manifest in narrow bands. As a result wood panels are a serious detriment to adequate bass response in concert halls. It is a common misunderstanding, particularly among musicians, that wood, and in particular thin wood panels that vibrate, contribute to good acoustical qualities of the hall. This no doubt arises from the connection in the mind between a musical instrument such as a violin and the hall itself. In fact, vibrating components in a hall tend to remove energy at their natural frequencies and return some of it back to the hall at a later time.

Perforated Panel Absorbers

If a perforated plate is suspended in a sound field, there is absorption due to the mass reactance of the plate itself, the mass of the air moving through the perforations, and the flow resistance of the material. If the perforated plate is mounted over an air cavity, there is also its impedance to be considered. There are quite a number of details in the treatment of this subject, whose consideration extends past the scope of this book. The goal here is to present enough detail to give an understanding of the phenomena without undue mathematical complication.

In a perforated plate the perforations form small tubes of air, which have a mass and thus a mass reactance to the sound wave. Figure 7.37 illustrates the geometry of a perforated plate. The holes in the plate have a radius a, and are spaced a distance e apart. The fluid velocity $\mathbf{u}_e$ on the exterior of the plate is raised to a higher interior velocity $\mathbf{u}_i$ as the fluid

FIGURE 7.37 Geometry of a Perforated Panel Absorber

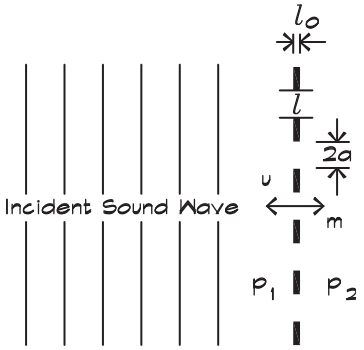

is forced through the holes. The ratio of velocities can be written in terms of the ratio of the areas, which is the porosity

$$\frac{\mathbf{u}_e}{\mathbf{u}_i} = \frac{\pi\, a^2}{e^2} = \sigma \tag{7.106}$$

The impedance due to the inertial mass of the air moving through the pores is

$$\frac{\mathbf{p}_1 - \mathbf{p}_2}{\mathbf{u}_e} = \frac{j\,\omega\,\pi\, a^2\,\rho_0\, l}{e^2} = \frac{j\,\omega\,\rho_0\, l}{\sigma} \tag{7.107}$$

so the effective mass per unit area is

$$m = \frac{\rho_0\, l}{\sigma} \tag{7.108}$$

The effective length of the tube made by the perforated hole in Eq. 7.107 is slightly longer than the actual thickness of the panel. This is because the air in the tube does not instantaneously accelerate from the exterior velocity to the interior velocity. There is an area on either side of the plate that contains a region of higher velocity and thus a slightly longer length. This correction is written in terms of the effective length

$$l = l_0 + 2\,(0.8\,a) \tag{7.109}$$

Usually the air mass is very small compared to the mass of the panel itself so that the panel is not affected by the motion of the fluid. If the area of the perforations is large and the panel mass M is small, the combined mass of the air and the panel must be used.

$$m_c = m\,\frac{M}{M + m} \tag{7.110}$$

When M is large compared with the mass of the air, m, then the combined mass is just the air mass.

The absorption coefficient for a perforated panel is obtained from Eq. 7.97, using the combined mass of the air and the panel. In commercially available products, perforated

FIGURE 7.38 Absorption of a Coated Perforated Panel (Wilhelmi Corp. Data, 2000)

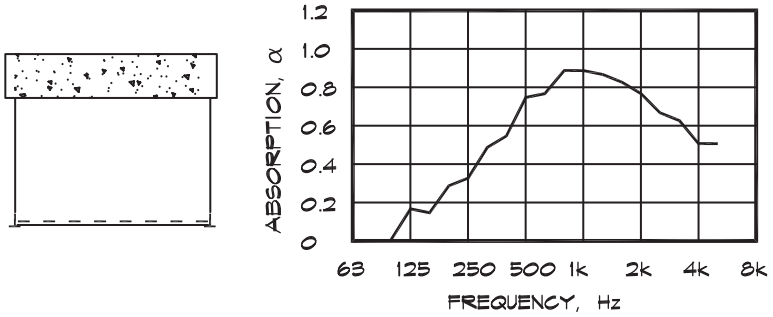

metal sheets are available with an air resistant coating, which adds flow resistance to the mass reactance of the air. These materials can be supported by T-bar systems and are effective absorbers. Absorption data for a typical product are shown in Fig. 7.38.

Perforated Metal Grilles

When a perforated panel is being used as a grille to provide a transparent cover for a porous absorber, it is important that there is sufficient open area that the sound passage is not blocked. In these cases the sound "absorbed" by the panel is actually the sound transmitted through the grille into the space beyond. The normal incidence absorption coefficient in this case is the same as the normal incidence transmissivity. Thus we can set it equal to the expression shown in Eq. 7.97

$$\tau = \left[1 + \left(\frac{\omega \, m_c}{2 \, \rho_0 \, c_0}\right)^2\right]^{-1} \tag{7.111}$$

If the loss through a perforated panel is to be less than about 0.5 dB, the transmission coefficient should be greater than about 0.9, and the term inside the parenthesis becomes 0.33. At 1000 Hz the combined panel mass should be 0.04 kg / m^2. For a 2 mm thick (.079") thick panel with 3 mm (.125") diameter holes, the effective length is about 4 mm and the required porosity calculates out to about 11%. This compares well with the data shown in Fig. 7.38, even though the calculation done here is for normal incidence and the data are for a diffuse-field measurement.

If a perforated panel is to be used as a loudspeaker grille, the open area should be greater, on the order of 30 to 40%. Increasing the porosity preserves more of the off-axis directional character of the loudspeaker's sound. Porosities beyond 40% are difficult to achieve in a perforated panel while still retaining structural integrity.

Air Backed Perforated Panels

When a perforated panel is backed with an airspace of a given depth, the back impedance of the airspace must be considered. The three contributing factors are the mass reactance of the air/panel system, the flow resistance of any filler material, and the stiffness of the air cavity behind the panel. The overall impedance is the sum of these three contributors, which at low

frequencies was given in Eq. 7.102

$$\mathbf{z} = \mathrm{j}\,\omega\,\mathrm{m_c} + \mathrm{r_f} - \frac{\mathrm{j}\,\rho_0\,\mathrm{c_0^2}}{\omega\,\mathrm{d}} \tag{7.112}$$

In the case of a perforated panel the combined mass of the panel and the air through the pores is used. We obtain the same result as Eq. 7.102, which we used for the absorption coefficient of a closed panel, and it is expressed in terms of the resonant frequency of the panel-cavity-spring-mass system.

$$\omega_0 = \left(\frac{\rho_0\,\mathrm{c_0^2}}{\mathrm{m_c\,d}}\right)^{\frac{1}{2}} \tag{7.113}$$

When we substitute the mass of the moving air in terms of the length of the tube and the porosity we get a familiar result—the Helmholtz resonator natural frequency. Here we have assumed that the mass of the air is much smaller than the panel mass

$$\mathrm{m_c} = \frac{\rho_0\,l}{\sigma} = \frac{\rho_0\,l\,\mathrm{e^2}}{\pi\,\mathrm{a^2}} = \frac{\rho_0\,l\,\mathrm{V}}{\mathrm{S\,d}} \tag{7.114}$$

and

$$\omega_0 = \left(\frac{\rho_0\,\mathrm{c_0^2}}{\rho_0\,l\,\mathrm{V/S}}\right)^{\frac{1}{2}} = \mathrm{c_0}\sqrt{\frac{\mathrm{S}}{l\,\mathrm{V}}} \tag{7.115}$$

It is apparent that a perforated panel with an air backing is acting like a Helmholtz resonator absorber and will exhibit similar characteristics, just as the solid panel did. The major difference is that the moving mass, in this case the air in the holes, is much lighter than the panel and thus the resonant frequency is much higher. These perforated absorbers are mainly utilized where mid-frequency absorption is needed.

The flow resistance of perforated panels can be measured directly or can be calculated from empirical formulas, such as that given by Cremer and Muller (1982)

$$\mathrm{r_f} \cong 0.53\,\frac{\mathrm{e^2}\,l_0}{\mathrm{a^3}}\,\sqrt{\mathrm{f}}\cdot 10^{-2}\ \text{mks rayls} \tag{7.116}$$

Figure 7.39 shows the absorption coefficient of a perforated plate in front of an airspace filled with absorptive material.

7.6 ABSORPTION BY RESONANT ABSORBERS

Helmholtz Resonator Absorbers

When a series of Helmholtz resonators is used as an absorbing surface, the absorption coefficient can be calculated in a manner similar to that used for a perforated plate.

FIGURE 7.39 Absorption of a Perforated Panel (Cremer and Muller, 1982)

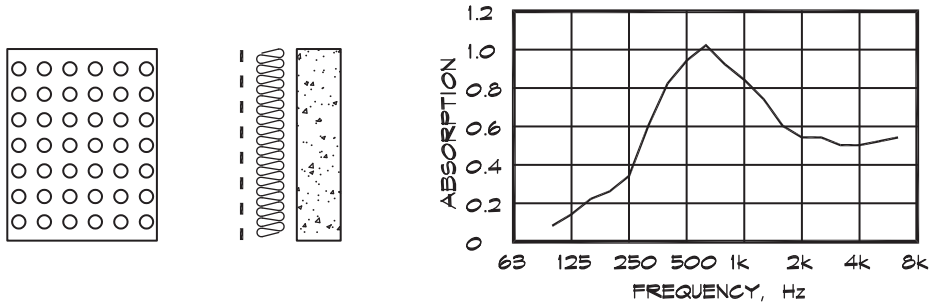

The resonant frequency is given by

$$f_0 = \frac{c_0}{2\pi}\sqrt{\frac{\pi a^2}{(l_0 + 1.7a)V}} \tag{7.117}$$

where a is the radius of the resonator neck, l_0 is its length, and V its volume. The question then is how to calculate the depth, d, of the cavity. With a perforated plate the volume of the airspace was

$$d = \frac{V}{e^2} \tag{7.118}$$

where e is the spacing between perforations. Using V as the volume of the Helmholtz resonator the normal-incidence absorption coefficient for a series of resonators is (Cremer and Muller, 1982)

$$\alpha_n = \frac{4r_f}{\rho_0 c_0}\left[\left(1 + \frac{r_f}{\rho_0 c_0}\right)^2 + \left(\frac{c_0 e^2}{2\pi f_0 V}\right)^2\left(\frac{f_0}{f} - \frac{f}{f_0}\right)^2\right]^{-1} \tag{7.119}$$

Products based on the Helmholtz resonator principle are commercially available. Some are constructed as concrete masonry units with slotted openings having a fibrous or metallic septum interior fill. Absorption data on typical units are given in Fig. 7.40.

Mass-Air-Mass Resonators

A mass-air-mass resonant system is one in which two free masses are separated by an air cavity that provides the spring force between them. A typical example is a drywall stud wall, which acts much like the resonant panel absorber, except that both sides are free to move. The equation is similar to that used in the single-panel equation (Eq. 7.104) except that both masses are included. The resonant frequency is

$$f_{mam} = 600\sqrt{\frac{m_1 + m_2}{d\, m_1\, m_2}} \tag{7.120}$$

where m_1 and m_2 are the surface mass densities of the two surfaces in kg/m^2 and d is the separation distance between the sides in cm. When the cavity is filled with batt insulation,

FIGURE 7.40 Helmholtz Resonator Absorbers (Doelle, 1972)

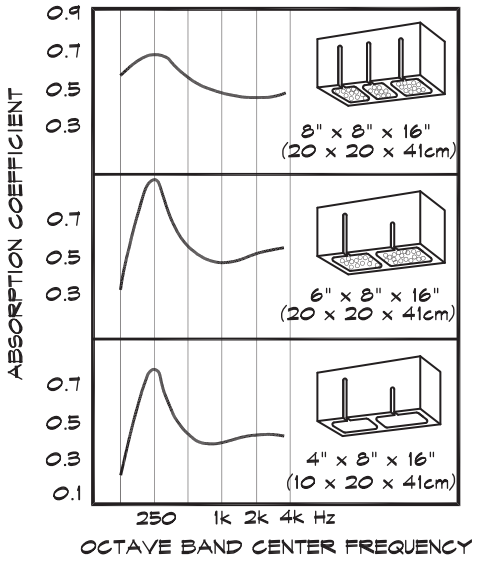

the constant changes from 600 to 500 because the sound velocity goes from adiabatic to isothermal. Away from resonance the absorption coefficient follows the relationship (Bradley, 1997)

$$\alpha(\mathrm{f}) = \alpha_{\mathrm{mam}} \left(\frac{\mathrm{f}_{\mathrm{mam}}}{\mathrm{f}} \right)^2 + \alpha_{\mathrm{s}} \tag{7.121}$$

where $\alpha(\mathrm{f})$ = diffuse field absorption coefficient
α_{mam} = maximum absorption coefficient at $\mathrm{f}_{\mathrm{mam}}$
α_{s} = residual surface absorption coefficient at high frequencies
f = frequency (Hz)
$\mathrm{f}_{\mathrm{mam}}$ = mass-air-mass resonant frequency (Hz)

Figure 7.41 shows the absorption coefficient for a single and double-layer drywall stud wall using $\alpha_{\mathrm{mam}} = 0.44$ and $\alpha_{\mathrm{s}} = 0.045$ for the single-layer wall and $\alpha_{\mathrm{mam}} = 0.44$ and $\alpha_{\mathrm{s}} = 0.06$ in the double-layer case. The same constants are used for batt-filled stud walls. The agreement shown in the figure between measured and predicted values is quite good.

Quarter-Wave Resonators

A hard surface having a well of depth d and diameter 2 a can provide absorption through reradiation of sound that is out of phase with the incident sound. These wells, shown in Fig. 7.42, are known as quarter-wave resonators because a wave reflected from the bottom returns a half wavelength or 180° out of phase with the wave reflected from the surface. When the length of the tube is an odd-integer multiple of a quarter wavelength it is out of phase with the incident wave and perfectly absorbing. The tube acts as a small resonant radiator, which can have both absorptive and diffusive properties.

As was the case in Eq. 7.89, the interaction impedance of a tube having a depth d is

$$\mathbf{z}_{\mathrm{t}} = -\mathrm{j}\,\rho_0\,\mathrm{c}_0\,\cot(\boldsymbol{q}\,\mathrm{d}) \tag{7.122}$$

FIGURE 7.41 Resonant Absorption by a Stud Wall (Bradley, 1997)

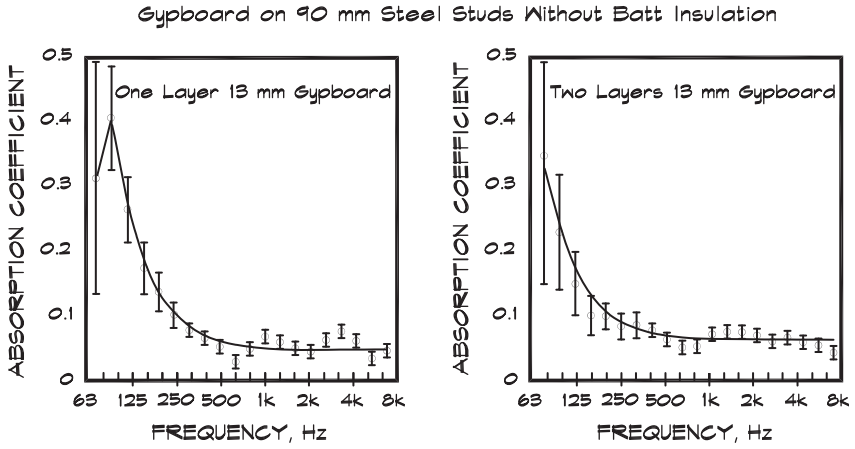

FIGURE 7.42 Quarter Wave Resonator

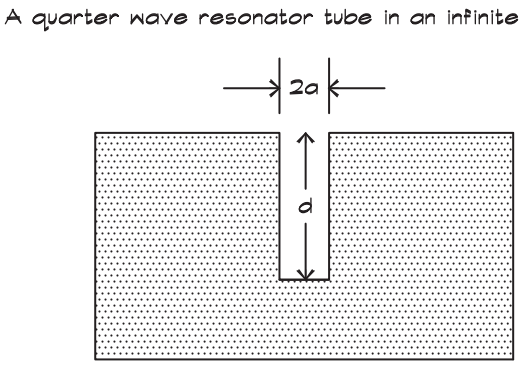

where $\boldsymbol{q}$ is the propagation constant. The tube has small viscous and thermal loss components and the imaginary part of the propagation constant, from an approximation originally due to Kirchoff, can be used to account for them

$$\boldsymbol{q} \cong \mathrm{k}\left[1 + \frac{0.31\,\mathrm{j}}{2\,\mathrm{a}\sqrt{\mathrm{f}}}\right] \tag{7.123}$$

There are two impedances to be included in the analysis: one having to do with the interaction between the incoming wave and the end of the tube, which was given in Eq. 7.122; and the other having to do with the radiation of sound back out of the tube. The radiation impedance of the tube is that of a piston in a baffle and was examined in Eq. 6.67 and 6.69 in the near field. For low frequencies, where the width of the opening is much smaller than a wavelength, the radiation impedance is approximately (Morse, 1948)

$$\mathbf{z}_\mathrm{r} \cong \rho_0 \mathrm{c}_0\left[\frac{1}{2}(\mathrm{k\,a})^2 + \frac{2\,\mathrm{j}}{\pi\,\mathrm{k\,a}}\right] \tag{7.124}$$

The pressure just outside the opening to the tube is the pressure radiated by the tube, plus twice the incident pressure, which is doubled due to its reflection off the rest of the hard

FIGURE 7.43 Absorption and Scattering Cross Sections of a Tube Resonator in a Wall (Ingard, 1994)

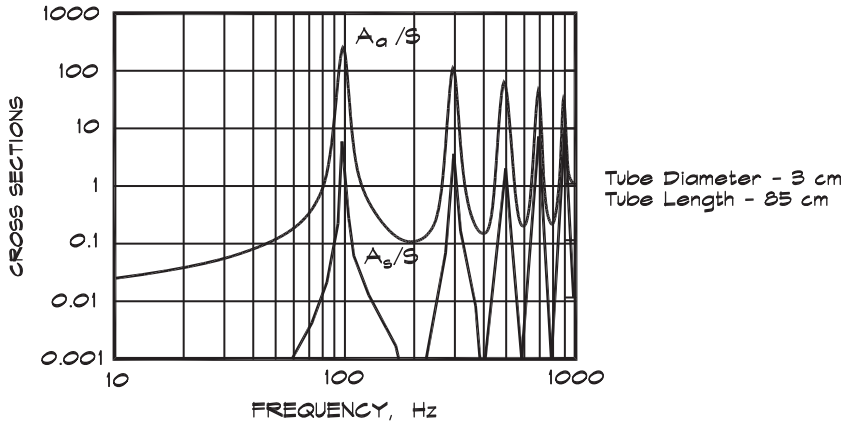

surface, $\mathbf{p}_{\text{outside}} = 2\,\mathbf{p}_{\text{i}} + \mathbf{p}_{\text{r}}$ where $\mathbf{p}_{\text{r}} = \mathbf{u}\,\mathbf{z}_{\text{r}}$. The pressure just outside the opening must match the pressure just inside the end of the tube, which is $\mathbf{p}_{\text{inside}} = -\mathbf{u}\,\mathbf{z}_{\text{t}}$. At the surface the pressures and the velocities must match, which leads to

$$\mathbf{u} = \frac{2\,\mathbf{p}_{\text{i}}}{\mathbf{z}_{\text{t}} + \mathbf{z}_{\text{r}}} \tag{7.125}$$

The absorption of a well in a surface can be expressed in terms of a cross section, defined (Ingard, 1994) as the power absorbed by the well divided by the intensity of the incident wave. The power absorbed by the resonator tube is

$$\mathrm{W_a} = \mathrm{S}\,|\,\mathbf{u}\,|^2 \;\; w_{\text{t}} = \mathrm{S}\,\frac{|\,\mathbf{p}_{\text{i}}\,|^2}{(\rho_0\,\mathrm{c}_0)}\,\frac{4\,\rho_0\,\mathrm{c}_0 w_{\text{t}}}{|\,\mathbf{z}_{\text{t}} + \mathbf{z}_{\text{r}}\,|^2} \tag{7.126}$$

where $\mathbf{z} = w + \mathrm{j}\,x$ and $\mathrm{S} = \pi \mathrm{a}^2$. Since $\mathrm{I_i} = |\,\mathbf{p}_{\text{i}}\,|^2 / (\rho_0\,\mathrm{c}_0)$ is the intensity of the incident wave, the power absorbed can be expressed as $\mathrm{W_a} = \mathrm{A_a}\,\mathrm{I_i}$, where $\mathrm{A_a}$ is the absorption cross section.

$$\mathrm{A_a} = \mathrm{S}\,\frac{4\,\rho_0\,\mathrm{c}_0\,w_{\text{t}}}{|\mathbf{z}_{\text{t}} + \mathbf{z}_{\text{r}}|^2} \tag{7.127}$$

A typical result, given in Fig. 7.43, shows strong peaks at the minima of the tube impedance. When the cross section is 100, it means that the tube is acting as a perfect absorber equal to 100 times its open area. Note that although a tube can be very effective at a given frequency, its bandwidth is very narrow.

The same figure shows the cross section of the power scattered back by the tube. The tube behaves like a piston in a baffle when it radiates sound back out. It continues to resonate even after the initial wave has been reflected and emits sound at its resonant frequency for a short period of time. When the tube mouth dimension is small compared with a wavelength, it acts as an omnidirectional source that diffuses sound at that frequency.

FIGURE 7.44 Seat Absorption (Schultz and Watters, 1964)

Anomalous sound attenuation (after correction for spherical divergence) for the early sound pressure level above the audience seating in a concert hall, as a function of frequency. —— Various seats on the main floor. —— First row in the first balcony.

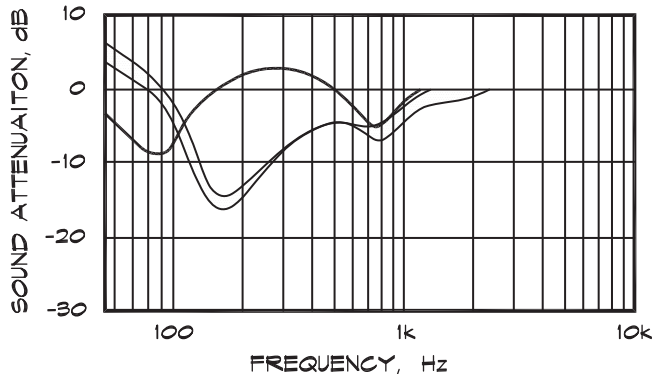

Absorption by Seats

It has been recognized for some time that theater seating, both occupied and unoccupied, produces excess attenuation of the direct sound coming from a stage, primarily at about 150 Hz, in much the same way as soft earth or vegetation contributes to excess ground attenuation. Padded opera chairs in a theater subdivide the floor into a regular lattice having a particular depth and spacing. As such they are like an array of quarter-wave resonators over which a sound wave, coming from the stage, grazes. In addition, the porous padding that covers them adds a resistive component to the impedance they present to a wave. A measurement of the excess attenuation due to theater seating, is shown in Fig. 7.44. Note that the dip is broader than the behavior predicted in Fig. 7.43 due to the resistive padding and the fact that the higher modes are not as prevalent. This may be due in part to the fact that the seat spacing is no longer small compared with a wavelength.

Ando (1985) published a detailed theoretical study of the absorptive properties of different chair-shaped periodic structures. Although the absorption varies somewhat with the precise shape selected, the basic pattern of the excess attenuation exhibits a steep dip at the frequency whose quarter wavelength is equal to the chair-back height above the floor. This agrees well with measurements made in concert halls. The excess grazing attenuation contributes to decreased bass response particularly in the orchestra seating section on the first floor of a hall. To help offset the extra attenuation, overhead reflectors can be used, which increase the angle of grazing incidence.

Quadratic-Residue Diffusers

One particular type of resonant tube absorber originally suggested by Schroeder (1979) uses a series of wells of different depths in a particular sequential order. Since each well is a small narrow-band omnidirectional radiator, a series of wells of different depths can cover a range of frequencies and provide diffusion over a reasonable bandwidth. The depth d_n of the n^{th} well is chosen such that

$$d_n = \left(\frac{\lambda}{2N}\right) s_n \tag{7.128}$$

where the sequence $s_n = (n^2 \bmod N)$ for $n = 0, 1, 2, \ldots$ and N is an odd prime number. For example, for $N = 11$ starting with $n = 0$, the sequence is [0, 1, 4, 9, 5, 3, 3, 5, 9, 4, 1] and then it repeats so that the period is N numbers long. This sequence of wells produces an essentially hemispheric polar reflection pattern within certain frequency limits. For a more detailed treatment, refer to Ando (1985).

The design process for a quadratic-residue diffuser is as follows:

1. Determine the frequency range f_{high} to f_{low} for the diffuser. The period N is given by the ratio f_{high} / f_{low}.
2. The width w of each well must be small compared with the wavelength of the highest frequency.

$$w \leq \frac{c_0}{2 f_{high}} \tag{7.129}$$

3. Calculate the depth of each well using Eq. 7.128, where $\lambda = \frac{c_0}{f_{low}}$ is called the design wavelength.

Figure 7.45 shows a side view of a quadratic-residue diffuser. One feature of quadratic-residue diffusers is that they absorb sound at low frequencies as might be expected from our previous analysis.

FIGURE 7.45 Quadratic Residue Diffusers

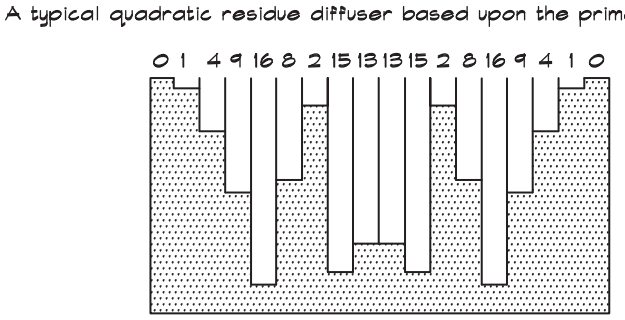

This page intentionally left blank

8 SOUND IN ENCLOSED SPACES

8.1 STANDING WAVES IN PIPES AND TUBES

Resonances in Closed Tubes

When a sound is generated within a solid enclosure such as a pipe, tube, or room, it expands naturally to fill the space. If the lateral dimensions of the space are small compared with a wavelength, as is the case with a tube, duct, or organ pipe, the sound propagates along the tube as a plane wave until it encounters an impedance boundary. If the tube is closed, the impedance at the end is very high, assumed to be infinite in a simple model, and the wave reflects back along the tube in the direction from which it came. If both ends are closed, the wave can reflect back and forth many times with little attenuation. The length of the tube in the direction of wave propagation determines the frequencies of the sound waves that persist under these conditions. These resonant frequencies are self-reinforcing since they combine in phase and continue for a long time after an exciting source is turned off. Other frequencies may be present initially; however, because of the geometry of the tube, they tend to cancel each other and average out to zero.

The behavior of the pressure in a one-dimensional plane wave propagating along a tube can be described using the formula

$$\mathbf{p} = \mathbf{A} \cos (\mathrm{k\,x} + \phi) \tag{8.1}$$

where x is the distance from the end of the tube. If both ends of the tube are rigid this fact establishes the mathematical boundary conditions at the end points. At $\mathrm{x} = 0$, the rigid boundary condition requires that the change in pressure with distance be zero at the boundary,

$$\left(\frac{\partial \mathbf{p}}{\partial \mathrm{x}}\right)_{\mathrm{x}=0} = 0 \quad \text{consequently } \phi = 0 \tag{8.2}$$

If the same condition is applied at the other termination

$$\left(\frac{\partial \mathbf{p}}{\partial \mathrm{x}}\right)_{\mathrm{x}=l} = \sin \mathrm{k}\, l = 0 \tag{8.3}$$

which is satisfied for $k\,l = n\,\pi$. The resonant frequencies of the sound wave in a closed tube are given by

$$f_n = \frac{n\,c}{2\,l} \tag{8.4}$$

where n is an integer. The lowest frequency is called the fundamental mode, where $n = 1$, and the length of the tube is half of the fundamental wavelength.

Standing Waves in Closed Tubes

There are two possible solutions for plane wave propagation in a closed tube, one for sound moving in each direction. They take the form of two traveling waves

$$\mathbf{p} = \mathbf{A}\,\cos(-k\,x + \omega\,t) + \mathbf{A}\,\cos(k\,x + \omega\,t) \tag{8.5}$$

Using a trigonometric identity for the sum of two cosine waves, the equation can be written as

$$\mathbf{p} = 2\,\mathbf{A}\,\cos(k\,x)\,\cos(\omega\,t) \tag{8.6}$$

which is a standing wave. At any particular point a particle vibrates back and forth in simple harmonic motion at a particular frequency; however, its amplitude is larger or smaller depending on its location along the x axis.

The locations of the values of maximum pressure, called *antinodes*, occur at positions where

$$k\,x = 0, \pi, 2\pi, 3\pi, \ldots \tag{8.7}$$

which means

$$x = 0, \frac{\lambda}{2}, \frac{2\,\lambda}{2}, \frac{3\,\lambda}{2}, \ldots = \frac{n\,\lambda}{2} \tag{8.8}$$

These pressure antinodes occur at the rigid boundaries and have an amplitude that is twice the amplitude of a free traveling wave.

If we compare the behavior of a sound wave near a solid boundary to that of a water wave there is considerable similarity. When an ocean wave washes up against a sea wall the water rises to a height twice that of a freely propagating surface wave and falls by a similar amount. A water particle close to the wall experiences the maximum displacement up and down in response to the impact of the wave. With a sound wave there is a pressure doubling at a solid boundary resulting in a 6 dB increase in sound pressure level.

Minimum values of the sound pressure are called *nodes* and occur at positions where

$$k\,x = \frac{\pi}{2}, \frac{3\,\pi}{2}, \frac{5\,\pi}{2}, \ldots \tag{8.9}$$

and

$$x = \frac{\lambda}{4}, \frac{2\,\lambda}{4}, \frac{3\,\lambda}{4}, \ldots = \frac{n\,\lambda}{4} \tag{8.10}$$

The pressure node in the fundamental occurs at the quarter-wavelength point, which is at the midpoint of the enclosure. This leads to a phenomenon in studios, graphically described as

FIGURE 8.1 Standing Waves in a Closed-Closed Tube

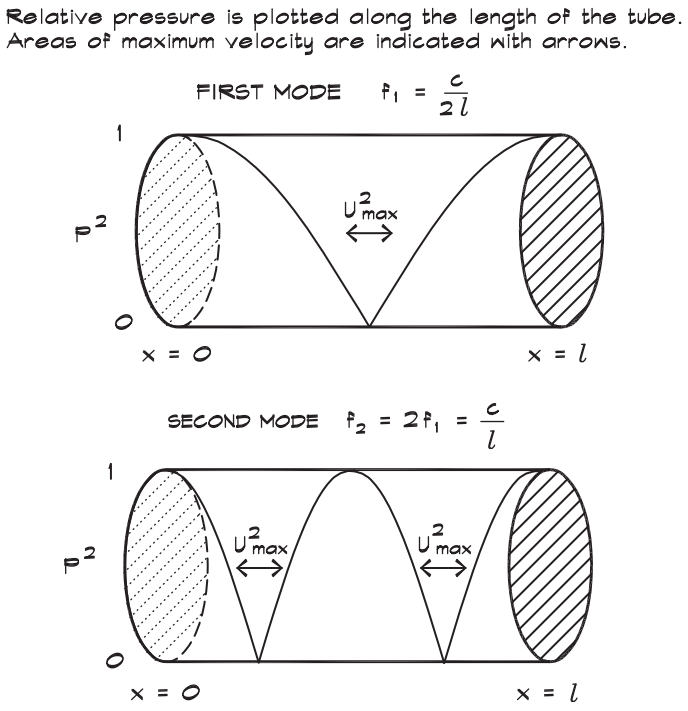

bass suckout—a lack of low-frequency energy at the mixer position near the center of the room, which is accentuated by the placement of bass loudspeakers at the ends of the room where the fundamental mode is easily excited.

An example of standing waves is shown in Fig. 8.1. These are constructed from continuously propagating rightward and leftward traveling waves. As they move past one another and combine, their sum produces the nodes and antinodes shown in the figure.

Standing Waves in Open Tubes

When a plane wave propagates along a tube that is open at the end, some of the sound energy is reflected from the open boundary. The reflection at this pressure release surface comes about due to the mass and springiness of the air column. An analogy may be drawn using the example of a toy paddle ball, where a rubber ball is attached to the paddle by means of an elastic band. When the ball strikes the paddle it is like a sound wave reflecting off the closed end of the tube. There is a pressure maximum, corresponding to squeezing the ball together, which forces a rebound. When the ball reaches the end of the elastic tether, it acts like the open end of the tube. A mass of air moves beyond the end of the tube and is pulled back by the elastic-spring force caused by the low-pressure region behind it. Air that is confined by the boundaries of the tube acts like a spring since the pressure cannot equalize in directions normal to the direction of wave propagation.

When both ends of the tube are open, the boundary condition requires that the acoustic pressure goes to zero at each end. The allowed solutions for the pressure take the form of a

FIGURE 8.2 Standing Waves in an Open-Open Tube

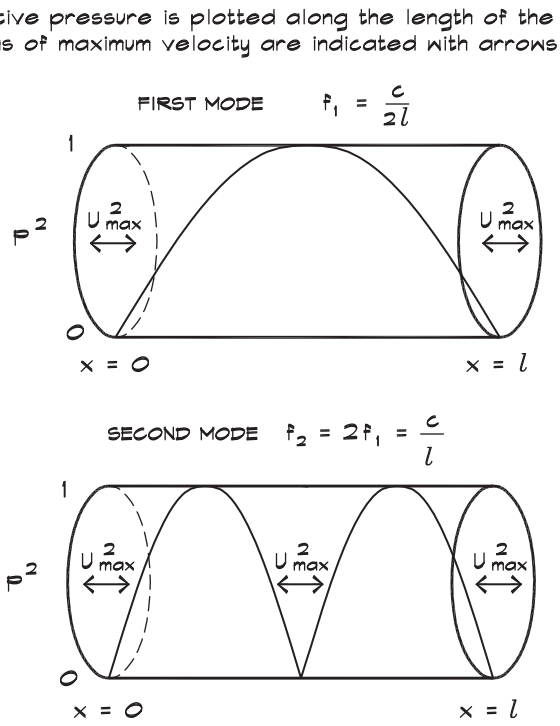

sine wave

$$\mathbf{p} = \mathbf{A} \sin k x = \mathbf{A} \sin \frac{n \pi x}{l} \tag{8.11}$$

having the same resonant frequencies as those given in Eq. 8.4. The difference between a totally open pipe and a totally closed pipe is that, with an open pipe, the pressure maximum (antinode) in the fundamental frequency is at the center of the pipe, rather than at the ends, as shown in Fig. 8.2. This is to be expected since a sine wave is simply a cosine wave shifted by 90°.

In a real pipe the boundary condition is not as simple as a perfect pressure null. Instead there is a finite impedance at the end, which introduces a length correction much like that discussed in Chapt. 7 for perforated plates. For long pipes, this correction is generally small. Refer to Kinsler et al., (1982) for a more detailed treatment.

Combined Open and Closed Tubes

When a tube has one open end and one closed end, the boundary conditions can be applied to a sine wave to obtain

$$\mathbf{p} = \mathbf{A} \sin k x = \mathbf{A} \sin \frac{(2n - 1) \pi x}{2} \tag{8.12}$$

where $n = 1, 2$, and so on, and the resonant frequencies are

$$f_n = \frac{(2n - 1) c_0}{4 l} \tag{8.13}$$

FIGURE 8.3 Standing Waves in a Closed-Open Tube

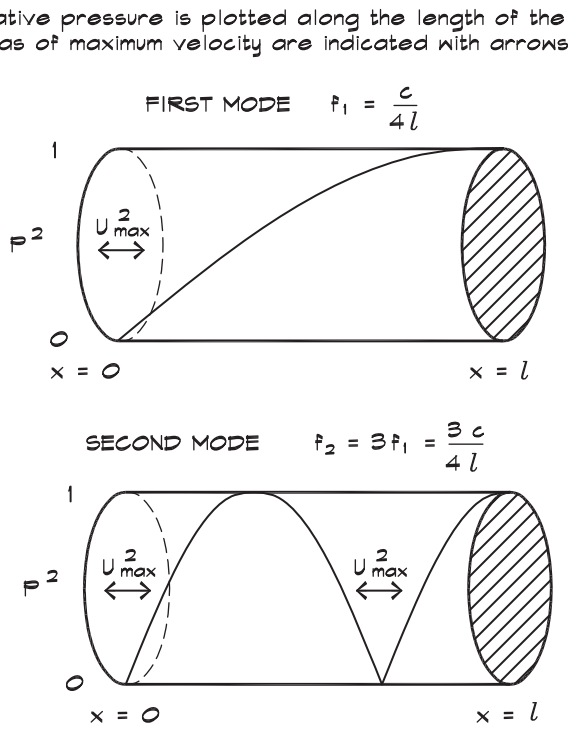

An organ pipe is open at the source end and can be either open or closed at the opposite end. For a given length the fundamental is one octave lower in a pipe, closed at one end, compared to one that is open. The even harmonics are missing; however, the density of modes remains the same as in the previous two examples. Fig. 8.3 shows the fundamental mode shapes.

8.2 SOUND PROPAGATION IN DUCTS

Rectangular Ducts

Sound waves that can propagate down a duct take on a form that is controlled by the duct dimensions relative to a wavelength. If a long duct is rectangular in cross section, standing waves can form in the lateral directions and a traveling wave in the third direction. The equation for the pressure takes the form

$$\mathbf{p} = \mathbf{A} \cos(k_x x) \cos(k_y y)\, e^{-j k_z z}\, e^{j \omega t} \tag{8.14}$$

where, in the lateral directions, there are allowed values of the wave number

$$k_x = m\pi/a \quad m = 0, 1, 2, \ldots \tag{8.15}$$

and

$$k_y = n\pi/b \quad n = 0, 1, 2, \ldots \tag{8.16}$$

where a and b are the lateral dimensions of the duct. The wave number k is related to its components

$$k^2 = k_x^2 + k_y^2 + k_z^2 \tag{8.17}$$

and to the frequency

$$k = \frac{2\pi f}{c} = \frac{2\pi}{\lambda} \tag{8.18}$$

The z-component of the wave number can be written as

$$k_z = \sqrt{k^2 - (k_x^2 + k_y^2)} \tag{8.19}$$

and inserting Eq. 8.15 and Eq. 8.16 into Eq. 8.19 we obtain

$$k_z = k\sqrt{1 - (f_{mn}/f)^2} \qquad f \geq f_{mn} \tag{8.20}$$

where

$$f_{m,n} = \frac{c}{2\pi}\sqrt{k_x^2 + k_y^2} = \frac{c}{2}\sqrt{\left(\frac{m}{a}\right)^2 + \left(\frac{n}{b}\right)^2} \tag{8.21}$$

is known as the *cutoff frequency* for a given mode (m,n). The indices take on integer values $m, n = 0, 1, 2$, and so on. By examining Eq. 8.20 it is clear that when $f = f_{m,n}$, $k_z(m, n) = 0$, and there is no wave propagation in the z direction for that particular mode. If the frequency is above cutoff, then $k_z(m, n)$ is real and positive and the mode m,n is called a propagating mode. Consequently plane waves will not be formed when the lateral dimensions of the duct are wider than half a wavelength.

When the frequency is below cutoff for a particular mode, the wave number is imaginary and the mode, which dies out exponentially, is called *evanescent*.

$$\mathbf{k}_z = -j\,\mathbf{k}\sqrt{(f_{mn}/f)^2 - 1} \qquad f < f_{mn} \tag{8.22}$$

Note that when m and n are zero, the wave is planar, and the lower cutoff frequency is zero. Thus there is no lower cutoff frequency for plane waves. The phenomenon of cutoff does not mean that the propagation of sound is cut off. It only means that below the cutoff frequency only plane waves propagate, and above the cutoff frequency only nonplane waves can be formed.

The propagation angle is the angle that a particular mode makes with the z axis. It is determined by using the relationship

$$k_z = k\cos\theta_{m,n} \tag{8.23}$$

where the propagation angle is defined as

$$\theta_{m,n} = \cos^{-1}\left(\sqrt{1 - \left(f_{mn}/f\right)^2}\right) \qquad f \geq f_{mn} \tag{8.24}$$

For plane waves the propagation direction is along the z axis since the cutoff frequency is zero. For a nonzero cutoff frequency, the propagation direction at cutoff for a particular mode is perpendicular to the z axis, so the wave does not propagate down the duct.

At high frequencies the propagation angle is small and the propagation direction approaches the z axis, which means that these modes tend to beam and have very little interaction with the duct walls. We will see the effects of this behavior in a later chapter. Lined ducts provide little attenuation both at very low frequencies, where the thickness of the lining is small compared with a wavelength, and at very high frequencies, where the wave does not interact with the lining due to beaming.

For a circular duct the cutoff frequency for the lowest mode is given by

$$f_{co} = 0.586 \frac{c_0}{d} \tag{8.25}$$

where d is the duct diameter. Above that frequency, modes can be formed across the duct, which combine with waves moving down the duct to generate cross or spinning modes depending on their shape.

Changes in Duct Area

If a plane wave, below the cutoff frequency, propagates down a duct that contains an abrupt change in area, energy will be reflected from the discontinuity. In Fig. 8.4 the area of the rectangular or conical duct changes abruptly from S_1 to S_2 at a point in the duct that marks the transition from region 1 to 2. At this point the pressure and volume velocity amplitudes must be continuous.

$$\mathbf{p}_i + \mathbf{p}_r = \mathbf{p}_t \quad \text{and} \quad S_1 \left(\mathbf{u}_i - \mathbf{u}_r\right) = S_2 \, \mathbf{u}_t \tag{8.26}$$

FIGURE 8.4 Area Changes in Various Types of Ducts

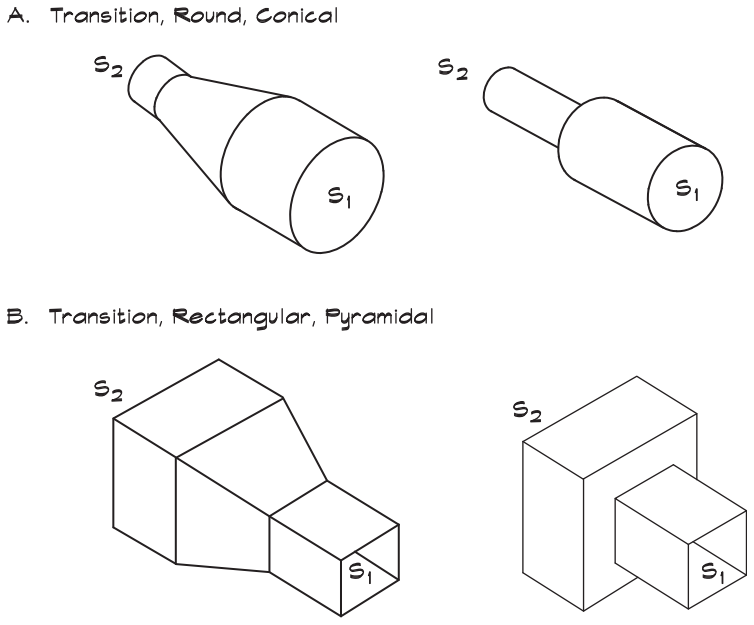

where the subscript i refers to the incident wave, r to the reflected wave, and t to the transmitted wave. The boundary conditions yield

$$\frac{\mathbf{p}_i + \mathbf{p}_r}{\mathbf{u}_i - \mathbf{u}_r} = \frac{S_1}{S_2}\left(\frac{\mathbf{p}_t}{\mathbf{u}_t}\right) \tag{8.27}$$

and using the plane wave relationships $\mathbf{u} = \mathbf{p}/\rho_0 c_0$

$$\frac{\rho_0 c_0 (\mathbf{p}_i + \mathbf{p}_r)}{\mathbf{p}_i - \mathbf{p}_r} = \frac{S_1}{S_2}\left(\frac{\mathbf{p}_t}{\mathbf{p}_t/\rho_0 c_0}\right) = \frac{\rho_0 c_0 S_1}{S_2} \tag{8.28}$$

The reflected amplitude coefficient is

$$\mathbf{r} = \frac{\mathbf{p}_r}{\mathbf{p}_i} = \frac{S_1 - S_2}{S_1 + S_2} \tag{8.29}$$

and the sound energy reflection coefficient is

$$\alpha_r = \left[\frac{S_1 - S_2}{S_1 + S_2}\right]^2 \tag{8.30}$$

and the transmission coefficient is

$$\tau = 1 - \left[\frac{S_1 - S_2}{S_1 + S_2}\right]^2 \tag{8.31}$$

The change in level in decibels, experienced by a plane wave passing through the area change boundary, is

$$\Delta L_a = 10 \log \tau = 10 \log \left[1 - \left(\frac{S_1 - S_2}{S_1 + S_2}\right)^2\right] \tag{8.32}$$

Clearly when the areas are equal there is no loss. For a 50% area reduction the loss is about 1.8 dB. Note that the formula can be used for an area increase or decrease with the same result. The loss due to changes in area contributes to the low-frequency attenuation in duct silencers as well as to the loss in plenums and expansion chambers.

Expansion Chambers and Mufflers

If a plane wave propagates down a duct and enters an area expansion for a certain distance followed by a contraction, there is an acoustical loss. This fundamental shape change is the basis of a reactive (nonlined) muffler used to quiet internal combustion engines and other noise sources, where a dissipative interior liner is not practical. It also furnishes most of the low-frequency loss in small plenums. Figure 8.5 illustrates the configuration.

When a plane wave encounters the changes in area, the pressure and volume velocities must be matched at the two boundaries. This leads to four boundary conditions similar to

FIGURE 8.5 Expansion Chamber Muffler

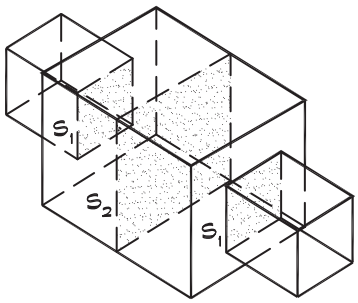

those in Eq. 8.26, which must be solved for the coefficients (Davis, 1957). At the first boundary

$$\mathbf{p}_{\mathrm{i}\,1} + \mathbf{p}_{\mathrm{r}\,1} = \mathbf{p}_{\mathrm{t}\,2} + \mathbf{p}_{\mathrm{r}\,2} \tag{8.33}$$

$$\left(\mathbf{u}_{\mathrm{i}\,1} - \mathbf{u}_{\mathrm{r}\,1}\right) = m\left(\mathbf{u}_{\mathrm{t}\,2} - \mathbf{u}_{\mathrm{r}\,2}\right) \tag{8.34}$$

where $\mathrm{m} = \mathrm{S}_2/\mathrm{S}_1$. At the second boundary

$$\mathbf{p}_{\mathrm{t}\,2}\, \mathrm{e}^{-\mathrm{j}\,\mathrm{k}\,l} + \mathbf{p}_{\mathrm{r}\,2}\, \mathrm{e}^{\mathrm{j}\,\mathrm{k}\,l} = \mathbf{p}_{\mathrm{t}\,3} \tag{8.35}$$

$$m\left[\mathbf{p}_{\mathrm{t}\,2}\, \mathrm{e}^{-\mathrm{j}\,\mathrm{k}\,l} - \mathbf{p}_{\mathrm{r}\,2}\, \mathrm{e}^{\mathrm{j}\,\mathrm{k}\,l}\right] = \mathbf{p}_{\mathrm{t}\,3} \tag{8.36}$$

When these four equations are solved simultaneously, the transmission coefficient can be obtained from $\boldsymbol{\tau} = \dfrac{\mathbf{p}_{\mathrm{t}\,3}}{\mathbf{p}_{\mathrm{i}\,1}}$

$$\boldsymbol{\tau} = \left[\cos \mathrm{k}\, l + \mathrm{j}\, \frac{1}{2}\left(m + \frac{1}{m}\right) \sin \mathrm{k}\, l\right]^{-1} \tag{8.37}$$

and the transmission loss through the expansion is

$$\Delta\, \mathrm{L_m} = 10 \log\left[1 + \frac{1}{4}\left(m - \frac{1}{m}\right)^2 \sin^2 \mathrm{k}\, l\right] \tag{8.38}$$

Recall that these equations were obtained by assuming plane waves in all three sections of the duct. For this equation to hold, the lateral dimensions of the chamber must be smaller than 0.8 λ (Beranek, 1992). A graph of the attenuation versus normalized length is shown in Fig. 8.6. Notice that the result repeats each time $\mathrm{k}\, l = \pi$.

8.3 SOUND IN ROOMS

The analysis of sound in rooms falls into regions according to the frequency (wavelength) of the sound under consideration. At low frequencies, where the wavelength is greater than twice the length of the longest dimension of the room, only plane waves can be formed and the room behaves like a duct. This condition can occur in very small rooms. Above the cutoff

FIGURE 8.6 Transmission Loss of a Single Expansion Chamber (Beranek, 1971)

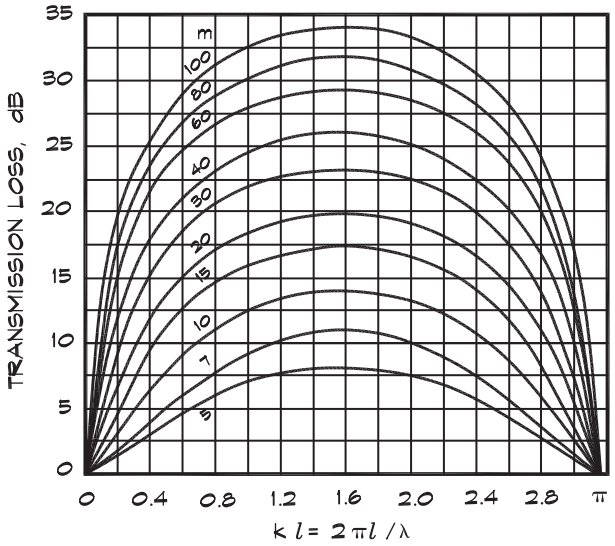

Transmission loss of a single expansion chamber of length l and $S_2/S_1 = m$. For values of kl above π use kl mod π.

frequency of a room, normal modes are formed, which are manifest as standing waves having localized regions of high and low pressure. At still higher frequencies the density of modes is so great that there is a virtual continuum in each frequency range and it becomes more useful to model room behavior based on the energy density or other statistical considerations.

Normal Modes in Rectangular Rooms

Let us consider a rectangular room having dimensions l_x, l_y, and l_z. When the room is ensonified and then the sound source removed, certain frequencies persist, much like those that remained in the case of a closed tube. In this case, however, the modes may develop in several directions, since no room dimension is small compared with a wavelength. If we apply the three-dimensional wave equation in rectangular coordinates given as Eq. 6.32 and write a general solution, it takes the form of

$$\mathbf{p} = \mathbf{A}\, e^{j(\omega t - k_x x - k_y y - k_z z)} \tag{8.39}$$

If this expression is substituted into Eq. 6.32, the values for the wave numbers k_x, k_y, and k_z must satisfy the relationship

$$k = \frac{\omega}{c} = \sqrt{k_x^2 + k_y^2 + k_z^2} \tag{8.40}$$

We can replace the negative signs in Eq. 8.39 with one or more positive signs to obtain seven additional equations, which represent the group of waves moving about the room and reflecting off the boundaries. When we apply the boundary conditions as we did for a closed tube, we find that the allowed values of the wave number are

$$k_i = \frac{n_i \pi}{l_i} \tag{8.41}$$

where i refers to the x, y, and z directions. The equation for the sound-pressure standing wave in the room, which has the same form as Eq. 8.6, is separable into three components

$$\mathbf{p} = 8\,\mathbf{A}\cos\left(\frac{n_x\,\pi x}{l_x}\right)\cos\left(\frac{n_y\,\pi y}{l_y}\right)\cos\left(\frac{n_z\,\pi z}{l_z}\right)e^{j\omega t} \tag{8.42}$$

The natural frequencies are

$$f_{\ell\,m\,n} = \frac{c_0}{2}\left[\left(\frac{\ell}{l_x}\right)^2 + \left(\frac{m}{l_y}\right)^2 + \left(\frac{n}{l_z}\right)^2\right]^{\frac{1}{2}} \tag{8.43}$$

where the ℓ, m, and n are integers that indicate the number of nodal planes perpendicular to the x, y, and z axes.

The normal modes of a rectangular room are referenced by whole number indices represented by the three letters ℓ, m, and n. The 1,0,0 mode, for example, would be the fundamental frequency in the x direction. The 2,1,0 mode is a tangential mode in the x and y directions as in Fig. 8.7. If we take a room having dimensions $7 \times 5 \times 3$ m high ($23 \times 16.4 \times 9.8$ ft) and calculate the first few modes, the results would be those in Table 8.1.

Several things are important to notice. If the room dimensions are a low integer multiple of one another, then modal frequencies will coincide. Under these conditions the energy in

FIGURE 8.7 Standing Waves in a Rectangular Room (Bruel and Kjaer, 1978)

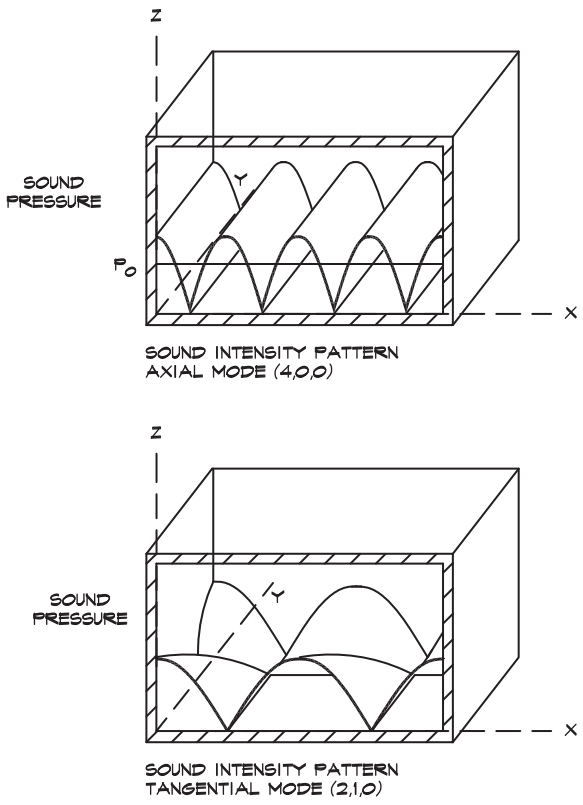

TABLE 8.1 Normal Modes of a Rectangular Room

Number	n_x	n_y	n_z	f_n (Hz)
1	1	0	0	24.6
2	0	1	0	34.5
3	1	1	0	42.4
4	2	0	0	49.2
5	0	0	1	57.4
6	2	1	0	60.1

the room will tend to coalesce into a few modes, which will strongly color the sound. Note also that as the frequency increases, the resonances move closer and closer together. They segue from a discrete set of identifiable frequencies into a continuum of modes.

The number of normal modes in a given frequency range can be calculated by plotting the allowed wave numbers in a three-dimensional graph, known as k-space (Fig. 8.8), having dimensions of wave number in the x, y, and z directions. A given value of k in Eq. 8.40 is represented as a point at the intersection of three lattice lines. The total number of frequencies is contained in a sphere having radius k in the positive octant of the sphere divided by the unit volume per k point. The distance between each k_i value is $\frac{\pi}{l_x}$, $\frac{\pi}{l_y}$, or $\frac{\pi}{l_z}$ and the unit volume per k point is $\frac{\pi^3}{V}$, where $V = l_x\, l_y\, l_z$ is the volume of the room. The number of allowed k values between 0 and a given value of k is

$$N_f = \frac{\pi k^3/6}{\pi^3/V} = \frac{4\pi}{3}\left(\frac{f}{c_0}\right)^3 \tag{8.44}$$

In calculating this number we have left out all k values outside of the positive octant, so we need to add back a correction for frequencies located on the axis planes, which are counted

FIGURE 8.8 Normal Modes Falling between Two Frequencies

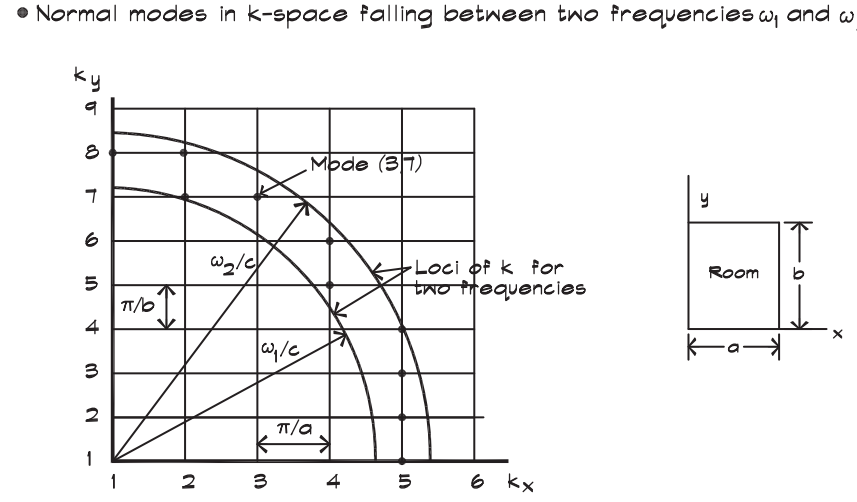

as one half, and on the axes themselves, which are counted as one quarter of their actual value. This yields

$$N_f = \frac{4\pi}{3} V \left(\frac{f}{c_0}\right)^3 + \frac{\pi}{4} S \left(\frac{f}{c_0}\right)^2 + \frac{L}{8}\left(\frac{f}{c_0}\right) \tag{8.45}$$

where S is the area of all the walls and L is the sum of all the edge lengths.

The number of modes in a given frequency range can be determined by taking the derivative of Eq. 8.45 with respect to frequency,

$$\frac{d\,N_f}{d\,f} = 4\pi V \frac{f^2}{c_0^3} + \frac{\pi}{2} S \frac{f}{c_0^2} + \frac{L}{8\,c_0} \tag{8.46}$$

At high frequencies the density of modes is extremely large—for all practical purposes, a continuum. For the room dimensions given in Fig. 8.8, at 1000 Hz, the modal density is 34 modes per Hertz.

Preferred Room Dimensions

A number of authors, including Bolt, Rettinger, and others have offered suggestions on preferred room dimensions for listening rooms and studios. These are given in terms of the ratios of the lengths of the sides of a rectangular room. The one published by Bolt is shown in Fig. 8.9.

FIGURE 8.9 Preferred Dimensions of a Rectangular Room (Bolt, 1946)

The curve encloses dimension ratios of width to length of a rectangular room having a unity ceiling height to give a smooth response at low frequencies.

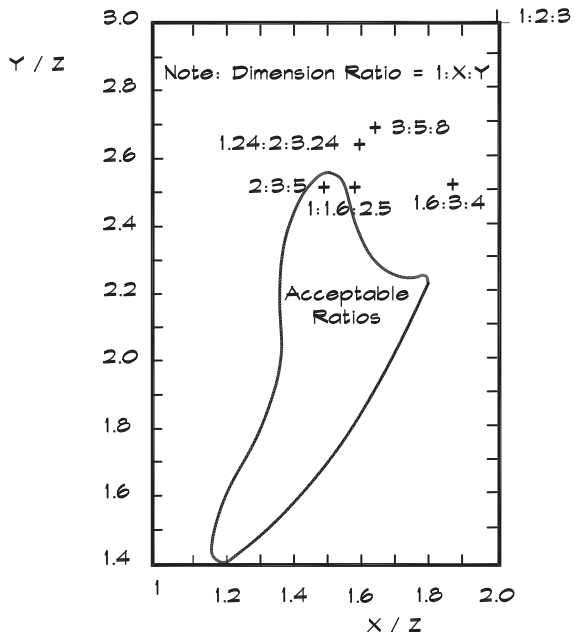

Recommendations such as those shown in Fig. 8.9 are most useful in designing reverberation chambers for acoustical-testing purposes, when a rectangular room is desired. They could be useful in the design of small studios; however, sound studios are rarely built in a rectangular shape. Normal-mode calculations for nonrectangular rooms are more difficult and can be done using finite element methods.

8.4 DIFFUSE-FIELD MODEL OF ROOMS

In a room whose dimensions are large enough that there is a sufficient density of modes, it is customary to describe the space in terms of a statistical model known as a diffuse field. A diffuse field is one in which there is an equal energy density at all points in the room. This implies that there is an equal probability that sound will arrive from any direction.

Schroeder Frequency

The transition between the normal-mode model and the statistical model is not a bright line, but is generally taken to occur at a modal spacing that has at least three modes within a given mode's half-power bandwidth. This point is marked by the so-called *Schroeder frequency* (Schroeder, 1954 and 1996), which is defined in metric units as

$$f_s = 2000\sqrt{\frac{T}{V}} \tag{8.47}$$

where V is the volume of the room and T is the reverberation time. In FP units, where V is in cubic feet, the multiplication constant is 12,000. Above the Schroeder frequency it is appropriate to analyze the room without having to take into account the behavior of its normal modes.

The Schroeder frequency allows us to subdivide the room behavior into regions. Figure 8.10 (Davis and Davis, 1987) shows a plot of the type of behavior we can expect from the sound pressure level in a room plotted against frequency. It also indicates the techniques that can be used to control the steady state room response. In small rooms, where the normal mode region can extend to several hundred Hertz, a statistical model can only be used at relatively high frequencies.

FIGURE 8.10 Controllers in Steady State Room Response (Davis and Davis, 1987)

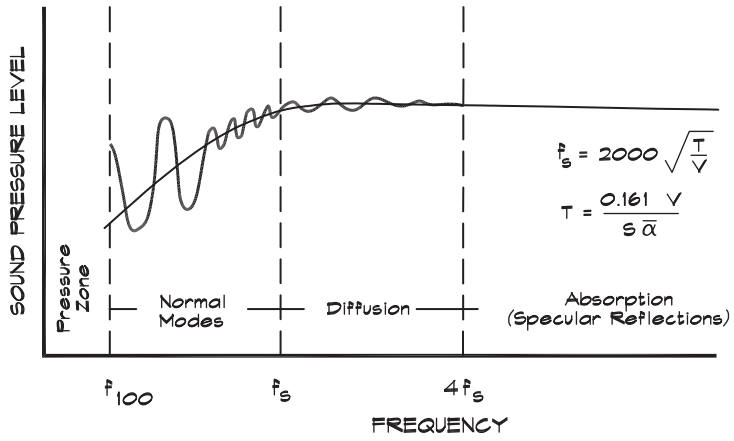

Mean Free Path

Above the Schroeder frequency, sound waves in a room can be treated as rays or particles in terms of their reflections off the room's surfaces. This can be done by following the ray path around a room and studying its interaction with the walls, or by constructing an image source for each reflecting surface and summing their contributions at the receiver. If we follow a sound ray around a room it will travel until it encounters a surface. The sound particle travels a distance (c_0 t) in time t and if it undergoes N collisions during that time, the average distance between collisions is

$$\Lambda = \frac{c_0\, t}{N} = \frac{c_0}{n} \tag{8.48}$$

where n is the average number of collisions per unit time and Λ is the *mean free path* between collisions. Knudsen (1932) determined the mean free path experimentally for a number of differently shaped rectangular rooms, and others (Kuttruff, 1973) have derived the equation from first principles. The result is

$$\Lambda = \frac{4\,V}{S_T} \tag{8.49}$$

where V is the volume and S_T is the total surface area of the room. Here both Λ and n are averages and Eq. 8.49 holds only for diffuse-field conditions. Using Eq. 8.48 the average collision frequency can be obtained

$$n = \frac{c_0\, S_T}{4\,V} \tag{8.50}$$

Decay Rate of Sound in a Room

The reciprocal of the average collision frequency is the mean time between collisions, which for a diffuse field is

$$t = \frac{4\,V}{c_0\, S_T} \tag{8.51}$$

If we ride along with the sound ray, the energy density in the vicinity of the ray after each reflection, shown in Fig. 8.11, is

$$\begin{aligned} D\,(t) &= D_0\,(1-\overline{\alpha}) \\ D\,(2\,t) &= D_0\,(1-\overline{\alpha})^2 \\ D\,(\mathrm{n}\,t) &= D_0\,(1-\overline{\alpha})^{\mathrm{n}} \end{aligned} \tag{8.52}$$

The total number of reflections n is the total time divided by the mean time between reflections, so we can write

$$D\,(\mathrm{t}) = D_0\,(1-\overline{\alpha})^{(c_0\ S_T/4\ V)\ t} \tag{8.53}$$

Now using the identity

$$(1-\overline{\alpha}) = \mathrm{e}^{\ln\,(1\,-\,\overline{\alpha})} \tag{8.54}$$

FIGURE 8.11 Path of a Sound Ray Having Energy Density D

Path of a sound wave modelled as a ray as it reflects off of surfaces having an average absorption coefficient $\bar{\alpha}$. The surfaces are spaced a distance equal to the mean free path $l = 4\,V/S_T$ apart.

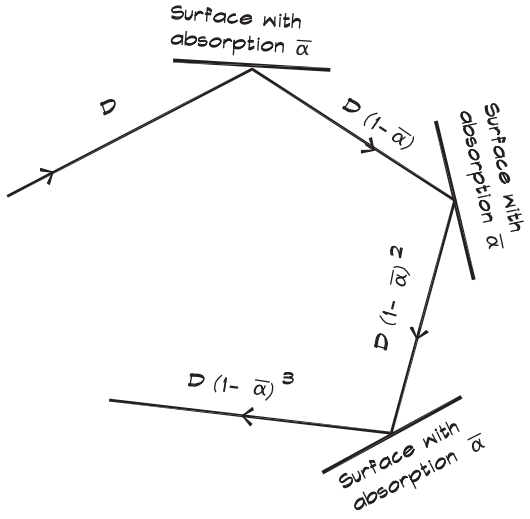

we obtain

$$D\,(\mathrm{t}) = D_0\, \mathrm{e}^{-(c_0\, S_T / 4\, V)\,[-\ln\,(1-\bar{\alpha})]\,\mathrm{t}} \tag{8.55}$$

Multiplying each side by the speed of sound, we can convert this equation into a sound pressure level as a function of time

$$L_p(\mathrm{t}) = L_p\,(\mathrm{t}=0) - 4.34\,\frac{c_0\, S_T}{4V}\,[-\ln\,(1-\bar{\alpha})]\,\mathrm{t} \tag{8.56}$$

which is the rate of decay of sound in a room under diffuse-field conditions. Note that the average absorption coefficient can be expressed as a weighted average of the individual coefficients for each of the surfaces of the room.

$$\bar{\alpha} = \frac{S_1\,\alpha_1 + S_2\,\alpha_2 + S_3\,\alpha_3 + \cdots + S_n\alpha_n}{S_T} \tag{8.57}$$

Sabine Reverberation Time

The idea that there exists a characteristic time for sound to die out in a room originated with Wallace Clement Sabine. When he undertook the task of correcting a problem of unintelligible speech in the Fogg Art Museum lecture hall at Harvard College; the sound in the room would persist for over 5 seconds. Because an English-speaking person can complete about 15 syllables in that time, most of the words were impossible to understand (Egan, 1988). Sabine measured the *reverberation time*, the time it took for the sound level to drop 60 dB, for varying amounts of absorptive materials. He borrowed 3-inch thick seat cushions from the nearby Sanders Theater and found that the more cushions he placed around the room, the more quickly the sound would die out. When 550 cushions were arranged in the

space on the platform, seats, aisles and the rear wall, the reverberation time had decreased to about 1 second. The empirical formula he discovered, now called the Sabine reverberation time, is

$$T_{60} = .049 \frac{V}{A} \tag{8.58}$$

where T_{60} = reverberation time,or the time it takes for sound to decrease by 60 dB in a room (s)
V = volume of the room (cu ft)
A = total area of absorption in the room (sabins)
$= S_1 \alpha_1 + S_2 \alpha_2 + S_3 \alpha_3 + \cdots + S_n \alpha_n$

The standard unit of absorption, now called the sabin in his honor, has units of sq ft. The metric sabin has units of sq m. In metric units the Sabine formula is

$$T_{60} = 0.161 \frac{V}{A} \tag{8.59}$$

Norris Eyring Reverberation Time

Carl Eyring published (1930) a theory of reverberation time in rooms based on an idea that was attributed to R. F. Norris (Andree, 1932). Using the arguments that lead to Eq. 8.56, he set the difference in level to 60 dB and calculated the resulting decay time

$$T_{60} = \frac{4\,V\,(60)}{-4.34\,c_0\,S_T\,\ln(1-\overline{\alpha})} = \frac{0.161\,V}{-S_T\,\ln(1-\overline{\alpha})} \tag{8.60}$$

where the volume is in metric units. In FP units the equation is

$$T_{60} = \frac{.049\,V}{-S_T\,\ln(1-\overline{\alpha})} \tag{8.61}$$

This equation is more accurate in dead (very absorptive) rooms than the Sabine equation. For example, in a perfectly absorbing room with a given area of absorption, the Sabine equation will give a nonzero result whereas the Eyring equation will correctly give zero. Care must be exercised in using the Norris Eyring equation with absorption coefficients measured with the Sabine equation, since occasionally an absorption coefficient greater than one is obtained. All Norris Eyring coefficients must be less than one.

Derivation of the Sabine Equation

When value of the average absorption coefficient is small, that is when we have an acoustically live space, we can use a series expansion for the natural logarithm,

$$\ln(x) = (x-1) - \frac{1}{2}(x-1)^2 + \frac{1}{3}(x-1)^3 - \ldots$$

to obtain an approximation for small ($\overline{\alpha} < 0.2$) values of the average absorption coefficient,

$$-\ln(1-\overline{\alpha}) \cong \overline{\alpha} \tag{8.62}$$

This leads us back to the Sabine equation, which is accurate under these conditions. The Sabine equation is the preferred formula for use in normal rooms and auditoria.

Millington Sette Equation

The average absorption coefficient for a given room is usually not readily available, but may be calculated from the absorption coefficients of the individual surfaces (Millington, 1932 and Sette, 1933)

$$S_T\,\overline{\alpha} = \sum_{i=1}^{n} S_i\,\alpha_i \tag{8.63}$$

which was adopted by Eyring.

$$T_{60} = \frac{0.161\ V}{-S_T\ \ln\left[1 - \sum (S_i\ \alpha_i / S_T)\right]} \tag{8.64}$$

Highly Absorptive Rooms

When the average absorption coefficient for a room is large ($\overline{\alpha} > 0.5$), another series expansion for the natural logarithm can be applied to the Norris Eyring equation, namely

$$\ln\,(x) = \frac{x-1}{x} + \frac{1}{2}\left(\frac{x-1}{x}\right)^2 + \frac{1}{3}\left(\frac{x-1}{x}\right)^3 + \ldots$$

to obtain

$$-\ln\,(1-\overline{\alpha}) \cong \frac{\overline{\alpha}}{1-\overline{\alpha}} \tag{8.65}$$

which yields the absorbent room approximation for the reverberation time

$$T_{60} \cong \frac{0.161V}{S_T\left(\dfrac{\overline{\alpha}}{1-\overline{\alpha}}\right)} \tag{8.66}$$

This equation is limited to relatively high values of the average absorption coefficient. Neither Eq. 8.66 or the Norris Eyring equation can be used when average absorption coefficients exceed a value of one—a relatively common occurrence since we use the Sabine formula to measure absorption.

Air Attenuation in Rooms

In Chapt. 4 we discussed how sound is attenuated as it moves through the atmosphere due to its interaction with the air molecules. If we assume there is an attenuation constant that characterizes the atmospheric loss in terms of so much per distance, we can write an equation in terms of the loss, m, in energy density per meter. After a given time, say the mean time between collisions, the ray has traveled a certain distance, in this case the mean free path, and the resulting energy density has the form

$$D\,(t) = D_0\,e^{-m\,\Lambda} \tag{8.67}$$

By inserting this relationship into Eq. 8.53 and recalculating Eq. 8.55 we get

$$D(t) = D_0 e^{-(c_0 S_T / 4V)\left[-\ln(1-\bar{\alpha}) - 4mV/S_T\right]t} \tag{8.68}$$

and the Norris Eyring reverberation time with air attenuation becomes

$$T_{60} = \frac{0.161\ V}{-S_T \ln(1-\bar{\alpha}) + 4mV} \tag{8.69}$$

in metric units and

$$T_{60} = \frac{.049\ V}{-S_T \ln(1-\bar{\alpha}) + 4mV} \tag{8.70}$$

in FP units. In terms of loss in dB/m or dB/ft the relationship is

$$m = \frac{\Delta L_{air}}{4.34} \tag{8.71}$$

where m has units of inverse meters or feet.

Air losses can be included in the Sabine reverberation time formulas, which devolve from the Eqs. 8.68 and 8.69, in the limit of small values of the average absorption coefficient. In metric

$$T_{60} = \frac{0.161\ V}{A + 4mV} \tag{8.72}$$

and in FP units,

$$T_{60} = \frac{.049\ V}{A + 4mV} \tag{8.73}$$

The total absorption in a room, including the air absorption, is called the room constant and is given the designation R

$$R = A + 4mV \tag{8.74}$$

The units are in sabins or metric sabins.

Laboratory Measurement of the Absorption Coefficient

It is standard practice (ASTM C423) to measure the absorption of an architectural material in a reverberant test chamber using the reverberation time method. A reverberation chamber is a hard room with concrete surfaces and a long reverberation time, with sufficient volume to have an adequate density of modes at the frequency of interest. Since the average absorption coefficient in the room is quite small under these conditions, the Sabine equation can be used. The reverberation time of the empty chamber is

$$T_{60}(1) = \frac{0.161\ V}{S_T\ \bar{\alpha}} \tag{8.75}$$

If a sample of absorptive material having an area S_1 is placed on the floor and the test repeated, the new reverberation time is

$$T_{60}(2) = \frac{0.161\ V}{S_T\ \overline{\alpha} - S_1\alpha_0 + S_1\alpha_1} \tag{8.76}$$

where α_0 is the absorption coefficient of the covered portion of the floor and α_1 is the absorption coefficient of the sample material under test. Combining Eqs. 8.75 and 8.76 we obtain the desired coefficient

$$\alpha_1 = \alpha_0 + \frac{0.161\ V}{S_1}\left(\frac{1}{T_{60}(2)} - \frac{1}{T_{60}(1)}\right) \tag{8.77}$$

In these tests there is some dependence on the position of the sample in the room. Materials placed in the center of a surface are more effective absorbers, and yield higher absorption coefficients, than materials located in the corners. This is because the average particle velocity is higher there. There are also diffraction effects and edge absorption attributable to the sides of the sample. For these reasons Sabine absorption coefficients that are greater than one sometimes are obtained and must be used with caution in the Norris Eyring equation.

8.5 REVERBERANT FIELD EFFECTS

Energy Density and Intensity

We have seen that, as the modal spacing gets closer and closer together, it becomes less useful to consider individual modes and we must seek other ways of describing the behavior of sound in a room. One concept is the energy density . A plane wave moves a distance c_0 in one second and carries an energy per unit area equal to its intensity, I. The direct-field energy density D_d per unit volume is

$$D_d = \frac{I_d}{c_0} = \frac{p^2}{\rho_0\, c_0^2} \tag{8.78}$$

where p^2 is the rms acoustic pressure.

The energy density in a diffuse field has the same relationship to the pressure squared, which is not a vector quantity, but a different relationship to the intensity. In a diffuse field the sound energy can be coming from any direction. The intensity is defined as the power passing through an area in a given direction. In a diffuse field, half the energy is passing through the area plane in the opposite direction to the one of interest. When we integrate the energy incident on the area in the remaining half sphere, the cosine term reduces the intensity by another factor of two. Thus in a reverberant field the intensity is only a quarter of the total power passing through the area. This is shown in Fig. 8.12.

$$I_r = \frac{1}{4}\left(\frac{p^2}{\rho_0\, c_0}\right) \tag{8.79}$$

FIGURE 8.12 Intensity in a Reverberant Field

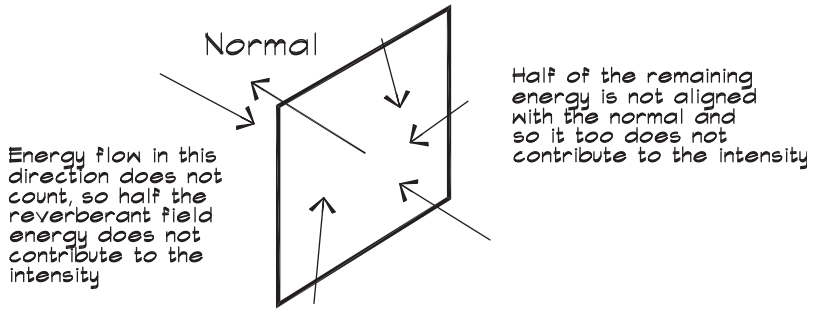

Semireverberant Fields

Occasionally we encounter a semireverberant field, where energy falls onto one side of a plane with equal probability from any direction. Most often this occurs when sound is propagating from a reverberant field through an opening in a surface of the room. Under these conditions the power passing through the plane of an opening having area S_w is given by

$$W_{sr} = \frac{S_w}{2}\left(\frac{p^2}{\rho_0 c_0}\right) \tag{8.80}$$

Room Effect

When a sound source that emits a sound power W_S is placed in a room, the energy density will rise until the energy flow is balanced between the energy being created by the source and the energy removed from the room due to absorption. After a long time the total energy in a room having a volume V due to a source having a sound power W_S is

$$V D_r = \frac{W_S \Lambda}{c_0}\left[1 + (1-\overline{\alpha}) + (1-\overline{\alpha})^2 + \cdots\right] = \frac{W_S \Lambda}{c_0 \overline{\alpha}} \tag{8.81}$$

which has been simplified using the limit of a power series for $\overline{\alpha}^2 < 1$

$$V D_r = \frac{4 W_S V}{c_0 S_T \overline{\alpha}} \tag{8.82}$$

and the sound pressure in the room will be

$$\frac{p^2}{\rho_0 c_0} = \frac{4 W_S}{S_T \overline{\alpha}} = \frac{4 W_S}{R} \tag{8.83}$$

Equation 8.83 is the reverberant-field contribution to the sound pressure measured in a room and can be combined with the direct-field contribution to obtain

$$\frac{p^2}{\rho_0 c_0} = \frac{Q W_S}{4\pi r^2} + \frac{4 W_S}{R} \tag{8.84}$$

Taking the logarithm of each side we can express this equation as a level

$$L_p = L_W + 10 \log \left[\frac{Q}{4 \pi r^2} + \frac{4}{R} \right] + K \tag{8.85}$$

where K is 0.1 for metric units and 10.5 for FP units. The numerical constants follow from the reasoning given in Eq. 2.67.

Equation 8.85 is based on Sabine's theory and was published in 1948 by Hopkins and Stryker. It is a useful workhorse for the calculation of the sound level in a room given the sound power level of one or more sources. It holds reasonably well where the diffuse field condition exists; that is, in relatively large rooms with adequate diffusion if we are not too close (usually within $\frac{\lambda}{2}$) to reflecting surfaces. The increase in sound pressure level due to the reverberant field over that which we would expect from free field falloff is called the room effect.

Figure 8.13 gives the result from Eq. 8.85 for various values of the room constant. Near the source the direct-field contribution is larger than the reverberant-field contribution and the falloff behavior is that of a point source in a free field. In the far field the direct-field contribution has dropped below the reverberant-field energy, and the sound pressure level is constant throughout the space. The level in the reverberant field can be reduced only by adding more absorption to the room. According to this theory, only the total amount of absorption is important, not where it is placed in the room. In practice absorption placed where the particle velocity is the highest has the greatest effect. Thus absorption mounted in a corner, where the pressure has a maximum and the velocity a minimum, would be less effective than absorption placed in the middle of a wall or other surface. Absorption, which is hung in the center of a space, has the greatest effect but this is not a practical location.

FIGURE 8.13 Difference between Sound Power and Pressure Level in a Diffuse Room Due to an Omnidirectional Source

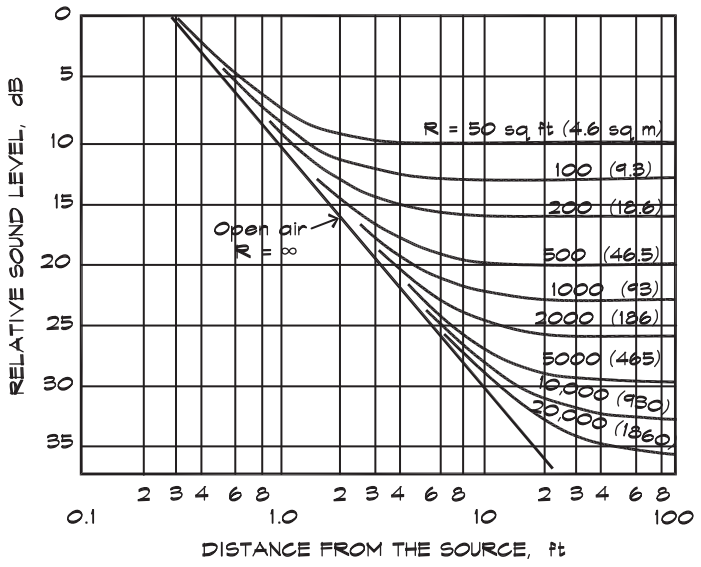

At a given distance, known as the *critical distance*, the direct-field level equals the reverberant-field level. We can solve for the distance by setting the direct and reverberant contributions equal.

$$r_c = \sqrt{\frac{Q R}{16 \pi}} \tag{8.86}$$

Beyond the critical distance the reverberant field predominates.

Radiation from Large Sources

When the source of sound is physically large, such as the wall of a room, it can radiate energy over its entire surface area. The idea of a displaced center was introduced in Eq. 2.91 to relate the sound power to the sound pressure level in free space for a receiver located close to a large radiating surface. Similarly in a reverberant space the direct and reverberant contributions are combined

$$L_p = L_W + 10 \log \left[\frac{Q}{4 \pi \left[z + \sqrt{\frac{S Q}{4 \pi}} \right]^2} + \frac{4}{R} \right] + K \tag{8.87}$$

where K is 0.5 for metric and 10.5 for FP units.

As the distance z, between the surface of the source and the receiver, is reduced to zero, Eq. 8.87 can be simplified to

$$L_p \cong L_W + 10 \log \left[\frac{1}{S} + \frac{4}{R} \right] + K \tag{8.88}$$

where S is the surface area of the source. When the receiver is far from the source the area contribution is small and the distance to the surface of the source and to its acoustic center are nearly equal ($z \cong r$). The equation then reverts to its previous form

$$L_p = L_W + 10 \log \left[\frac{Q}{4 \pi r^2} + \frac{4}{R} \right] + K \tag{8.89}$$

Departure from Diffuse Field Behavior

In the power-pressure conversion, when we do not measure the sound pressure level close to the reflecting surfaces, we neglect some energy near the boundary given in Eq. 8.74. Waterhouse (1955) has investigated this energy and has suggested the addition of a correction term to the room constant, which is only significant at low frequencies.

$$R = A \left(1 + \frac{S_T \lambda}{8 V} \right) + 4 m V \tag{8.90}$$

where S_T is the total surface area and V the volume of the room. The correction is used in certain test procedures (e.g., ISO 3741 and ASTM E336).

FIGURE 8.14 Measured (Power – Pressure) Level Differences (Davis and Davis, 1978)

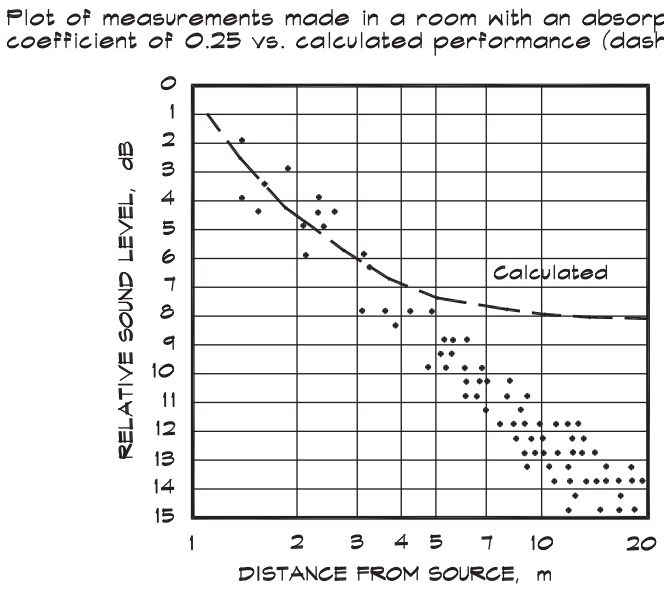

FIGURE 8.15 Rectangular Room with Source Wall ($x = -\ell_x$), Absorbing End-Wall ($x = 0$), and Absorbing Side Surfaces ($y = \ell_y$ and $z = \ell_z$) (Franzoni, 2001)

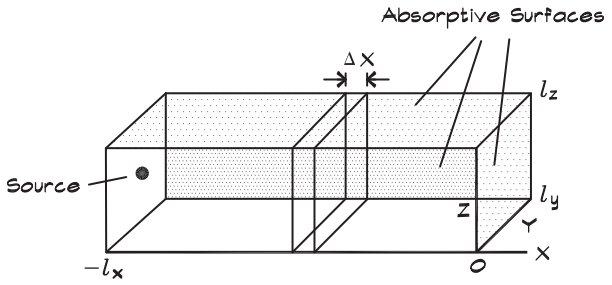

When rooms have a significant dimensional variation in different directions, particularly where there are low ceilings with a large amount of absorption, there is a departure from the behavior predicted by the Hopkins Stryker equation. Figure 8.14 shows measurements taken by Ogawa (1965) in Japan. A number of authors have attempted to account for this behavior by adding additional empirical terms or multipliers to the equation. Hodgson (1998) has published a review of several of these methods.

Franzoni and Labrozzi (1999) developed an empirical formula that applies to long, narrow, rectangular rooms, when the absorption is not uniformly distributed on all surfaces. For a source positioned near one wall and the geometry shown in Fig. 8.15,

$$\overline{p}^2_{rev} = \frac{4\,\rho_0\,c_0\,W}{A}\left[\frac{(1-\overline{\alpha}_{total})(1-\overline{\alpha}_{total}/2)}{(1-\overline{\alpha}_w\,\overline{S}/2)}\right] e^{-(1/2)\,\overline{\alpha}_w\,\overline{S}\overline{x}} \tag{8.91}$$

where $\overline{p}^2_{rev}$ = cross-sectionally averaged mean square acoustic pressure (Pa^2) at a distance x from the origin (not the source)
A = total area of absorption in the room (sabins)
$= S_1 \alpha_1 + S_2 \alpha_2 + S_3 \alpha_3 + \cdots + S_n \alpha_n$
$\overline{\alpha}_{total} = A / S_{total}$
$\overline{\alpha}_w$ = total absorption of the side surfaces divided by the area of the side surfaces
$\overline{x} = x / l_x$
$\overline{S}$ = ratio of the side wall surface area to the cross sectional surface area

Reverberant Falloff in Long Narrow Rooms

Franzoni (2001) also published a theoretical treatment of the long-narrow room problem by considering an energy balance for diffuse-field components traveling to the right and to the left using the geometry in Fig. 8.15. She assumes that there is a locally diffuse condition, where energy incidence is equally probable in all directions from a hemisphere at a planar slice across the room, but the rightward energy does not necessarily equal the leftward energy. The total energy at a point is taken to be uncorrelated and can be expressed as the sum of the two directional components

$$\overline{p}^{\,2} = \overline{p}^{\,2}_{+x} + \overline{p}^{\,2}_{-x} \tag{8.92}$$

At a given slice the reverberant intensity, due to rightward moving waves, is

$$I_{+x} = \frac{\overline{p}^{\,2}_{+x}}{\rho_0 c_0} \tag{8.93}$$

and similarly for the leftward moving waves.

To evaluate the effect of reflections from the side surfaces we write the mean square pressure near the wall as the sum of the incident and reflected components interacting with the sides

$$\overline{p}^{\,2}_{+x} = \overline{p}^{\,2}_{+x_{incident}} + \overline{p}^{\,2}_{+x_{incident}}(1 - \alpha_w) = (2 - \alpha_w)\overline{p}^{\,2}_{+x_{incident}} \tag{8.94}$$

The incident intensity into the side wall boundary (y or z) is

$$I_{sidewall} = I_s = I_y = I_z = \frac{\overline{p}^{\,2}_{+x_{incident}}}{2\rho_0 c_0} = \frac{\overline{p}^{\,2}_{+x}}{2\rho_0 c_0}\left[\frac{1}{2 - \alpha_w}\right] \tag{8.95}$$

where $\overline{p}^{\,2}_{+x}$ = mean square pressure associated with rightward traveling waves, incident plus reflected.

If we define β as the fraction of the surface area at a cross section, covered with an absorbing material having a random incidence absorption coefficient α_w, and l_p and S as the perimeter and area of the cross section, we can write a power balance relation equating the power in to the power out of the cross section.

$$I_x S = \left(I_x + \frac{d I_x}{d x}\Delta x\right) S + \alpha_w \beta l_p \Delta x I_s \tag{8.96}$$

This can be written as a differential equation

$$\frac{\mathrm{d}\left(\overline{\mathrm{p}}_{+\mathrm{x}}^{2}\right)}{\mathrm{d}\,\mathrm{x}} + \frac{\alpha_{\mathrm{w}}\,\beta\,l_{\mathrm{p}}}{(2-\alpha_{\mathrm{w}})\,S}\;\overline{\mathrm{p}}_{+\mathrm{x}}^{2} = 0 \tag{8.97}$$

which has a solution for right-running waves

$$\overline{\mathrm{p}}_{+\mathrm{x}}^{2} = \mathrm{P}_{+\mathrm{x}}\mathrm{e}^{-(\alpha_{\mathrm{w}}\,\beta\,l_{\mathrm{p}})/((2-\alpha_{\mathrm{w}})\,S)\,\mathrm{x}} \tag{8.98}$$

and another for left-running waves

$$\overline{\mathrm{p}}_{-\mathrm{x}}^{2} = \mathrm{P}_{-\mathrm{x}}\mathrm{e}^{+(\alpha_{\mathrm{w}}\,\beta\,l_{\mathrm{p}})/((2-\alpha_{\mathrm{w}})\,S)\,\mathrm{x}} \tag{8.99}$$

where $\mathrm{P}_{-\mathrm{x}}$ and $\mathrm{P}_{+\mathrm{x}}$ are coefficients to be determined by the boundary conditions at each end. At the absorbing end ($\mathrm{x} = 0$) the right and left intensities are related

$$\mathrm{I}_{-\mathrm{x}}(0) = (1-\alpha_{\mathrm{b}})\,\mathrm{I}_{+\mathrm{x}}(0) \tag{8.100}$$

with α_{b} being the end wall random incidence absorption coefficient. The coefficients in Eqs. 8.98 and 8.99 are related

$$\mathrm{P}_{-\mathrm{x}} = (1-\alpha_{\mathrm{b}})\,\mathrm{P}_{+\mathrm{x}} \tag{8.101}$$

At the source-end wall, the power of the sources is equal to the power difference in right and left traveling waves

$$\mathrm{W} = S\left[\mathrm{I}_{+\mathrm{x}}(-l_{\mathrm{x}}) - \mathrm{I}_{-\mathrm{x}}(-l_{\mathrm{x}})\right] \tag{8.102}$$

Plugging in the mean square pressure terms and using Eq. 8.101 (Franzoni, 2001),

$$\overline{\mathrm{p}}^{\,2}(\mathrm{x}) = \frac{2\,\rho_0\,\mathrm{c}_0\,\mathrm{W}}{S}\left[\frac{\cosh(\gamma\mathrm{x}) - \dfrac{1}{2}\,\alpha_{\mathrm{b}}\,\mathrm{e}^{+\gamma\mathrm{x}}}{\sinh(\gamma\,l_{\mathrm{x}}) + \dfrac{1}{2}\,\alpha_{\mathrm{b}}\,\mathrm{e}^{-\gamma l_{\mathrm{x}}}}\right] \tag{8.103}$$

where $\gamma = \alpha_{\mathrm{w}}\,\beta\,l_{\mathrm{p}}/\left[(2-\alpha_{\mathrm{w}})\,S\right]$. Although this formula is somewhat more complicated than Eq. 8.91 it is still straightforward to use.

The result given by Eqs. 8.91 and 8.103 can be compared to more detailed calculations in Fig. 8.16. The agreement is good for both equations. Franzoni (2001) gives several other examples for different absorption coefficients, which also yield good agreement.

Reverberant Energy Balance in Long Narrow Rooms

An energy balance must still be maintained, where the energy produced by the source is absorbed by the materials in the room. In the Sabine theory, the balance is expressed as Eq. 8.83 and the reverberant field energy is assumed to be equally distributed throughout the room. In Franzoni's modified Sabine approach, the average reverberant field energy is the same as Sabine's, but the distribution is uneven. The average energy can be obtained either by integrating Eq. 8.103 over the length of the room or from the following arguments.

FIGURE 8.16 Comparison of Falloff Data—Empirical Fit and Theoretical (Franzoni, 2001)

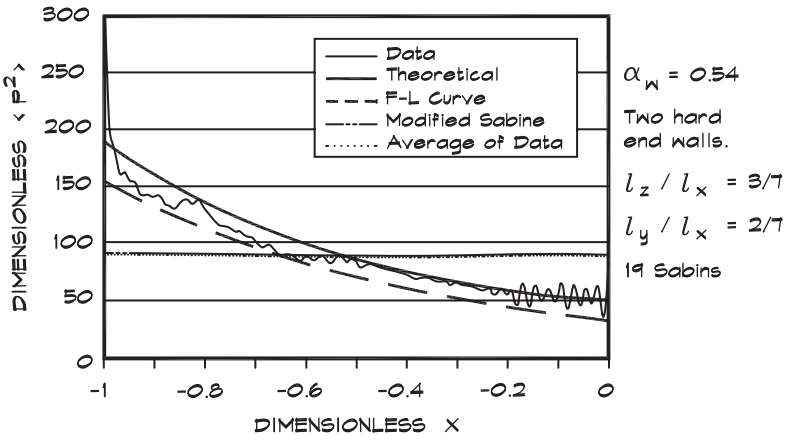

The power removed from the room is

$$W_{out} = \sum_{\substack{\text{absorbing} \\ \text{surfaces, i}}} I_{\substack{\text{into} \\ \text{surface}}} \alpha_i S_i \tag{8.104}$$

The intensity incident on a surface is due to both the direct and reverberant-field components. From Eq. 8.94 the reverberant energy into a boundary surface is

$$I_r = \frac{\overline{p}^2_{\text{incident}}}{2\rho_0 c_0} = \frac{\overline{p}^2}{2\rho_0 c_0} \frac{1}{(2-\alpha_i)} \tag{8.105}$$

and the average direct-field energy is

$$I_d = \frac{W_{in}}{S_{total}} \tag{8.106}$$

The power removed by the absorbing surfaces is

$$W_{out} = \sum_i \frac{\overline{p}^2}{2\rho_0 c_0 (2-\alpha_i)} \alpha_i S_i + \sum_i \frac{W_{in}}{S_{total}} \alpha_i S_i \tag{8.107}$$

which in terms of the average mean square pressure is the modified Sabine equation (Franzoni, 2001)

$$\overline{p}^2_{\substack{\text{spatial} \\ \text{average}}} = \sum_i \frac{4 W_{in} \rho_0 c_0}{\sum_i \alpha_i S_i/(1-\alpha_i/2)} \left(1 - \sum_i \alpha_i S_i / S_{total}\right) \tag{8.108}$$

When the same absorption coefficient applies to all surfaces this simplifies to

$$\overline{p}^{\,2}_{\substack{\text{spatial}\\ \text{average}}} = \frac{4\,W_{in}\,\rho_0\,c_0}{A}(1-\alpha/2)\,(1-A/S_{total}) \tag{8.109}$$

The first term in the parentheses is a correction to the Sabine formula for the difference between the incoming and outgoing waves, and the second term is the power removed by the first reflection. Figure 8.16 also shows the results to be quite close to exact numerical simulations of the sound field.

Fine Structure of the Sound Decay

When an impulsive source such as a gunshot, bursting balloon, or electronically induced pulse excites a room with a brief impulsive sound, the room response contains a great deal of information about the acoustic properties of the space. First there is the initial sound decay in the first 10 to 20 msec of drop after the initial burst. The reverberation time based on this region is called the early decay time (EDT) and it is the time we react to. After the first impulse there is a string of pulses, which are the reflections from surfaces nearest the source and receiver. Thereafter follows a complicated train of pulses, which are the first few orders of reflections from the room surfaces. In this region the acoustical defects present in the room begin to appear. Long-delayed reflections show up as isolated pulses. Flutter echoes appear as repeated reflections that do not die out as quickly as the normal reverberant tail. Focusing can cause sound concentrations, which increase the reflected sound above the initial impulse. If the energy-time behavior of the room is filtered, it can be used to explore regions where modal patterns have formed and can contribute to coloration. A typical graph is shown in Fig. 8.17.

When two rooms are acoustically coupled the reverberation pattern in one room affects the sound in the other. When one has a longer reverberation time it may lead to a dual-slope reverberation pattern in the other. Consequently it is good practice to match the decay patterns of adjacent rooms unless it is the purpose to use one to augment the reverberant tail of the other.

FIGURE 8.17 Energy vs Time for an Impulsive Source

Sound pressure level at a point in a room for an impulsive sound. The direct sound arrives first followed by discrete reflections separated in time. Multiple reflections merge to become the reverberant field.

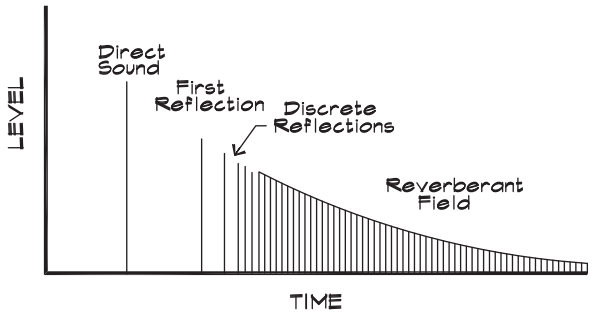

The room resonances that we examined in earlier sections contribute to the long-term behavior of the sound field. If an initial source of sound is turned on, the direct-field energy reaches a listener first, followed closely by the early reflections and lastly by the reverberant field. In the low frequencies the reverberant field is colored by the room modes where energy is preferentially stored. These modes build up and persist longer than nonresonant sound fields. The early reflections are determined by the position and orientation of reflecting surfaces near the source, whereas the reverberant field is defined by the total absorption and position of materials in the room, by the presence of diffusion in the space, and the room modes by the room size and surface orientation. By controlling these variables we can shape the room response according to its use.

This page intentionally left blank